Networks in Financial Markets

Inauguraldissertation zur Erlangung des akademischen Grades
eines Doktors der Wirtschafts- und Sozialwissenschaften
der Wirtschafts- und Sozialwissenschaftlichen Fakultät
der Christian-Albrechts-Universität zu Kiel

vorgelegt von
Diplom-Volkswirt Matthias Raddant
aus Bad Segeberg
Kiel, April 2012

Gedruckt mit Genehmigung der Wirtschafts- und Sozialwissenschaftlichen Fakultät
der Christian-Albrechts-Universität zu Kiel
Dekan: Professor Horst Raff, Ph.D.
Erstberichterstattender: Professor Dr. Thomas Lux
Zweitberichterstattender: Professor Dr. Simone Alfarano
Drittberichterstattender: Professor Dr. Stefan Reitz
Tag der Abgabe der Arbeit: 24.04.2012
Tag der mündlichen Prüfung: 11.07.2012

Networks in Financial Markets

Inauguraldissertation zur Erlangung des akademischen Grades
eines Doktors der Wirtschafts- und Sozialwissenschaften
der Wirtschafts- und Sozialwissenschaftlichen Fakultät
der Christian-Albrechts-Universität zu Kiel

vorgelegt von Diplom-Volkswirt Matthias Raddant aus Bad Segeberg
Kiel, April 2012

CONTENTS

LIST OF FIGURES

LIST OF TABLES

Acknowledgments

First I would like to thank my supervisor Thomas Lux for his support during the last years, for showing me an approach to economics which made the subject interesting for me in the first place, and for being "the most relaxed person I ever met" (quote from a former colleague). I also want to thank Mishael Milaković for guiding me through large parts of my Ph.D., for sharing his view on economics, economists, and some more.

I am indebted to Simone Alfarano, for showing dynamic systems to me, and for his advice over the last years. I thank Eshel Ben-Jacob and Dror Y. Kenett for our inspiring collaboration and their hospitality.

My gratitude goes out as well to all the members of Icelab, for providing office space when needed, and to all the helpful colleagues at the CAU and IfW Kiel. I want to thank my fellow students and friends, especially Laura Birg, Nadine Heitmann, Markus Pape, and Wan-Hsin Liu, for the good time that we had in Kiel. Lastly, I thank Fariba for her help, patience, and kindness.

1. INTRODUCTION

1.1 Why We Need to Study Networks in Economics

For some reasons, social scientists and physicists are not very close academic friends. This might be due to the fact that physicists analyze the behavior of particles or matter, while social scientists analyze the action of men. Men is able to make rational decisions, while matter just behaves accordingly to the laws of nature. In general, the author's impression is that human behavior in economics is seen as something that happens separated from natural sciences, postulated in various models that sometimes lack explanatory power with respect to real macroeconomic behavior. Interestingly, economists and especially physicists share one topic in their research: Both have to consistently explain behavior of systems on very different scales. In economics these scales are labeled micro and macro. Physicists talk about meso and macro to differentiate between issues of classical and quantum mechanics. Among physicists there is agreement that different toolboxes are needed to explain effects on different scales, and a lot of these toolboxes have in fact been developed. It seems incomprehensible why economists then care so little about methods from the natural sciences.

Let me explain some points of this slightly exaggerated critic: Modern mathematical methods have been introduced into economics decades ago and they have taken us a long way in understanding dynamical systems, market clearing conditions, and optimal planning and control. The concept of the utility maximizing household is working fine as a cornerstone in microeconomic models, even if no real household will ever solve any equation system. However, the last financial crisis has revealed that despite their technical complexity our recent macroeconomic models too often lack practical usability aside from narrowly defined research questions.[1]

In these models society is mostly represented by a representative consumer or producer, whose decision is implicitly duplicated for the rest of the society. Economists accept that methods which are good for predicting the economy on the household level are not always very helpful to describe aggregate behavior and vice versa.

[1] See, e.g., Krugman (2009), "What went wrong with economics".

Nevertheless, macroeconomics is very much based on the methodology of microeconomics, which sometimes works fine, but at some point, especially when it comes to explaining crisis and interactions, totally breaks down. In the wording of physics, the required information for the prediction of aggregate behavior is not only the knowledge about isolated particles, but also the knowledge about the distribution of relevant attributes of these particles, and their interactions. This means that even if the behavior of a single particles can be predicted, it is known that on the aggregate level other forces come into play and that not even the aggregation over all predictable particles does necessarily say anything about the behavior of the aggregate.

Moreover, many systems that we analyze in economics are so complex that we cannot assume that single participants or macroscopic groups have full knowledge of the consequences of their decisions and actions. While it seems reasonable that decisions involving a limited number of counterparts and a manageable set of information will be taken rationally, this becomes doubtful for models which assume rational expectations about large sets of macroeconomic variables. If we accept that the so-called micro-foundation of our macroeconomic models is problematic, because it will not necessarily lead to a sufficient explanation of aggregate behavior, we might sometimes be better off to treat the people in our models like 'particles', which can do nothing else than behave according to the laws of nature.

Network science, and especially the physics community, has developed powerful tools to work on some of the above mentioned problems. They allow us to build upon an agent or household based description of behavior. They allow us to describe heterogeneity in society and they are intended to analyze connections, interdependencies, and interactions – all ingredients which are likely to improve our understanding of economics.

Even though it is evident that the economic and social systems that we want to analyze all inhibit a network structure, it is not very common in economics to describe and model problems in terms of networks. In this thesis, I will present four topics where networks are explicitly used to do this. The second chapter deals with a theoretical model about opinion formation, as it can be used to describe investors in financial markets. Chapter 3 is pure empirical work. We analyze the network of board members of German companies. In the forth chapter, the view is back on a classical finance topic. The network here is not given directly, it is a latent one, given by the similarity graph derived from an analysis of correlations of stock returns. The last chapter finally relates directly to the financial crisis of 2008 and financial contagion. We investigate the Italian interbank loan market and analyze

how it has changed since the crisis.

In the following we will discuss basic principles of network science. A more detailed summary of the chapters can be found in Section 1.5.

1.2 Heritage and Development of Network Science

Network science has always been an interdisciplinary field. It is almost forgotten that around 70 years ago many foundations of what we today call *social network analysis* have been developed by sociologists and social psychologists, see e.g. Moreno and Jennings (1938). They used graph theory and basic concepts of statistics to study human relationship and thus introduced these methods into the field of sociology. Studies based on questionnaires gave an idea about the average number of social contacts of people. Moreno called his approach *Sociometry*. He used systematically collected data from schools and work groups and analyzed the connections and attitudes between the people in the samples. This modeling lay the foundations of social network analysis, (see, e.g., Wasserman and Faust, 1994; Freeman, 2004).

It was then White et al. (1976) whose description of people, acting dependent on their position and role in their network, gave another important impulse for modern sociology and for the use of quantitative methods. White studied mathematics, made a PhD in physics and a bit later turned to sociology. He introduced modern structural analysis into social network analysis, and is very well known for the concept of *structural equivalence*. Lorrain and White (1971) showed, how nodes can be compared to each other, which enables us to detect relationship patterns in networks. White inspired a huge number of scientists, many of them his students, to carry on his research. It became evident from their research that the position which people have in their social network is crucial for their development in life, and that for this reason more research had to be done on network structure.

Especially since the 1990s much of this kind of research has been carried on by physicists. Computer scientists have become active in the field as well, motivated by datasets of growing online-communities in the world wide web.

It is obvious that there is some gap between the introduction of network science into sociology and the more recent approaches. The reason for this was the lack of reliable larger datasets and the possibility to analyze them (see Rosvall, 2006). As a result, for quite some time it was not evident to most researchers, how larger real world social networks look like. In a seminal paper Travers and Milgram (1969) found out that the average separation of two people in our society is about six, which means that through friends, and friends of friends, you can reach another

person mostly after six 'steps'. At that time this was an overwhelming finding and gave an idea at least on average distances and connectivity in social networks. After that a lot of theoretical work was done on so-called random networks of the Erdös and Renyi (1959) type, in which links are evenly distributed between nodes with respect to number and destination. Despite some evidence that these kind of networks do not resemble reality, it took up to the late 1990s to realize that networks in real life mostly have a scale-free degree distribution following a power-law. Albert et al. (1999) show this fact by analyzing connections of web-sites in the world wide web. The finding that nodes differ dramatically in the number of connections they have, gave a new impulse to the field, since this stylized fact could explain patterns of information and disease spreading.

In some disciplines network theory has been used for a long time, for example in medicine for a description of the immune system, like in Hoffman (1975). After the stylized facts of social networks are to some extend known, the usage has grown even more. In biology and medicine the spread of disease is modeled with concepts from network science. Liljeros et al. (2001) show that policies on HIV prevention can be derived, Eubank et al. (2003) model the spread of disease in urban networks. Biologists an ecologists analyze food webs (e.g. Dunne et al., 2002) and other parts of the ecosystem with network science methods.

1.3 Basic Concepts in Network Science

1.3.1 Graphs, Nodes, and Edges

The terminology in network science is sometimes rather lose. A network is a *graph*, which consists of *vertices* and *edges* connecting them. In the language of the mathematician, this graph will only be a network, if the edges have weights (or distances) assigned to them. In this case, vertices are also called *nodes* and edges become *links*. However, in the literature this condition is mostly dropped and the above mentioned terms are used synonymously (see, e.g., Jackson, 2008; Rosvall, 2006).

Nodes mostly represent objects or people and edges represent relationships between them. Links can be unidirectional or bidirectional. In the latter case we explicitly differentiate the direction of a connection while in the case of unidirectionality this is not possible. The intensity of a relationship can be expressed by assigning a weight to each link. The resulting network is then also called a *weighted network*.

In order to work with network data, these are mostly mapped to a matrix. The most common method is to use an *adjacency matrix*. An example is shown in Figure

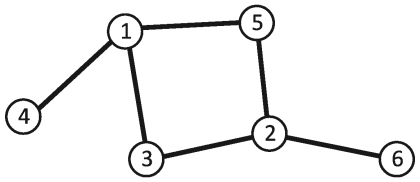

$$\begin{pmatrix} 1 & 0 & 1 & 1 & 1 & 0 \\ 0 & 1 & 1 & 0 & 1 & 1 \\ 1 & 1 & 1 & 0 & 0 & 0 \\ 1 & 0 & 0 & 1 & 0 & 0 \\ 1 & 1 & 0 & 0 & 1 & 0 \\ 0 & 1 & 0 & 0 & 0 & 1 \end{pmatrix}$$

Fig. 1.1: Network and adjacency matrix
The small network on the left can be described by the adjacency matrix to the right. Node 1 is connected to the nodes 4,5 and 3. These connections are represented by the 1 entries in the first row of the matrix. Here the entries on the trace are 1 by definition.

1.1. Given a network with N nodes we define a matrix $A_{[N\times N]}$ such that each entry in row i column j is 1 if the nodes i and j are connected. For weighted networks the values a_{ij} can take any value. A is symmetric if the network is unidirectional.

1.3.2 Degree

The term degree describes the number of links that a node has. More interesting than the degree of a single node is of course the degree distribution of a network. In a random network, for example, the probability of each node to be connected to any other node is the same for all nodes in the network. As a result, the degree distribution is Binomial. As mentioned above, we mostly find scale-free networks in the real world. This term refers to the stylized fact that the degree distribution of most networks follow, at least in approximation, a power law, such that the number of links l follows $P(l) \propto l^{-\gamma}$. These networks have many nodes with a low degree and only few with a high degree. This has implications for the length of the shortest path when tracing from each node to any other node. It explains, for example, Milgram's finding of humans only being six degrees of separation apart. This feature is driven by the existence of high degree nodes, so-called hubs, which, similarly to big airports, link to all parts of the network.

1.3.3 The Special Case of Bipartite Graphs

A special type of network can be derived from a bipartite graph. Such a graph consists of two sets of vertices, edges show the relations between edges from the different sets. A graph can be called bipartite, if we can group the vertices into two sets, such that no edges exist within the groups and each vertex has at least one edge. These kind of graphs mostly show some kind of membership or incidence of vertices for the two sets.

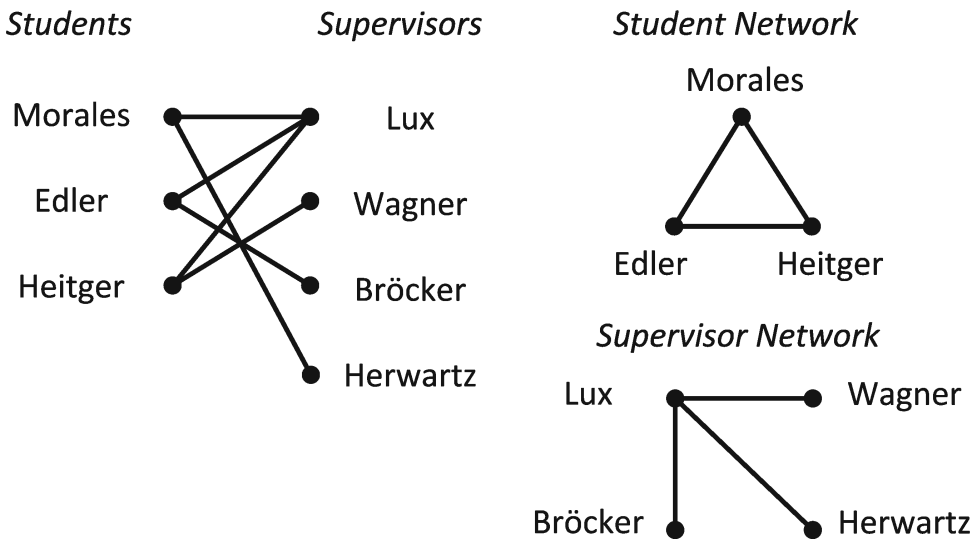

Fig. 1.2: Bipartite graph
The network on the left is a bipartite graph, it consists of two sets, the set of students and the set of their supervisors. From this graph we can come up with two projections, the network of supervisors and the network of students. Students are connected if they share at least one supervisor. Supervisors are connected if they share at least one student. Since Lux is a supervisor to all students, the network of students is complete while the network of supervisors is not.

The incidences that a bipartite graph shows can be projected into two directions, into the network of nodes from the first set (being connected by sharing a vertex from the second set) and vice versa the network of the second set. An example of a bipartite graph is given in Figure 1.2. This graph consists of the set of supervisors and the set of students that they supervised. Since every student is normally supervised by two supervisors, the projection of the graph on the students network shows a dense network between the students. The other projection from this graph is the network of supervisors.

Instead of using an adjacency matrix, this graph can be described by an *incidence matrix*. In this case the bipartite graph is mapped to a matrix $I_{N\times L}$ where $i_{ij} = 1$ if vertex i is adjacent to edge j.

When we define the students as vertices and the supervisors (or professors) as edges which point to them, we can use the incidence matrix $I_{[S\times P]}$ and derive the adjacency matrix of the network of students as $S = II^T$ and the adjacency matrix for the network of professors from $P = I^T I$.

Bipartite graphs will show up again in Chapter 3 when we turn to analyze executives and their membership in different company boards.

1.3.4 Assortativity and Clustering

Whether a node in a network is rather important or not is one of the general questions in network science. Being important is mostly associated with having a lot of links, but also where links lead can be decisive.

The first concept to describe how nodes are linked is based on very basic measure of degree. Networks in which nodes with a high degree are mostly connected to other nodes of high degree are called *assortative*, while the converse is called *disassortative*. Assortativity can also refer to other properties of nodes then just degree, *assortative mixing* describes the correlation between all attributes of connected nodes (see Newman, 2002).

Social networks mostly show a high degree of *clustering*, in this case the probability that two nodes which are linked to the same other node are also connected among each other is very high. Interestingly, this redundancy of connections has been found to make links which lead outside of such a clustered group rather valuable. This is called the concept of the *strength of weak ties* named by Granovetter (1973). According to his work, society consists of strongly wired communities, linked by weak ties, which hold the community together.

While the concept of clustering describes properties of the entire network, there are some measures to describe single nodes, the best known might be *centrality*. To calculate the betweenness centrality of a node, we have to count how many shortest paths between any two other nodes run through the node for which we calculate the betweenness centrality. This gives an idea of how critical this node is for the overall network (see Newman, 2010).

1.3.5 Community Structures

Following the idea of Granovetter about the existence of strongly connected components within networks, numerous methods have been developed to identify clusters. The goal of *graph partitioning* or *community detection* is to split the nodes of a network into groups, such that many links exist inside the groups and only few links remain in between nodes of different groups.

There are two streams of literature on this topic, the first (and older one) on *graph partitioning* tries to split the network into a fixed number of subgraphs. The method of *spectral partitioning* for example achieves this by evaluating the eigenvalues of the *Graph Laplacian*[2]. In larger datasets it is mostly inconvenient to work with a predefined number of clusters. Moreover, some matrix calculations become very time

[2] The Laplacian is a special form of the adjacency matrix of the network, where the trace of the Laplacian correspond to the number of links between nodes, see Sections 3.3 and 3.4.

consuming. *Community detection* therefore has developed algorithmic procedures, which endogenously detect the number of subgraphs in the partitioning process (see, e.g., Newman, 2010; von Luxburg, 2007).

The method by Newman and Girvan (2004) is based on betweenness centrality. In a given network, their algorithm removes the links with the lowest betweenness score until the graph falls apart into two pieces. The procedure can be repeated with the remaining subgraphs up to the desired level of partitioning. This algorithm works fine with networks of all sizes.

The algorithm by Rosvall and Bergstrom (2008) is an approach based on information theory. It detects communities by optimizing the path that an imaginary 'random walker' would take through the network. The problem of clustering is then equivalent to finding an efficient description of his path.

A known problem of graph partitioning is that communities often overlap. Palla et al. (2005) try to deal with this problem with their 'clique percolation' approach, which allows to detect overlapping communities in networks.

1.3.6 Correlation-Based Networks

Networks can be used to describe all kind of systems, what is needed is a definition of the edges and the vertices. Empirical networks can sometimes be observed, but often they have to be derived from latent variables. Edges can be described as connected if they show some kind of proximity in time or space. Networks can also be derived from patterns of communication, reference, or pure coexistence (see da Rocha, 2011). Networks that are based on correlation, for example of time-series, are only recently gaining more attention (see Tumminello et al., 2007; Lacasa et al., 2008).

Figure 1.3 shows how proximity (or similarity) can be inferred from financial market time series. The plot is based on the returns time series of the largest German publicly listed firms on a daily basis for the years 2008–2009. We can calculate the matrix of correlation coefficients for all time series and assign a color coding to the correlation coefficients. The matrix has been sorted such that firms with similar correlations coefficients are closely together and that overall correlation is decreasing top to bottom. We observe that the correlations differs significantly and that at least two groups seem to exist which are more correlated which each other than with the rest of the market. The correlation coefficients can then also be interpreted as weights or distances of the firms in a network. For more details see Section A in the Appendix and the work in Chapter 4.

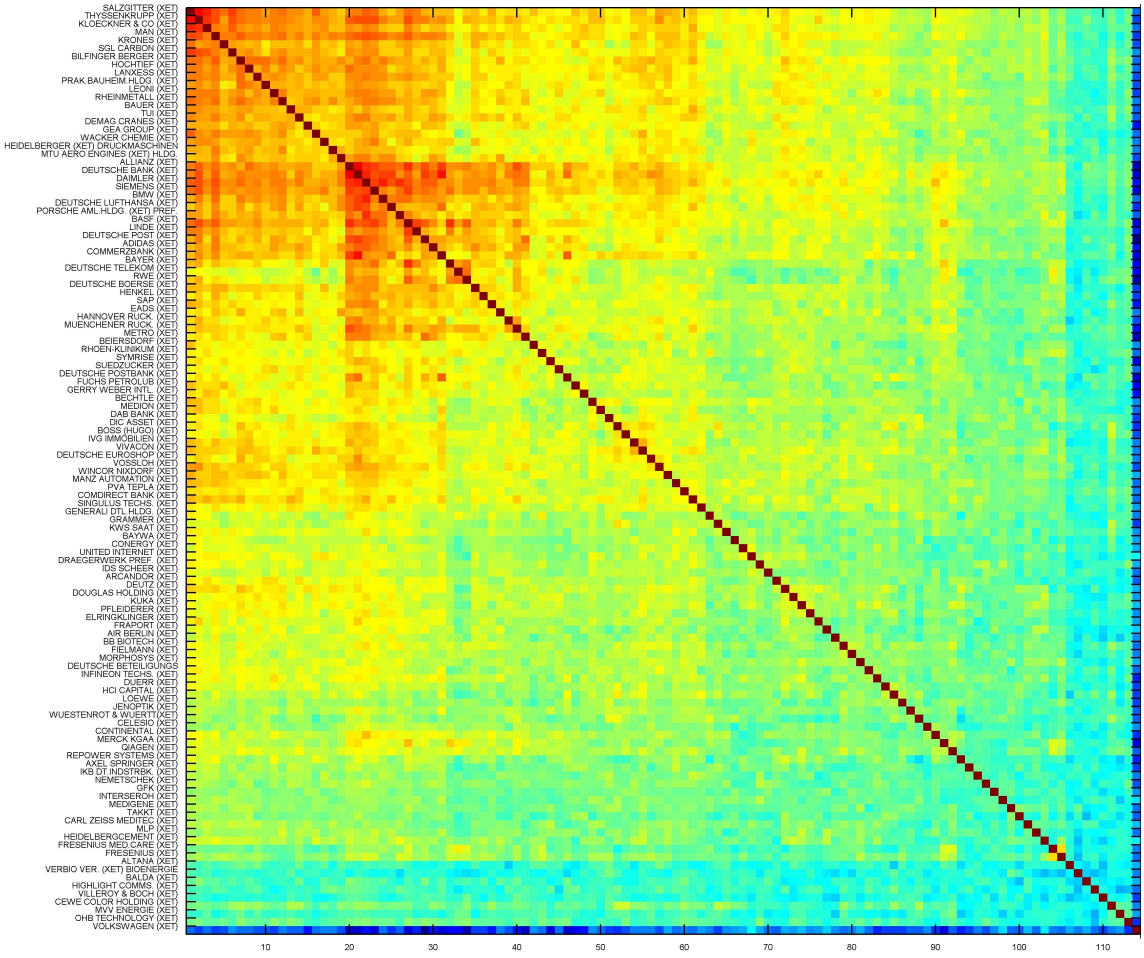

Fig. 1.3: Correlation of stock returns

The matrix is ordered according to the outcome of a dendrogram clustering algorithm. The strength of the correlation is given by a color code from 0 (dark blue) to 1 (red).

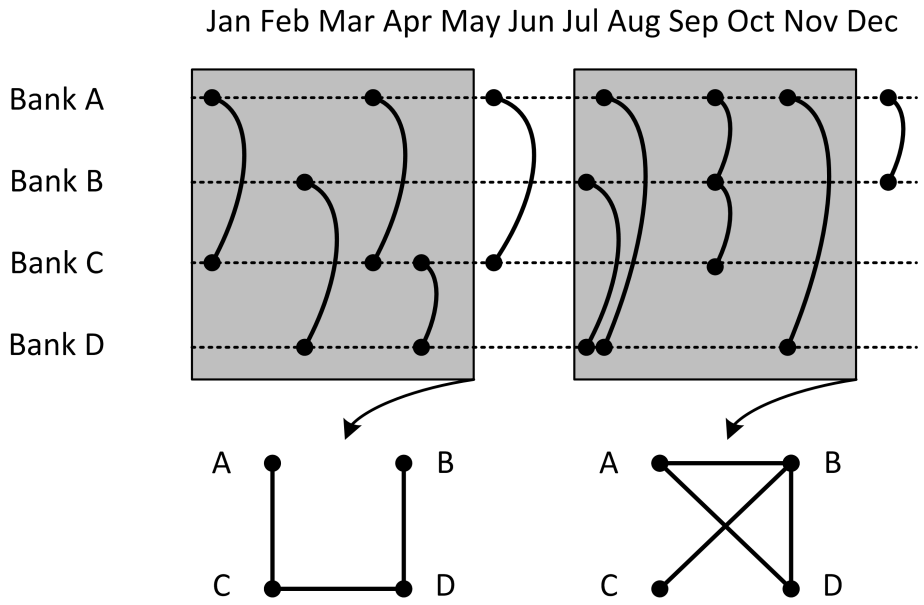

Fig. 1.4: Temporal network
The top panel shows the engagement of banks in the overnight loan market in a stylized example. A bilateral contract is represented by an arc between the dotted lines. The bottom panels show the resulting networks that emerge trough interactions between banks in a time window illustrated by the gray boxes. The example shows that the resulting network critically depends on the position and length of the time window.

1.3.7 Temporal Networks

A still relatively new topic in network science are temporal networks (also called dynamic networks). Holme and Saramaki (2012) stress that one has to account for the fact that links are not necessarily active continuously. A simple example from an economic setting in shown in Figure 1.4. The nodes in this network are banks which trade loans between each other. While the banks will exist for a rather long time, the links between each other change on a high frequency. The network that we can infer from these loan contracts will depend on the time window.

In choosing an appropriate time window we are faced with trade-offs. While general features of the network structure only become visible when we observe it over a long time window, dynamics of the networks might become difficult to identify. On short time scales networks typically show a high degree of randomness in connections, but the dynamics of the micro-structure become observable. We will extend on this topic in Section 5.

1.4 Fault Lines

The interest in networks in economics has increased noticeably with the financial turmoil of 2008. Suddenly, it was evident to most economists that much of the mechanism that transfered the financial crisis from the U.S. housing market into almost every other country can be described as a network effect. Even more, the relationships between banks and other financial institutions, their ability of domino-like collapse fostered by bilateral exposures, resembles a network. The concept of *financial contagion* has been on the agenda for some time but has not gained much popularity besides the article by Allen and Gale (2001), who discuss the effect in a small-scale model. Empirical studies on the stability of the banking system have been performed for the Italian market by Iori et al. (2008) and for the U.S. by Soramäki et al. (2007). These studies gained some interest from regulators and central banks, however, it has to be noted that most of this work stems from the interdisciplinary physics community.

Most contributions to network science from economists have their roots in game theory. In this context, it is discussed, why two individuals should initiate a link between each other (see Jackson and Wolinsky, 1996) and which network configurations are stable, given that there is some benefit from a connection and some cost of upkeep in a game of link formation. According to Bala and Goyal (2000), 'stable' structures resulting from such games are circles or fully connected networks.

Even if some results from this kind of research are very interesting, it is easily noticed that most of their methods have never spilled over to researchers in other disciplines. The reason for this seems to be that in the mean time, many stylized facts of social and economic networks have been pinned down. The networks, however, that are the result of the before mentioned 'microapproaches' do not resemble these stylized facts. They mostly do not have a power law degree distribution, they do not show clustering, and above all, they are mostly very small.

I hope that the research presented in the following chapters is a small step of bringing economic research on networks closer to the interdisciplinary community which has established over the last 15 years.

1.5 The Chapters in Brief

Networks and Herding

Herding models have been developed to explain the joint behavior of interacting individuals. The model presented here is based on the model of Kirman (1993). It

describes the switching of a population of individuals between two groups. While the original model uses an aggregate description of the system, where all of its individuals are identical, Chapter 2 provides a setting where individuals are given different weights, and where the network structure between actors is varied. The results obtained from the simulations hint at problems associated with the concentration of investment decisions. The main contribution of this work is to show that hierarchical networks not only warrant non-Gaussian properties for any system size, but also lead to an increase in system-wide volatility. Viewed from this perspective, the mere existence of institutional structures like managed funds, which essentially correspond to hierarchical networks, would represent a source of financial volatility.

Board Networks

Chapter 3 deals with the evolution of the network of German companies. Board director who serve on more than one board connect the respective firms for which they work. Directors on the other side are connected by working for the same company. We examine the bipartite graphs of the German corporate boards in 1993, 1999 and 2005, and identify cores of directors who are highly central in the entire network while being densely connected among themselves.

Although mergers and acquisitions have reshaped large part of these companies, and although corporate governance policy on multiple mandates has changed, the statistical patterns of this network have been maintained. The dynamic analysis of links and the selection of new board members suggests that the recruitment decisions of new managers follows a strategy that explains the prevalence of a stable cluster in the network of firms.

The Network of International Stock Markets

In this chapter we start out by examining the dynamics of the correlation structure in six different stock markets. These markets are the U.S., the U.K., Japan, Germany, China and India. We find that the correlations within most of these markets have increased over time. Moreover we find that bursts of strong correlation seem to happen jointly in different markets. We try to quantify these meta-correlations over the period from 2000–2010. The results suggest that these meta-correlations are helpful to identify spill-overs of market stress better than a pure analysis of stock index comovements. Further our findings indicate that the growing volatility in financial markets is not necessarily a result of mutual foreign influence, but that also the separate markets have become more correlated internally.

The Network of Italian Banks

In the last chapter we analyze the Italian interbank loan market during the time of 1999–2010. The analysis of net trade flows shows a high imbalance caused by a few large net borrowers in the market. The trading volume shows a significant drop starting in 2007 and accelerates with the Lehman default in late 2008. The network, based on trading relationships, is very dense, hence we try to identify strong links by looking for preferential lending relationships expressed by discounts in the loan rate. Furthermore, we estimate the dynamics of credit spreads for each bank and find that economically significant spreads for the overnight market only developed in 2010. The analysis of bilateral loan relationships reveals that in the pre-crisis era large net borrowers used to borrowed at a slight discount. In the post-Lehman era borrowers with large net exposures paid more than the average market rate, which shows that the risk evaluation of market participants has changed considerably

1.6 Note on Joint Work

Parts of the material presented here are the result of joint work with other researchers. The network model in Chapter 2 was a joint work with Simone Alfarano and Mishael Milaković. The analysis of the board network in Chapter 3 was joined work with Laura Birg, who contributed the dataset, and Mishael Milaković, with whom I developed the paper. The analysis of stock returns in the Chapter 4 is joined work with Dror Y. Kenett, the resulting paper was co-authored by Eshel Ben-Jacob and Thomas Lux.

2. INSTITUTIONAL HIERARCHY AND VOLATILITY IN FINANCIAL MARKETS

2.1 Introduction to Herding Models

Financial time series exhibit ubiquitous non-Gaussian statistical regularities across different countries, assets, and time frequencies. The two most prominent features concern the fluctuations in the prices of financial assets, which exhibit heavy tails and clustered volatility (see, e.g., Cont, 2001; Pagan, 1996). From a statistical point of view, the prevalence of non-Gaussian distributions in returns and their volatilities testifies to the importance of long-range correlations, which ultimately prevent the application of the Central Limit Theorem (CLT). Traditional finance has paid little, if any, attention to the origins of these statistical regularities and to the possibly most challenging question implied by the violation of the CLT: how does a complex system like the financial market actually allow for a large scale coordination of the trading positions among millions of agents? The established literature on informational cascades (see, e.g., Banerjee, 1992; Bikhchandani et al., 1992; Chamley, 2004) does not address this question because it considers a static, sequential Bayesian updating approach with a constant 'true' state of the world and lacks any connection to the stylized facts of financial returns. The three major strands of the agent-based finance literature, on the other hand, argue in unison that it is precisely the perpetually alternating coordination of trading strategies over time that is responsible for the stylized facts of financial returns. Yet each of the approaches has to deal with its own set of problems.

Percolation models of herd behavior exploit the properties of well known critical systems from the statistical physics literature (see, e.g., Cont and Bouchaud, 2000; Iori, 2002; Bornholdt, 2001; Stauffer and Sornette, 1999) but rely on carefully adjusted model parameters near criticality to produce non-Gaussian statistics, en-

tirely leaving open how or why a financial market composed of millions of agents could self-organize into (and remain in) such a critical state. The second strand of models follows the seminal work of Brock and Hommes (1997) where agents interact globally rather than locally, namely through the price system and public information about the performance of strategies that is subject to noise (see, e.g., Hommes, 2006; Chang, 2007). The drawback of this class of models is that they need a careful fine-tuning of their 'signal-to-noise ratio' around unity in order to resemble the stylized facts. Finally the third strand, and starting point of the present paper, is inspired by entomological experiments concerning ants' foraging behavior that Kirman (1991,9) utilized to propose a stochastic herding model of opinion formation among financial investors. These models endogenously create swings and herding behavior in aggregate expectations through *social agent interaction*, while the stationary distribution of the stochastic process of opinion formation describes the *statistical equilibrium* of the model.

The 'ant model' has been reasonably successful in replicating the statistical features of financial returns, but Alfarano et al. (2008) have shown analytically that Kirman's original model suffers from the problem of *self-averaging* or *N-dependence*:[1] the model's ability to replicate the stylized facts vanishes for a given parametrization when the system size N increases, a quite common feature in agent-based models that has received relatively minor attention so far (see, e.g., Aoki, 2008; Egenter et al., 1999; Lux and Schornstein, 2005). Alfarano and Milaković (2009) establish a direct link between N-(in)dependence and the communication network among agents in a generalized version of Kirman's original model. They show that the model is immune to self-averaging if the relative communication range of agents remains unchanged under an enlargement of system size. Interestingly and rather counter-intuitively, other network features like the functional form of the degree distribution, the average clustering coefficient, the graph diameter, or the extent of assortative mixing have no impact on the N-dependence property. Put differently, the average number of neighbors per agent has to increase linearly with the total number of agents N in order to overcome the problem of self-averaging in the generic herding model. Among prototypical network structures such as regular lattices, small-world, or scale-free networks (see, e.g., Newman, 2003), it is only the random graph with constant linking probability that exhibits this feature, yet random graphs are hardly ever a realistic representation of socio-economic communication networks.

After all, the results of Alfarano et al. (2008) and Alfarano and Milaković (2009)

[1] Aoki utilizes the terms *(non) self-averaging* in lieu of N-(in)dependence, and we will subsequently use both terms interchangeably.

establish the model's behavior when the number of agents tends to infinity, at the same time illustrating that simple proto-typical network structures (with the exception of the empirically unsatisfactory random graph) cannot overcome the problem of N-dependence. The present paper builds on these insights and investigates whether a certain class of core-periphery networks might be capable of overcoming the self-averaging property of the original model. Here we consider a central network with bi-directional links between *core agents* or *opinion leaders* on one hand, and a relatively large number of uni-directionally linked *followers* in the periphery on the other. We vary the number of followers per core agent by randomly drawing from various distributions, and study the aggregate behavior of system-wide opinion dynamics under an increasing dispersion in the number of followers. In essence the hierarchical network corresponds to a weighted version of the original model. As we argue below, the weighted version is a reasonable first approximation of the institutional structure of financial fund investment. The central idea is that many investors effectively transfer control over investment decisions to fund managers who in turn are socially interacting, with the opinions of some fund managers carrying greater weight than others, for instance because they manage larger funds or have performed more successfully in the past. It turns out that the analytical mean-field prediction used in Alfarano and Milaković (2009) now significantly underestimates the volatility in system-wide opinion dynamics. The key implication of this result is that behavioral heterogeneity among interacting agents is not, as previously thought, the exclusive source of endogenously arising volatility in agent-based herding models, but that the hierarchical structure of fund investment is an important auxiliary source of financial volatility.

We take the position that investing in the presence of (actively managed) financial funds basically corresponds to the hierarchical core-periphery networks we study here. Investors who are not wealthy enough to afford a broadly diversified portfolio of assets, those who participate in retirement plans, or those who simply feel that they lack the skills or time to make investment decisions often invest in some type or other of managed fund. Effectively such agents, who correspond to followers in the periphery of the network, transfer their wealth to the fund managers in the core, and ultimately allow those to make decisions for them. If fund managers socially interact with their peers, and empirical evidence by Hong et al. (2005) and Wermers (1999) strongly suggests that this is indeed the case, we arrive at the core-periphery networks that we study in this paper.

Essentially, core-periphery networks will lead to an increase of system-wide volatility because fluctuations in a disproportionately small but central part of the network

are amplified on a system-wide level. Therefore it seems rather ironic that investors who want to 'play it safe' by investing in a variety of managed funds will actually end up increasing system-wide volatility if they delegate investment decisions to herding-prone fund managers.

2.2 Generic Herding Model

In a prototypical interaction-based herding model of the Kirman type, the agent population of size N is divided into two groups, say, X and Y of sizes n and $N-n$, respectively. The time evolution of the group sizes is modeled as a Markov chain, characterized by a pair of transition rates that are sometimes also referred to as birth and death rates. Depending on the particular financial market framework, the two groups are typically labeled as fundamentalists and chartists, or optimists and pessimists, or buyers and sellers. The basic idea is that agents change state for personal reasons or under the influence of the *neighbors* with whom they socially interact during a given time period. The transition rate for an agent i to switch from state X to state Y in the Markov chain is

$$\omega_i^- \equiv \rho_i(X \to Y) = a_i + \lambda_i \sum_{j \neq i} D_Y(i,j), \tag{2.1}$$

where a_i governs the possibility of self-conversion due to idiosyncratic factors, e.g. the arrival of new information, while λ_i governs the interaction strength between i and its neighbors. The function $D_Y(i,j)$ is an indicator function serving to count the number of i's neighbors that are in state Y,

$$D_Y(i,j) = \begin{cases} 1 & \text{if j is a Y-neighbor of i,} \\ 0 & \text{otherwise,} \end{cases} \tag{2.2}$$

hence the sum captures the (equally weighted) influence of the neighbors on agent i. Symmetrically, the transition rates in the opposite direction are given by

$$\omega_i^+ \equiv \rho_i(Y \to X) = a_i + \lambda_i \sum_{j \neq i} D_X(i,j) \ . \tag{2.3}$$

Let $a = \sum_i a_i/N$ and $\lambda = \sum_i \lambda_i/N$ denote the averages of the behavioral parameters over agents, and let D denote the average number of neighbors per agent. If all links are bi-directional, $\lambda_i > 0 \forall i \in \{1, \ldots, N\}$, a mean-field argument (see Alfarano and Milaković, 2009) shows that the transition rates for a single switch on

the aggregated system-wide level are

$$\omega^{-} = n \left(a + \frac{\lambda D}{N}(N - n) \right), \tag{2.4}$$

for a switch from X to Y, and symmetrically

$$\omega^{+} = (N - n) \left(a + \frac{\lambda D}{N} n \right), \tag{2.5}$$

for the reverse switch. An important result of the mean-field approach is that the *relative communication range* D/N ultimately determines whether the Markov chain is self-averaging or not. In the jargon of Alfarano et al. (2008), the non self-averaging case corresponds to "non-extensive" transition rates with a constant relative communication range, while the "extensive" transition rates, as in Kirman's original model, lead to self-averaging and hence to counter-factual statistics of returns.[2] Notice that non-extensive transition rates depend on the respective *occupation numbers* n and $N-n$, while extensive transition rates depend on the *concentrations* n/N and $(N-n)/N$ of agents in the opposite state, and therefore on the average communication range per time period in the network. This apparently minor modification has a crucial impact on the aggregate properties of the herding model, as illustrated in Figure 2.1. Hence, in contrast to Kirman's original model, the generalized transition rates (2.4) and (2.5) illustrate that network structure matters because the average number of neighbors explicitly enters the transition rates.

At any time, the *state of the system* refers to the concentration of agents in one of the two states, say, $z = n/N$, which can be treated as a continuous variable for large N. None of the possible states of $z \in [0, 1]$ is an equilibrium in itself nor are there multiple equilibria in the orthodox economic sense. Equilibrium rather refers to the stationary distribution of the birth and death process (2.4) and (2.5). The distribution, that is the statistical equilibrium, describes the proportion of time the system spends in state z and is known to be a Beta distribution (see, e.g., Alfarano et al., 2008; Alfarano and Milaković, 2009, for a detailed derivation of the following results),

$$p_e(z) = \frac{1}{B(\epsilon, \epsilon)} z^{\epsilon - 1} (1 - z)^{\epsilon - 1}, \tag{2.6}$$

where $B(\epsilon, \epsilon) = \Gamma(\epsilon)^2 / \Gamma(2\epsilon)$ is Euler's Beta function. The qualitative behavior of the process is parsimoniously encoded in the adimensional shape parameter ϵ of the

[2] The next section explains in more detail how the Markov chain typically enters Walrasian models of the financial market.

distribution

$$\epsilon = \frac{aN}{\lambda D}\,. \tag{2.7}$$

When $\epsilon < 1$, the distribution is bimodal with probability mass having maxima at $z = 0$ and $z = 1$. For $\epsilon > 1$ the distribution is unimodal, and in the "knife-edge" scenario $\epsilon = 1$ the distribution is uniform. The mean $E[z] = 1/2$ is independent of ϵ but the system exhibits very different characteristics depending on the modality of the distribution. In the bimodal case, the system spends least of its time around the mean, instead mostly exhibiting very pronounced herding in either of the extreme states, as illustrated in the top panel of Figure 2.1. Finally, the variance of z,

$$Var(z) = E(z^2) - E(z)^2 = \frac{1}{4(2\epsilon + 1)} = \left[4\left(\frac{2aN}{\lambda D} + 1\right)\right]^{-1}\,, \tag{2.8}$$

is known to be a convenient summary measure of the model properties with respect to an enlargement of system size. If the variance of z remains constant (or even increases) when the system is enlarged, the leptokurtosis and volatility clustering of returns will be preserved in a standard Walrasian model of market clearing. A decreasing variance under enlargement of system size, on the other hand, is characteristic of self-averaging and thus leads to counter-factual Gaussian properties of returns, as shown in the bottom panel of Figure 2.1 and explained in more detail in the following section.

2.3 Financial Market Framework

For the sake of completeness, we briefly discuss how the Markov chain of the previous section would enter into a parsimonious model of an artificial financial market with interacting heterogeneous agents, where it is typically used as a metaphor of information diffusion among investors (see, e.g., Kirman, 1991,9; Alfarano et al., 2005; Alfarano and Lux, 2007; Alfarano et al., 2008; Alfi et al., 2009; Irle et al., 2011, for more realistic or detailed implementations). Suppose that market participants are divided into two groups: the first group is populated by N_F *fundamentalists*, who buy (sell) assets when the price is below (above) its fundamental value P_F. Their excess demand for assets is given by $ED_F = N_F\gamma_F \log(P_F/P)$, where $\gamma_F > 0$ designates the sensitivity to deviations between the fundamental value and the market price P. Without loss of generality, the fundamental price is assumed to be constant over time. The second group is populated by N_{NT} *noise traders*, who are essentially driven by herd instincts in their investment strategies. Depending on their expectations of future price movements, noise traders can be either *optimists (subscript*

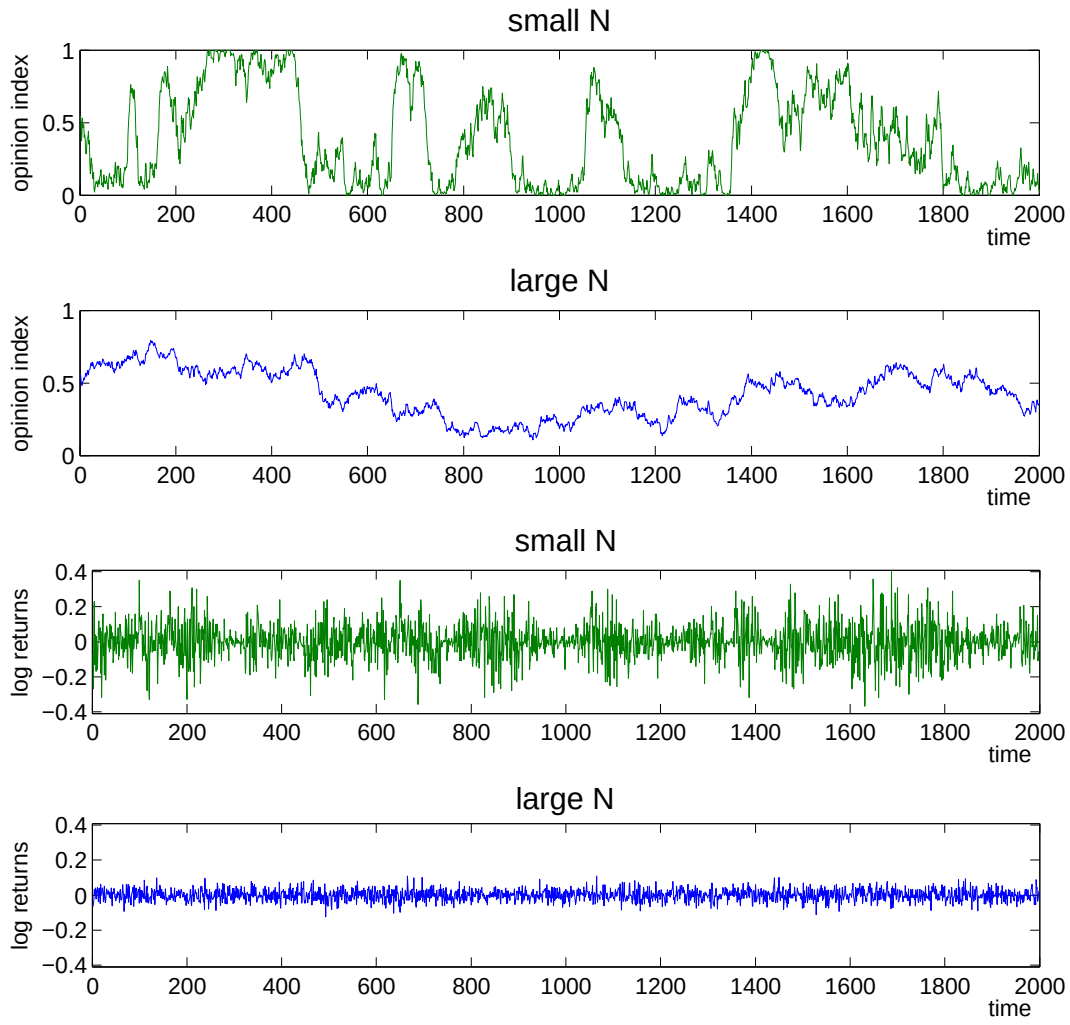

Fig. 2.1: Opinion dynamics in the herding model
The two panels on the top illustrate the time evolution of aggregate opinion dynamics measured as the fraction of agents in one of the two states, say, $z = n/N$ (top panel $N = 500$, $a = 0.5$, $\lambda = 1$, $D = N$; second panel $N = 10000$, $a = 0.5$, $\lambda = 1$, $D = 500$). The two panels on the bottom exhibit the corresponding time series of returns generated from a Walrasian pricing function, as for instance in Eq. (2.13) of Section 2.3 (with $\kappa = 1$), where the level of excess demand depends on z. The bottom panel illustrates that an enlargement of system size under extensive transition rates will lead to counter-factual Gaussian returns and absence of volatility clustering.

O) or *pessimists (subscript P)*. The excess demand of the noise trader group will be proportional to their aggregated state, $ED_{NT} = \gamma_{NT}(N_O - N_P)$, where N_O and N_P are the numbers of optimists and pessimists, respectively, with $N_{NT} = N_O + N_P$. The parameter $\gamma_{NT} > 0$ governs the impact of the noise traders' aggregate mood on the asset price. In line with the notation of the previous section, ED_{NT} can be parameterized as a function of $z = N_O/N_{NT}$, that is the fraction of optimists over

the total number of noise traders

$$ED_{NT} = \gamma_{NT} \cdot N_{NT}(2z - 1) \ . \tag{2.9}$$

While the share of fundamentalists and noise traders is constant over time (so there are no transitions between those two groups), switches from optimism to pessimism and vice versa do take place among the noise traders, and are governed by the Markov chain detailed in Section 2.2. Hence noise traders change their opinions about the future prospects of an asset for idiosyncratic reasons or because of a tendency to follow the majority opinion of their peers.

Assuming sluggish price adjustments by a market maker in the presence of excess demand, one typically formalizes the price dynamics as

$$\frac{dP}{P \cdot dt} = \theta \cdot ED = \theta[ED_F + ED_{NT}] \ , \tag{2.10}$$

where θ is the speed of price adjustment. As an approximation to the resulting disequilibrium dynamics, one may consider instantaneous market clearing ($\theta \to \infty$) or equivalently a Walrasian scenario ($ED = 0$) and solve (2.10) for the equilibrium price

$$P = P_F \exp\left[\frac{N_{NT} \cdot \gamma_{NT}}{N_F \cdot \gamma_F}(2z - 1)\right] = P_F \exp\left[\kappa(2z - 1)\right] \ , \tag{2.11}$$

where

$$\kappa = \frac{N_{NT} \cdot \gamma_{NT}}{N_F \cdot \gamma_F} \ . \tag{2.12}$$

Given a realization of the process z, we can see from (2.11) that periods of undervaluation (compared to the fundamental price) will alternate with episodes of overvaluation. In the first case the majority of noise traders are pessimists, while in the second case most are optimists.

Finally, returns are typically defined as the log-increment of prices

$$r(t, \Delta t) = \log\left(\frac{P(t + \Delta t)}{P(t)}\right) = \kappa \Delta z \ , \tag{2.13}$$

and the third panel of Figure 2.1 shows the corresponding time series of log-returns for a 'small' number of traders ($N_F = N_{NT} = 500$), visually already indicating a leptokurtic return distribution and volatility clustering. In fact, Alfarano and Lux (2007) have shown that this very simple model quantitatively reproduces the stylized facts of financial returns with (i) a fat-tailed distribution of returns, (ii) an absence of auto-correlation in raw returns, and (iii) a slowly decaying positive

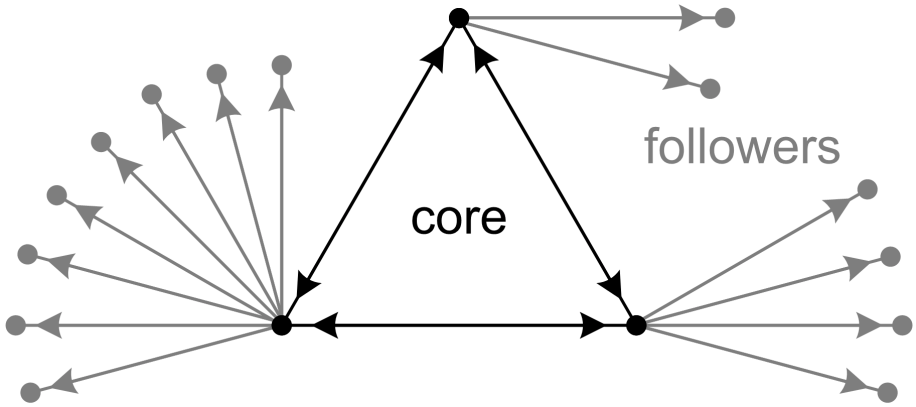

Fig. 2.2: A stylized representation of a hierarchical core-periphery network
Core agents (black; bi-directional links) influence each other in their opinion formation, while peripheral followers (grey; uni-directional links) simply mimic their respective core agents. This basically corresponds to a weighted version of Kirman's original model.

auto-correlation in even functions of returns, i.e. volatility clustering. Increasing the number of agents, for instance to $N_F = N_{NT} = 10,000$ (keeping $D = 500$) as shown in the bottom panel of Figure 2.1, turns the abrupt mood swings in z into much smoother paths and results in counter-factual Gaussian fluctuations of returns.

2.4 Network Hierarchy and Core Weights

Essentially, we know that the relative communication range D/N in the transition rates (2.4) and (2.5) determines whether or not the model is self-averaging. Alfarano and Milaković consider prototypical networks with bi-directional links, in particular regular lattices, random graphs, small-world networks of the Watts and Strogatz (1998) type, and the scale-free networks of Barabási and Albert (1999). Among these it is merely the random graph that exhibits a constant relative communication range since in that case $D = N\,\ell$, where ℓ designates the constant linking probability among agents in the random graph. On the other hand, D/N approaches zero for an increasing system size in the other network structures, unless one appropriately changes the respective parameters in the generating mechanisms of these networks.

From a socio-economic viewpoint, however, it is not at all clear how or why a complex system composed of many interacting agents could possibly coordinate an appropriate system-wide change in these parameters. The random graph is not a convincing mapping of socio-economic relationships either, because it implies that the average connectivity of agents increases linearly with system size.[3] Now sup-

[3] A simple example illustrates this implausibility. Suppose you live in Smallville, where you

pose instead that N core agents are still bi-directionally linked among themselves, i.e. they still obey the Markov chain in Section 2.2. Additionally, each core agent has a constant number W of followers in the periphery, with uni-directional links emanating from the core to the periphery. Uni-directional linking implies that the state of peripheral followers corresponds to the state of the respective core agents. Then the total number of followers is $W\,N = F$, with a total of $F + N$ agents in the entire network. In this case, the system-wide concentration of agents in state X will be

$$z = \frac{Wn + n}{F + N} = \frac{n(W + 1)}{N(W + 1)} = \frac{n}{N}, \tag{2.14}$$

which just amounts to a relabeling of variables. Put differently, in this special case the system size $F+N$ can be expanded at will by simply adding followers F without encountering the self-averaging problem. Thus we preserve system-wide fluctuations in a population of $F+N$ individuals, although only N socially interacting core agents are responsible for the fluctuations. At the same time, the hierarchical structure avoids the empirically unsatisfactory random graph structure in the entire population that would otherwise be necessary to preserve non self-averaging fluctuations. The assumption of a constant number of followers per core agent, however, is quite artificial and unsatisfactory. Therefore we want to investigate more general core-periphery structures by randomly drawing the number of followers per core agent from various distributions, keeping the total number of followers constant. We examine whether or how the dynamics of z change when the dispersion of followers increases. Notice that the respective numbers of followers now act as *weights* in the opinion formation process of core agents, otherwise we recover the unweighted and already well-understood cases resulting in the large-N limit of the generalized transition rates (2.4) and (2.5). Put differently, we would like to avoid the problem of self-averaging when enlarging the system, but without taking recourse to random graphs. Therefore we turn to core-periphery networks as a stylized representation of the institutional structure of financial markets, and investigate whether these hierarchical networks overcome the problem of self-averaging when the core remains small relative to the periphery.

Figure 2.2 provides a stylized representation of the resulting core-periphery networks that reflect the organizational structure of managed fund investment. On one hand, peripheral agents who invest in managed funds effectively delegate all subsequent investment decisions to fund managers until they decide to withdraw their

closely interact with, say, thirty people. Moving to Metropolis, with a population about three hundred times the size of Smallville, a constant linking probability would imply that you now closely interact with a number of agents on the order of 10^5.

capital again. On the other hand, the fund managers in the core influence each other and are prone to herding effects, as in the empirical findings of Hong et al. (2005) or Wermers (1999). We can also interpret the number of followers per core agent as the size distribution of funds, thereby implicitly assuming that the influence of fund managers on each other's opinion is proportional to the size of the fund they are managing. While we are not aware of evidence that directly supports this assumption, the empirical size distribution of funds does in fact exhibit wide dispersion and leptokurtosis (see, e.g., Gabaix et al., 2006; Schwarzkopf and Farmer, 2008).

2.5 Simulation Setup and Results

It is important to recall that we can study the (non) self-averaging property without actually increasing the number of agents in our subsequent simulations, because the addition of followers amounts to changing core agent *weights*. Notice that adding core agents instead of followers would correspond to the scenario that Alfarano and Milaković (2009) already studied in detail, where the structure of the bi-directional (core) network determines whether the model is self-averaging or not in the large N limit. The introduction of weights, however, prevents a straightforward application of their mean-field technique: when the weights are widely dispersed, the average number of followers per core agent obviously no longer provides a good approximation. Therefore we simulate the opinion dynamics in various core-periphery models, where we increase the dispersion of weights while drawing weights from different distributions, or altering the network structure in the core. We compare the resulting variance of z both to the mean-field prediction and to the variance in another limiting case that we have termed the *independent one-leader scenario* below.[4] After all, the variance of z is a useful summary measure of the different scenarios because we know that if it decreases relative to the mean-field benchmark, the weighted core-periphery networks will still suffer from the problem of self-averaging. If on the other hand the variance of z remains constant, the hierarchical model will be immune to self-averaging.

2.5.1 Network-Adapted Transition Rates

To implement individual transition probabilities, in line with the transition rates (2.1) and (2.3), we first consider the (symmetric) adjacency matrix $E = e_{ij}$ for $i, j \in \{1, \ldots, N\}$ that keeps track of the links or *edges* between core agents, with $e_{ij} = 1$ if

[4] Appendix B.1 contains an analytical treatment of this case.

i and j are neighbors and $e_{ij} = 0$ otherwise.[5] The key element in the implementation of the transition rates is to determine for each agent i the number of neighbors that are in the opposite state, say n_i.

Let $\mathbf{e}(i)$ denote the i-th column of the adjacency matrix E, which basically informs us of who is or is not an i-neighbor. While some of the neighbors will be in the same state as agent i, others will be in the opposite state, and these are the agents that we are interested in when implementing transition rates. To extract the i-neighbors that are in the opposite state, consider the projection matrix $S(i)$ of dimension $N \times N$ that keeps track of the i-neighbors that are in the opposite state: that is, for each i the off-diagonal elements of $S(i)$ are zero, $s_{ij} = 0$ if $i \neq j$, and obviously $s_{ii} = 0$ as well; on the diagonal of $S(i)$ we have $s_{jj} = 1$ if the state of neighbor j is opposite to that of agent i, and $s_{jj} = 0$ otherwise. Then the column vector $\mathbf{k}(i) = S(i)\ \mathbf{e}(i)$ expresses which i-neighbors are in the opposite state, and we finally have $n_i = \mathbf{k}^T(i)\,\mathbf{k}(i)$.

Thus *in the absence of followers* we would posit the transition probability $\tilde{\pi}_i = (a+\lambda\, n_i)\Delta t$ for switching states on the individual level. To ensure that $0 \leq \tilde{\pi}_i \leq 1\,\forall i$, we need $\Delta t \leq 1/(a+\lambda\, n_{max})$, where n_{max} designates the number of neighbors of the node(s) with the highest degree in the network. Since an agent can be connected at most to all other agents, we utilize the transition probability

$$\tilde{\pi}_i = \frac{a + \lambda n_i}{a + \lambda N} \tag{2.15}$$

for individual switches, hence agent i's probability to remain in the current state is $0 \leq 1 - \tilde{\pi}_i \leq 1$.

In the presence of followers, we first need to make sure that our simulation results are comparable with the mean-field prediction arising from (2.15), hence the individual transition probabilities need to be adapted to the core weights stemming from the hierarchical network setup. Let the column vector $\mathbf{w}$, with elements w_i, record the number of followers or weights for each core agent i, so $F = \sum_i w_i$ is the total number of followers in the network, and let $\langle f \rangle = F/N$ be the average number of followers per core agent. Now we are interested in the weighted sum of core agents who are in the opposite state of an agent i, denoted f_i. Since $\mathbf{k}(i)$ describes the i-neighbors that are in the opposite state, the weighted sum of core agents in the opposite state is straightforwardly computed as $f_i = \mathbf{k}^T(i)\ \mathbf{w} = \mathbf{e}^T(i)\ S(i)\ \mathbf{w}$, and the probability p_i to observe a change in the state of agent i in the weighted

[5] By convention, $e_{ii} = 0$, so there are no 'self-loops' in the network.

scenario is now given by

$$\pi_i = \frac{a + \lambda f_i / \langle f \rangle}{a + \lambda N} \tag{2.16}$$

Notice several points about the formulation of the herding term in the numerator of (2.16). First, using the definition of $\langle f \rangle$, we can rewrite it as $f_i / \langle f \rangle = N\, f_i / F$. Since $0 \leq f_i/F \leq 1$, we see that the denominator in (2.16) ensures $0 \leq \pi_i \leq 1 \forall i$. Put differently, since $0 \leq n_i \leq N$, the weighted formulation has the same boundaries as the unweighted one. Second, if all core agents have the same number of followers, we have that $\forall i\, f_i = n_i \langle f \rangle$, so we recover the unweighted original formulation (2.15). Third, the ratio $f_i / \langle f \rangle$ in the sum of (2.16) is a direct measure of the dispersion of core weights, readily illustrating why we should not expect the mean-field approximation to be accurate when the dispersion becomes large.[6]

2.5.2 Simulation Setup

In our simulations, we fix the number of core agents at $N = 500$ and draw the number of followers from Gaussian, uniform, exponential and Pareto distributions with mean $\langle f \rangle = 1000$ such that each randomly drawn number is rounded to the nearest (absolute) integer value. Let N^+ and F^+ respectively denote the number of core agents and followers that are in the optimistic state. The system-wide concentration of agents in the optimistic state is now $z = (N^+ + F^+)/M$, where $M = N + F$ is the total number of agents. In all scenarios we set the parameters a, λ in such a way that $\epsilon = 1$, which yields a uniform distribution of z with $Var(z) = 1/12 \approx .083$ when the mean-field approximation applies. One 'sweep' of the system corresponds to one round of sequential updating of all core agents in the system, thus requiring N steps per sweep, and each simulation run consists of half a million sweeps. Finally, we successively increase the standard deviation σ_f of the respective distribution while ensuring that the weights remain positive and record the variance of z for each sequence of increasing σ_f . Recall again that when $Var(z)$ increases (decreases) above (below) the "knife-edge" value of one twelfth, this implies that the distribution of z transforms from a uniform to a bimodal distribution with non-trivial averaging behavior (unimodal distribution with trivial self-averaging).

2.5.3 Core Structure and One-Leader Benchmark

The simulation results for a fully connected core are magnified in the inlay of Figure 2.3. When core weights are not overly dispersed, the mean-field prediction still performs well, but pronounced deviations ultimately do occur as the dispersion

[6] The source code of the algorithm can be found in Appendix B.2.

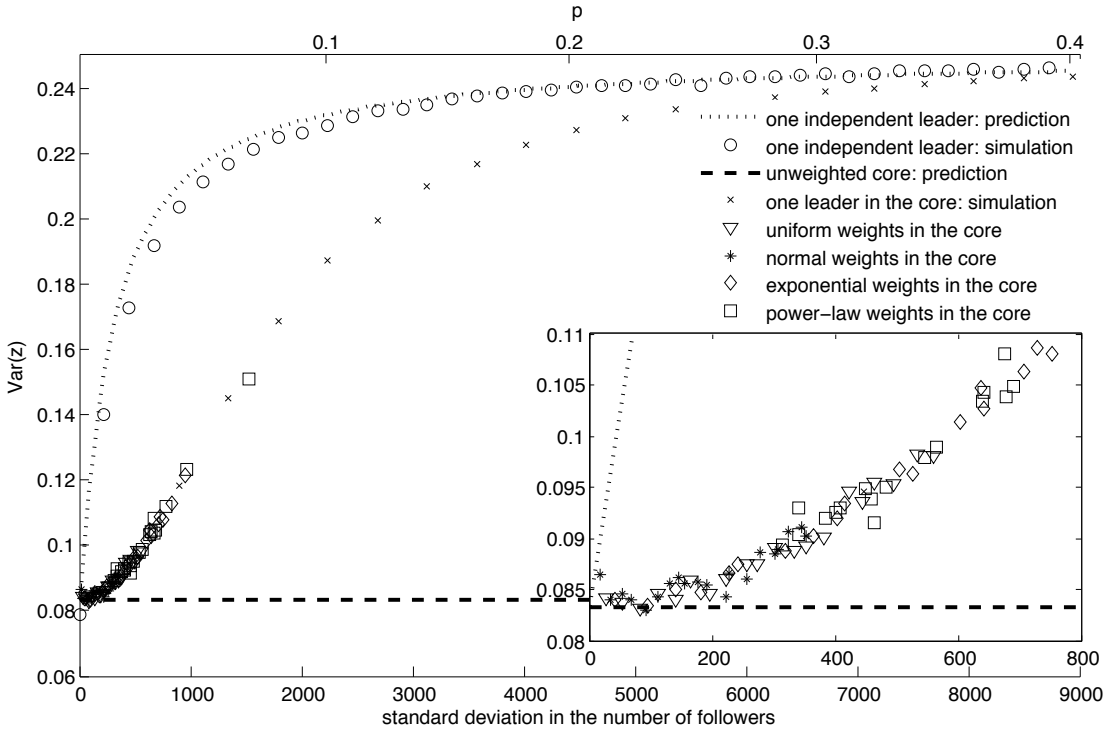

Fig. 2.3: The impact of increasing heterogeneity in core weights
The simulations (with a fully connected core $D = N$ and behavioral parameters $a = \lambda = 1$, so $\epsilon = 1$) demonstrate that rising heterogeneity leads to increasing volatility, irrespective of the particular distribution from which the weights are drawn.

of weights increases. Intuitively, this happens because a few core agents become increasingly influential in the opinion formation dynamics of the system, thereby increasing the time during which the system is near one of the two extreme states. Hence hierarchical networks are not only immune to self-averaging, but actually *amplify* volatility in the system. It is noteworthy that the outcome does not depend on the functional form of the distribution from which the weights are drawn.

In order to determine the limit of the variance amplification, we consider an extreme case that we label as the *one-leader* scenario. In this case, we allocate an equal number of followers to all but one core agent (the leader), who is then assigned a weight such that the average number of followers corresponds again to $\langle f \rangle = 1000$. Let $1/N < p < 1$ denote the fraction of followers that are connected to the one-leader, such that the leader has pF followers, and assume that the remaining $(1-p)F$ followers are allocated with equal weight among the $N-1$ remaining core agents. When $p = 1/N$, all core agents have the same number of followers, F/N. Conversely when $p \to 1$, the system is almost entirely represented by the leader. In

each new simulation run, we successively shift a larger number of followers to the leader by increasing p. The result is shown in Figure 2.3, with $Var(z)$ intuitively approaching a value of one-fourth since the leading agent will represent almost the entire system by itself, and cannot be influenced by others anymore. Thus its actions will consist of random switches between the two states, while the few remaining core agents mimic the leader's behavior. Hence the system spends half its time in one state and half in the other, resulting in a variance of one-fourth.

In addition, we present some analytical results for the related benchmark scenario of an *independent* leader who in a sense acts "outside" the core network: in contrast to the preceding one-leader scenario, the independent leader now does not care about the state of other core agents. We explain the details of this benchmark setup and how we simulated it in Appendix B.1. Figure 2.3 also illustrates the benchmark outcome of both the prediction and the simulation for the independent leader scenario. In summary, the figure establishes two central results. First, the mean-field approximation works reasonably well if the dispersion in the number of followers is relatively small, that is when the core is fairly homogeneously weighted. Second, a heterogeneously weighted core actually leads to increasing system-wide volatility, asymptotically approaching the independent one-leader scenario, which constitutes the most extreme degree of heterogeneity. The heterogeneity of core agents thus represents an auxiliary source of fluctuations in the model. Basically, the simulations establish the model's behavior between the mean-field and independent leader benchmarks, illustrating that the core-periphery setup quickly diverges from the mean-field approximation and asymptotically approaches the independent leader benchmark. The social interactions among core agents are crucial for overcoming N-dependence, because a vanishing herding propensity would lead to independently acting core agents, and thereby to a degenerate self-averaging distribution of their aggregate opinion with a sharply peaked mean of one-half. Moreover, if the core was enlarged (instead of the periphery) we would also confront the self-averaging problem, unless the core network was the empirically unsatisfactory random graph. It is therefore the contemporaneous presence of a hierarchical network with a relatively small core, and the social interactions in the core that ultimately overcomes the problem of N-dependence.

2.5.4 Varying the Core Structure

Our previous investigations show that a hierarchical network with a fully connected core not only overcomes the self-averaging problem, but also amplifies volatility. A remaining issue is whether these results are robust with respect to the network

structure in the core itself. On that account, we perform another series of simulations with varying core network structures, and record how the different core networks respond to an increasing dispersion of weights.

For comparison with our previous findings we keep the size of the core fixed at $N = 500$, and construct the following networks in the core: a circle with neighborhood forty, a random network with linking probability of ten percent, and a scale-free network with an average of five thousand links. For the random and the scale-free graph we construct ten different realizations of the core network, and run the simulations again for half a million sweeps, subsequently averaging over the ten respective core realizations. The details of the respective network parametrizations are not crucial, because in each scenario we set $\lambda = 1$ in the transition rates (2.16), and adapt the behavioral parameter a in light of a particular parametrization of D such that the mean-field prediction would again yield a uniform distribution ($\epsilon = 1$). The simulation results in Figure 2.4 demonstrate that core network structure has merely second-order effects on the macroscopic properties of the model. As before, an increasing dispersion of followers increases volatility, while the mean-field prediction holds true if the dispersion of weights is not too large.

We also simulated a very extreme scenario by considering a scale-free graph with deterministically assigned core weights that are proportional to the degree of a core agent. We can think of such a *proportional weights* structure as the asymptotic limit of *positive feedback* effects in the time evolution of the network, for instance if highly central core agents increasingly attract the interest and wealth of investors, or if core agents with a large weight become increasingly connected among their peers in the core. Whatever the ultimate reason might be for observing such a double-weighted hierarchy, it is noteworthy that volatility increases considerably compared to the other scenarios shown in Figure 2.4, even for very small deviations in the number of followers.

2.6 Discussion

Hierarchical core-periphery structures turn out to overcome the problem of N-dependence in probabilistic herding models of the Kirman type. On one hand, this is good news from the viewpoint of the model's asymptotic properties, because one is able to replicate the stylized facts of financial returns with behaviorally heterogeneous agents for any system size, without having to tune any of the behavioral parameters. On the other hand, our findings have somewhat stark implications from the viewpoint of investment strategy, and they also raise pressing new ques-

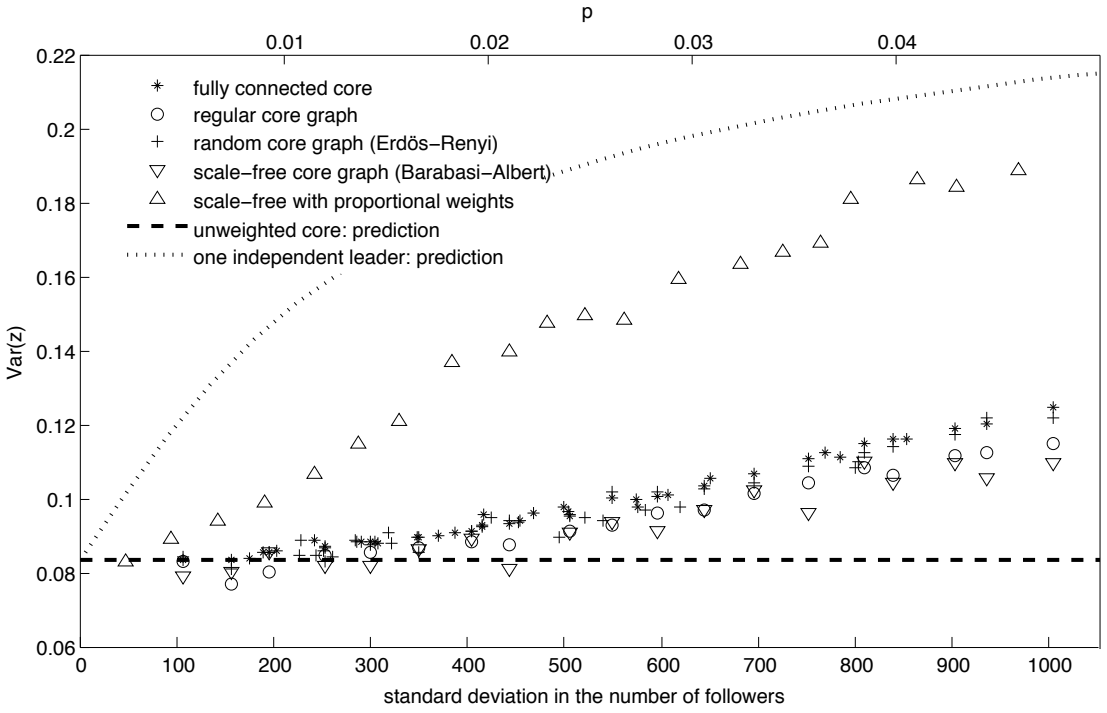

Fig. 2.4: Influence of network structure on volatility
The impact of different core network structures on system-wide volatility has merely second-order effects, except for the "proportional weights" scenario: if the core is a scale-free graph with core weights that are proportional to the degree of each agent in the core, the mean-field approximation immediately fails to produce accurate results and the variance of z rapidly increases, almost doubling compared to the other scenarios where core weights are still randomly assigned when varying the network structure in the core. As before, the simulations were conducted for $N = 500$ agents with $\lambda = 1$, and a and D set in such a way that $\epsilon = 1$.

tions about the origins of hierarchical network structures.

The introduction of hierarchical network structures represents an additional source of volatility on top of the behavioral heterogeneity that has previously been considered as the exclusive source of volatility in social interaction models. If one accepts our premise that hierarchical networks are a useful representation of fund investor relationships in financial markets, then popular and traditional investment advice to 'diversify one's portfolio' has to be judged with caution. Investors who are not wealthy enough to broadly diversify their portfolios, those who participate in funded retirement plans, or those who simply feel that they lack the skills or time to make appropriate investment decisions might very well delegate their investment decisions to institutional investors. But if these fund managers are socially interacting and influencing each other in their investment decisions, as the quoted empirical ev-

idence suggests, this becomes a self-defeating strategy because we have argued that system-wide volatility increases under such circumstances. Put in more provocative terms, all the good intentions of investors to diversify risk can lead to the opposite effect if fund managers are prone to social interaction effects. Moreover, the presence of positive feedback effects in the time evolution of hierarchical networks seems to worsen the situation further, rather than improving it, since positive feedbacks would significantly increase the level of volatility in our simulations.

From the viewpoint of policy-making, our study indicates that a reduction of financial volatility would be facilitated by a shrinking degree of hierarchical organization in financial markets, corresponding to an increasing decentralization of investment decisions. While such advice sounds straightforward in principle, its implementation would most likely be more painful and complex: our results suggest that already very small values of p (or market share for that matter) lead to a sudden and pronounced increase in volatility. Keeping p very close to zero, on the other hand, would more or less imply getting rid of managed funds altogether, which hardly appears to be a feasible option.

3. PERSISTENCE OF A NETWORK CORE IN THE TIME EVOLUTION OF INTERLOCKING DIRECTORATES

3.1 Introduction to Corporate Board Networks

We study the time evolution of German corporate director interlocks between 1993 and 2005, and detect a persistent core of directors who are highly central in the network while being densely connected among themselves. The statistical properties of the network core show little variation over time in spite of significant changes in corporate governance and considerable turnover in the identity of core directors, leading to questions about the mechanisms that are responsible for the origin of a persistent network core.

Traditional research in organization and management science has investigated the influence of shared directorships or ownerships on firm performance, profitability, and corporate strategy, including acquisition behavior, choice of financing, the magnitude and direction of political and charitable contributions, the adoption of poison pill practices, and many more, in fact generating such an abundance of results to warrant several recent surveys on different aspects of the subject (see, e.g., Borgatti and Foster, 2003; Brass et al., 2004; Galaskiewicz, 2007; Provan et al., 2007). Another strand of research, inspired by the interdisciplinary work of Barabási and Albert (1999), has emphasized the statistical properties of corporate networks (see, e.g., Battiston and Catanzaro, 2004; Caldarelli and Catanzaro, 2004; Newman et al., 2001) and concludes that director interlocks exhibit the *small world effect*, whereby the interpersonal distance between any two directors is several orders of magnitude smaller than the number of directors in the network. In addition, Davis et al. (2003) argue that director interlocks are also characterized by a high degree of clustering, typical of the *small world networks* introduced by Watts and Strogatz (1998).[1] Subsequently, however, Conyon and Muldoon (2006) and Robins and Alexander (2004) have shown from different yet complementary viewpoints that the high degree of clustering is present by construction, and should as such not be an unexpected feature in director interlocks. Intuitively, the reason is that directors of the same

[1] See Uzzi et al. (2007) for a review of small world networks in the social sciences.

company are linked by definition to all their colleagues, while the large majority of directors serves only on a single board in the network.

Conventional wisdom thus has it that the *small world effect* typically stems from the presence of 'hubs', i.e. nodes with a large number of links to other nodes in the network, and the degree distribution of nodes has been shown to obey a power law in many complex networks (see, e.g., the surveys by Newman, 2003; Schnettler, 2009). Still, in numerous social contexts the number of links and nodes exhibits a characteristic scale and does not span enough orders of magnitude to be a power law. In addition, the cost of forming a link on the World Wide Web or in an academic citation network is very small compared to the amount of resources that are involved in the hiring of corporate directors. Power-law degree distributions are in a strong combinatorial sense the most likely distributions when links are relatively costless, yet as links become costlier the functional form of the most likely degree distribution becomes an exponential (see Venkatasubramanian et al., 2005). Thus it seems fair to say that power laws are an inadequate or at best imperfect explanation for the small world property of director interlocks.

To understand the origins of the small world effect in director interlocks, we find it instructive to follow the approach of Milaković et al. (2010). They start from the fact that the large majority of directors serves on a single board, and ask whether the observed instances of multiple board membership deviate from a random benchmark. The benchmark assumes that board recruitment decisions are entirely random in the sense that each director is equally likely to obtain an additional board appointment, turning multiple board membership into a sequence of Bernoulli trials. The resulting binomial distribution and the empirically observed distribution display deviations over increasing orders of magnitude in each year of our sample, and it turns out that directors with multiple board memberships are to a very large extent connected among themselves, making them highly central in the overall network. From this viewpoint, the small world property of director interlocks is due to a relatively small number of 'big players' who are densely connected among themselves, thereby forming a core network that substantially shortens the distance between arbitrarily chosen directors in the entire network. While Milaković et al. show the existence of a network core in a more recent year, they lack observations on the time evolution of the board and director networks. One of the main findings of the present paper is that institutional ties among the largest German companies are maintained over time in spite of considerable turnover in the identity of directors. In light of this turnover, it becomes important to understand the origins of a persistent network core, and our analysis suggests that both the reconstruction of broken

ties among large corporations, as well as their preference for recruiting experienced directors with multiple board memberships, are responsible for the time persistence of a network core.

Finally, the idea that a core of director interlocks influences the degree of interest group formation has previously been put forward by Mintz and Schwartz (1981), and several authors have suggested procedures to classify or identify a core of key players in complex networks, both in the social sciences (see, e.g., Borgatti, 2006; Borgatti and Everett, 1999) and in interdisciplinary physics (see, e.g., Holme, 2005). But the existence of a network core also has implications beyond pressure group formation, particularly for a class of diffusion processes sometimes referred to as *duplication in walks* (see, e.g., Borgatti, 2005). An important illustration of such a process is the diffusion of states (e.g. expectations, tastes, opinions, trading positions, etc.) in a system made up of a large number of interacting heterogeneous agents. One can show, perhaps somewhat unexpectedly, that the existence of a core is often sufficient for the system-wide propagation of fashions and fads in such systems (see, e.g., Alfarano and Milaković, 2009; Alfarano et al., 2012), while more traditional network features like average clustering, diameter, small world coefficient, or degree distributions are not. The presence of a hierarchical core-periphery structure can oftentimes lead to system-wide conformity, including the possibility that the social interactions of core agents lead to coordinated "animal spirits" in a system that is several orders of magnitude larger than the size of the core. We believe that the potential implications of our empirical results are best discussed in light of this latter point.

There is quite some evidence that the corporate network, especially in Germany, is in a state of decline. The increased shareholder orientation of companies, the strategic reorientation of big banks, and the decreasing influence of the state in the infrastructure sector are made accountable for this process (see, e.g., Heemskerk, 2007; Beyer and Höpner, 2003). In the remainder of this chapter we will see that this decline is for real, but we also claim that the mechanism which keeps the corporate network alive is still present. After a description of the dataset we will proceed by identifying and comparing cores of directors for the different subsamples in Section 3.3. In Section 3.4 we will analyze how the process of re-wiring throughout the years takes place.

3.2 The Dataset

Our compilation of board composition data aimed for Germany's one hundred largest publicly traded companies in 1993, 1999, and 2005. The thirty largest companies are listed in the German stock index DAX (*Deutscher Aktienindex*), while the next largest companies are listed in the Mid-Cap-DAX, or MDAX. The MDAX was founded in 1996, containing the seventy largest companies that were not included in the DAX, which we also used in the 1993 sample. In 2003, the number of companies in the MDAX was reduced from seventy to fifty, so we used the survivors among the twenty companies that left the MDAX in the 2005 sample, or replaced those that no longer existed with the next largest companies in 2005.

For the purpose of our study, corporate boards consist of executive management (*Vorstand*) and supervisory board (*Aufsichtsrat*). According to the pertinent German legal code, they have to meet at least four times per year (§ 94(3) of *Aktiengesetz*, or *AktG*). Executives are appointed for a maximum of five years, and both appointment as well as potential reappointment need to be approved by the supervisory board (§ 84 *AktG*). In light of the five-year limit, we chose equally spaced intervals of six years to increase the likelihood of observing changes in the composition of corporate boards. We compiled the data by consulting various archives that keep records of the annual reports of these companies, and by writing to companies for whom we could not locate annual reports.[2] The descriptive statistics of our sample, reported in Table 3.2, show a decreasing average board size over time, which is mainly due to M&A activity among very large corporations,[3] and also to the fact that 2005 additions had only about half the sample's average board size in that year.

Let n be the number of directors in a year, and let c be the number of companies in that year. Then the *incidence matrix* $\mathbf{M}$ of dimension $n \times c$, with $m_{ij} = 1$ if director i is on the board of company j and zero otherwise, describes the corporate network in each year. The projection onto directors, $\mathbf{D} = \mathbf{M}\mathbf{M}^{\mathbf{T}}$, is the weighted adjacency matrix of director interlocks. Its diagonal entries equal the total number of board memberships of director i, while non-zero entries off the diagonal of $\mathbf{D}$ represent the weight of a link, showing on how many boards two directors serve together. Symmetrically the projection onto boards, $\mathbf{B} = \mathbf{M}^{\mathbf{T}}\mathbf{M}$, yields the weighted adjacency matrix of company interlocks, its diagonal entries correspond to the board

[2] Three companies in the 1993 sample did not reply to our inquiry, all three of them with relatively minor market capitalization, leaving us with 97 companies in that year.

[3] Dresdner Bank, for instance, was acquired by Allianz in the financial sector, while VEBA and VIAG merged to EON in the utilities industry.

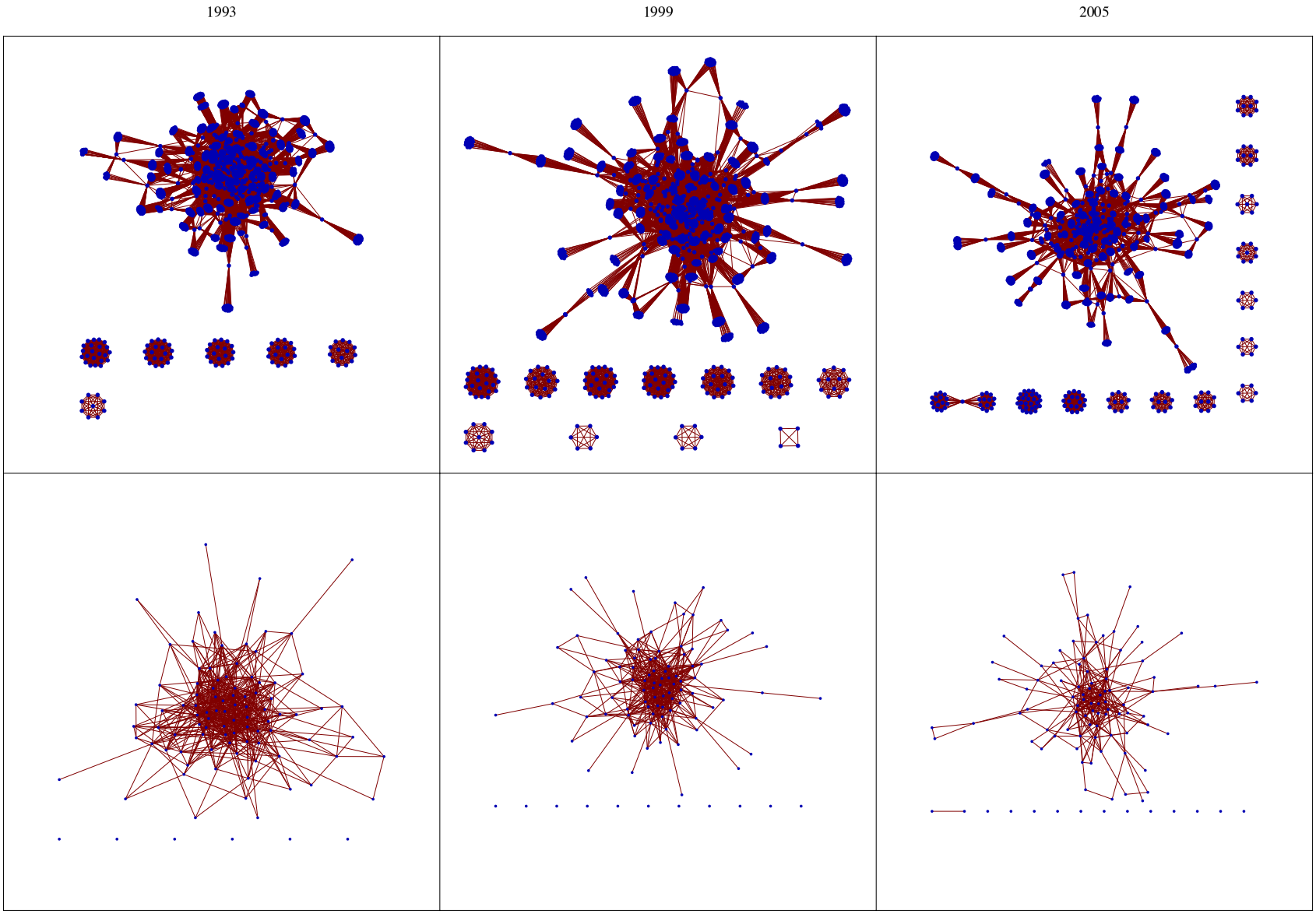

Fig. 3.1: Company networks

The network of German director (top panel) and company (bottom panel) interlocks in 1993, 1999 and 2005. Only a few companies are isolated from the large connected components, and a casual graphical inspection already suggests that each network has a core-periphery structure.

	1993	1999	2005
# of companies (distinct: 176)	97	100	100
# of directors (distinct: 3884)	1744	1711	1593
# of mandates	2143	2044	1833
average board size	22.9	20.4	18.3
average mandates per director	1.23	1.17	1.15
Company links (total)	803	657	375
Company links (unweighted)	597	490	291

Tab. 3.1: Mandates statistics

The descriptive statistics of our sample illustrate a slight decrease in the number of directors and mandates over time, and a highly nonlinear decrease in the number of links between companies that are formed by multiple board membership. The non-linearity is caused by the fact that a director with b mandates creates $l(b) = b!/2(b-2)!$ *links among companies. If, for instance, a director with* $b = 6$ *mandates retires and is replaced by different single-mandate directors each time, then* $l(6) = 15$ *links are removed from the network.*

size of company j, and off-diagonal non-zero elements indicate the number of directors that two companies have in common. The resulting networks are displayed in Figure 3.1 and readily reveal the existence of a core in each period, but the figure also suggests that the number of core companies and directors decreases over time. The question is then whether, as one might intuitively expect, core directors also become less influential in the sense that they are less central or less densely connected among themselves.

3.3 Analysis of Cores of Directors

3.3.1 Random Benchmark

To tackle the issue, we first need to identify a core of directors. For this purpose, it is instructive to consider the frequency of multiple board memberships, shown in Figure 3.2.

We start from the observation that the vast majority of directors serves on just one board, and conduct a simple thought experiment. Suppose that the directors in each sample are indistinguishable; then we can determine the probability of observing multiple board membership as a sequence of k independent Bernoulli trials, resulting in a binomial distribution for observing $B = b$ additional board memberships,

$$Pr[B = b] = \binom{k}{b} p^b (1-p)^{k-b},$$

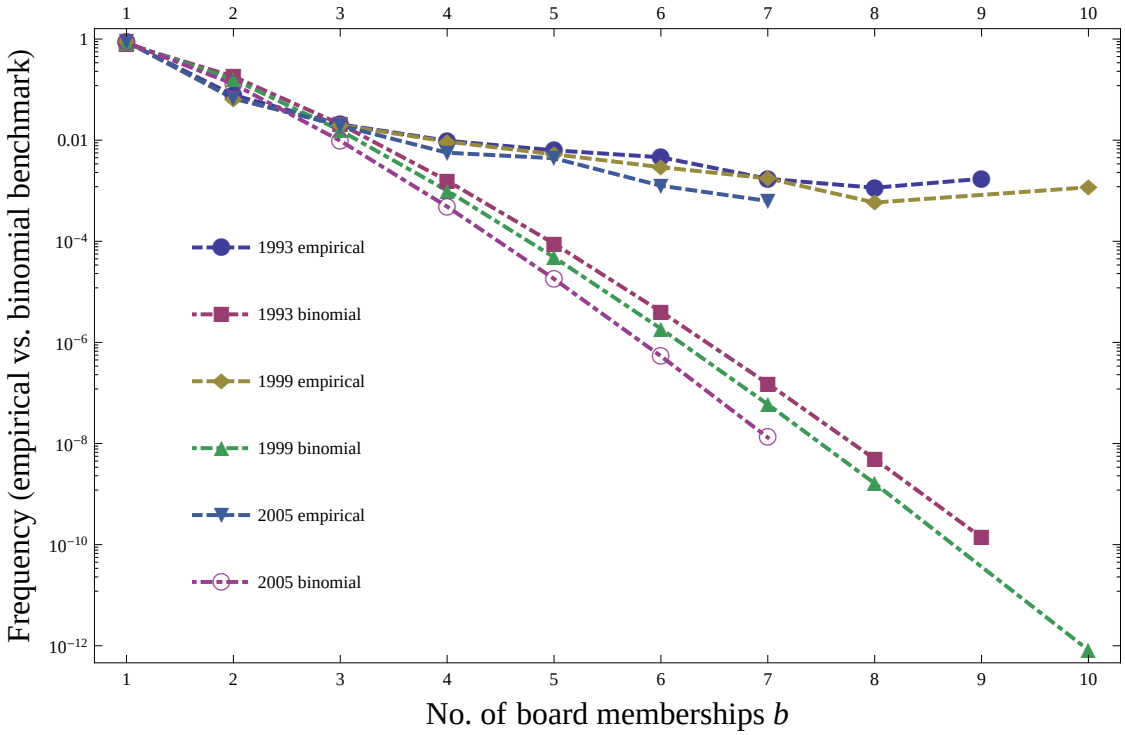

Fig. 3.2: Board membership benchmark
The top curves show the empirical relative frequency of multiple board membership in each of the three years, while the bottom curves illustrate the binomial probability of observing multiple board membership in the respective sequences of independent Bernoulli trials described in the text. The semi-log scale reveals deviations on increasing orders of magnitude for $b > 3$.

where p is the probability of success, i.e. of obtaining an additional board membership. To illustrate the procedure, consider for example the year 1993: there are 1744 directors in total, and the number of mandates is 2143, yielding $k = 2143 - 1744 = 399$, and $p = 1/1744$. Figure 3.2 illustrates the resulting binomial distributions and compares them to the empirical relative frequencies of multiple board membership.

For $b > 3$, the incidence of multiple board membership is several orders of magnitude higher than we would expect in a sequence of independent Bernoulli trials, which suggests that directors with three or more mandates are probabilistically distinct and in some sense special. One would expect to observe a network core if these directors were connected among themselves, thus we plot the network structure among directors with $B \geq b$ board memberships in Figure 3.3, which reveals that the resulting sub-graphs, or *b-cores*,[4] are indeed to a very large extent connected. We also observe that both the number of directors and the fraction of

[4] Notice that our b-cores are different from so-called k-cores, which are constructed using a node's minimum degree (see, e.g., Seidman, 1983).

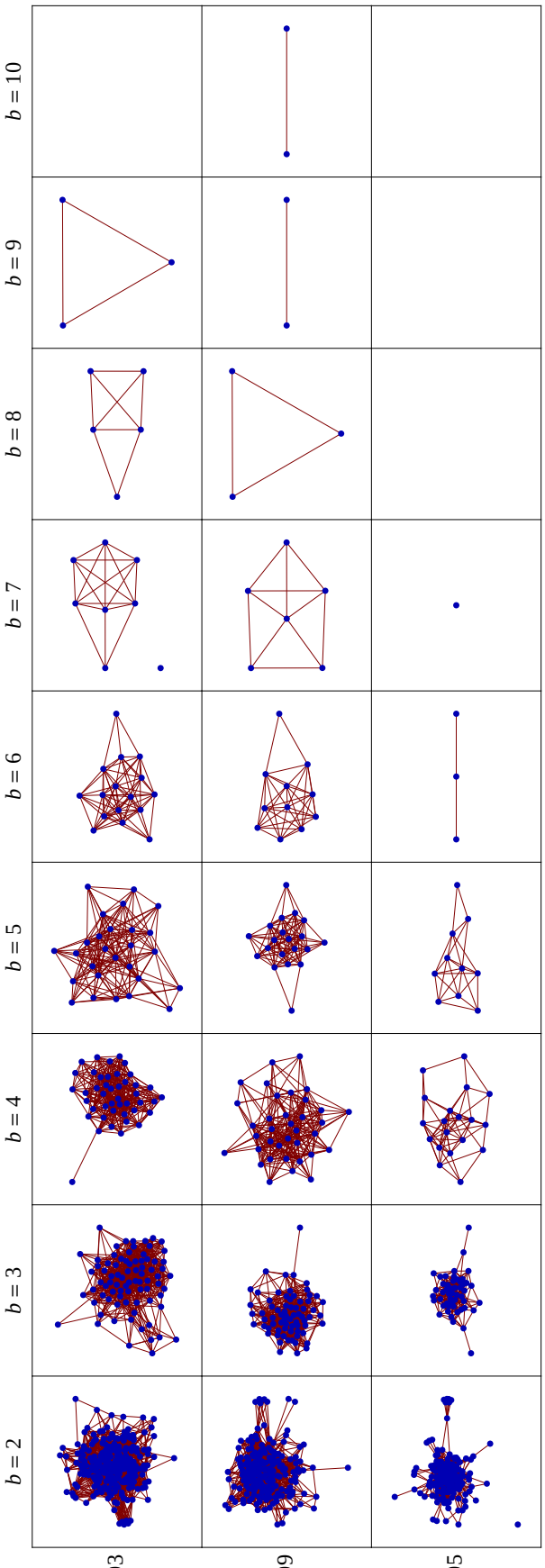

Fig. 3.3: Networks for different b-cores

Network structures formed by considering directors with an increasing threshold of board memberships $B \geq b$. Notice that there is only one instance of an isolated director with $b \geq 3$ mandates in any of the years (Alfred Pfeiffer in the 1993 $b-7$ core). The size of cores and the fraction of companies in the respective cores both decrease over time, shown in more detail in Figure 3.4.

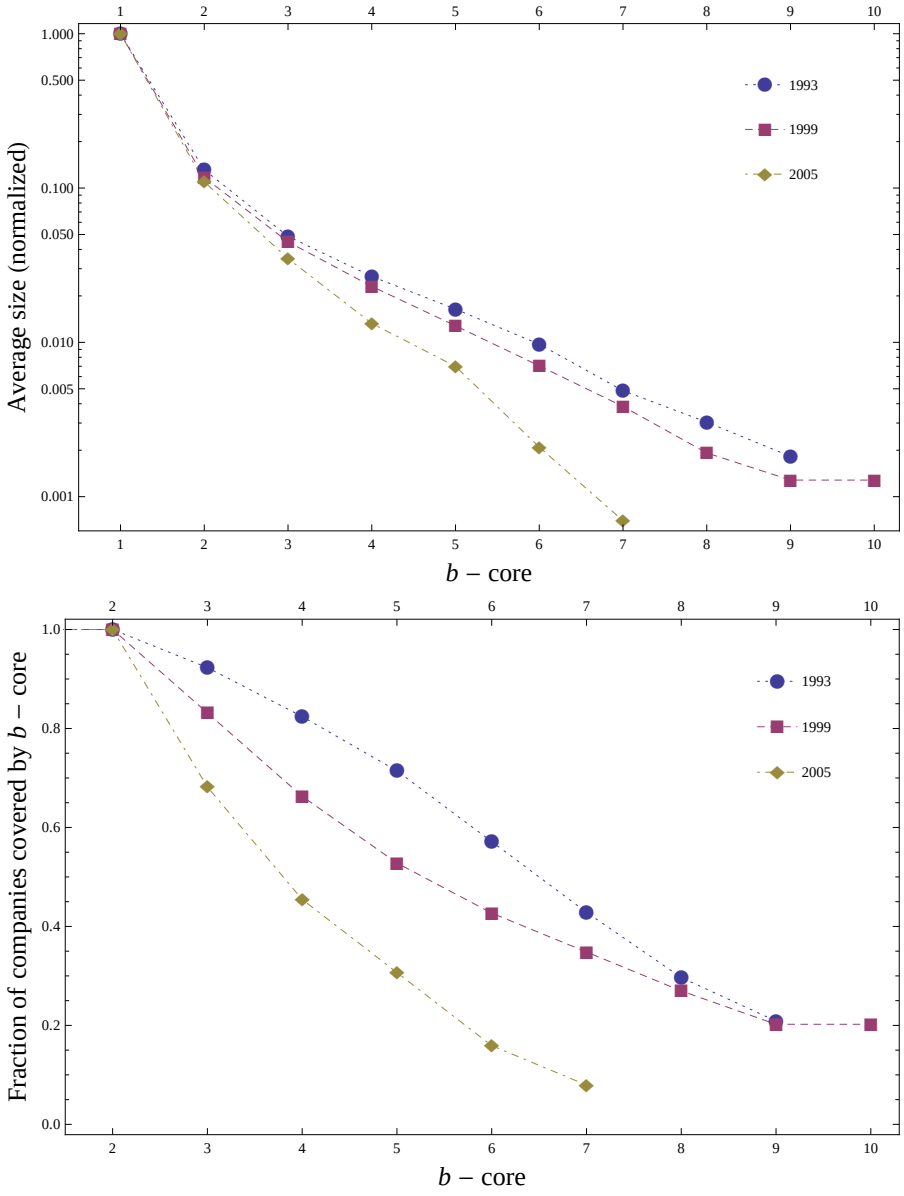

Fig. 3.4: Directors and companies of b-cores
The number of directors in the respective b-cores (top panel) decreases over time, as well as the fraction of companies that are linked by the respective b-core directors (bottom panel).

companies that are connected by the respective core directors decrease over time in our sample, shown in Figure 3.4. A major contributing factor to this development is certainly the recent reform of Germany's corporate governance code (DCGK).[5] The reform deals with a number of national and international criticisms that have been leveled against Germany's traditional corporate governance, mostly concerning the inadequate focus on shareholder interests, and the inadequate independence of supervisory boards, addressed for instance in DCGK paragraphs 5.1.2 (age limit for management board service), 5.4.2 (independence of supervisory board members), and 5.4.4 (deterrence of the hitherto custom that former chief executives serve as supervisory board chairmen). While the new code aims at standardizing best practices in corporate governance, it does not have the status of a formally binding law. Nevertheless, deviations from DCGK rules have to be explicitly justified and publicized on an annual basis (§ 161 *AktG*), and the observed decrease in the average number of board memberships is not an unexpected feature from this perspective. It is noteworthy that the code took effect in early 2002, while the pronounced decrease in average mandates indeed occurs between the 1999 and 2005 samples. At this point, one can speculate whether the DCGK is the ultimate cause of these developments or not, yet over the years we do in fact observe a pronounced decline in executive managers' supervisory board memberships:[6] Table C.2 in the appendix shows that in 1993 (1999, 2005), the 569 (441, 457) directors with executive positions additionally served on 228 (164, 83) supervisory boards of other corporations. The drop in the ratio of supervisory board memberships per executive ($228/569 = 0.4$ in 1993, 0.3 in 1999 and 0.17 in 2005) illustrates that corporate governance practices have indeed changed over the investigated time period. This brings us back to the question whether shrinking b-core sizes also imply that core directors become less influential over time, and how to formally define a network core in the first place.

3.3.2 Density and Corporate Reach

Intuitively a network core consists of directors that are highly central in the network and densely connected among themselves. The density of the (unweighted) graph $\mathbf{D}$ is given by the ratio of the existing number of links, denoted $|L|$, to the number of links in a complete graph of the same size, denoted $|N|$,

$$\text{density}_D = 2|L|/|N|(|N|-1), \tag{3.1}$$

[5] See `http://www.corporate-governance-code.de/index-e.html`.

[6] Current members of the management board must not simultaneously serve on the company's supervisory board (§ 105 *AktG*), but have routinely been allowed to serve as supervisory board members at other companies.

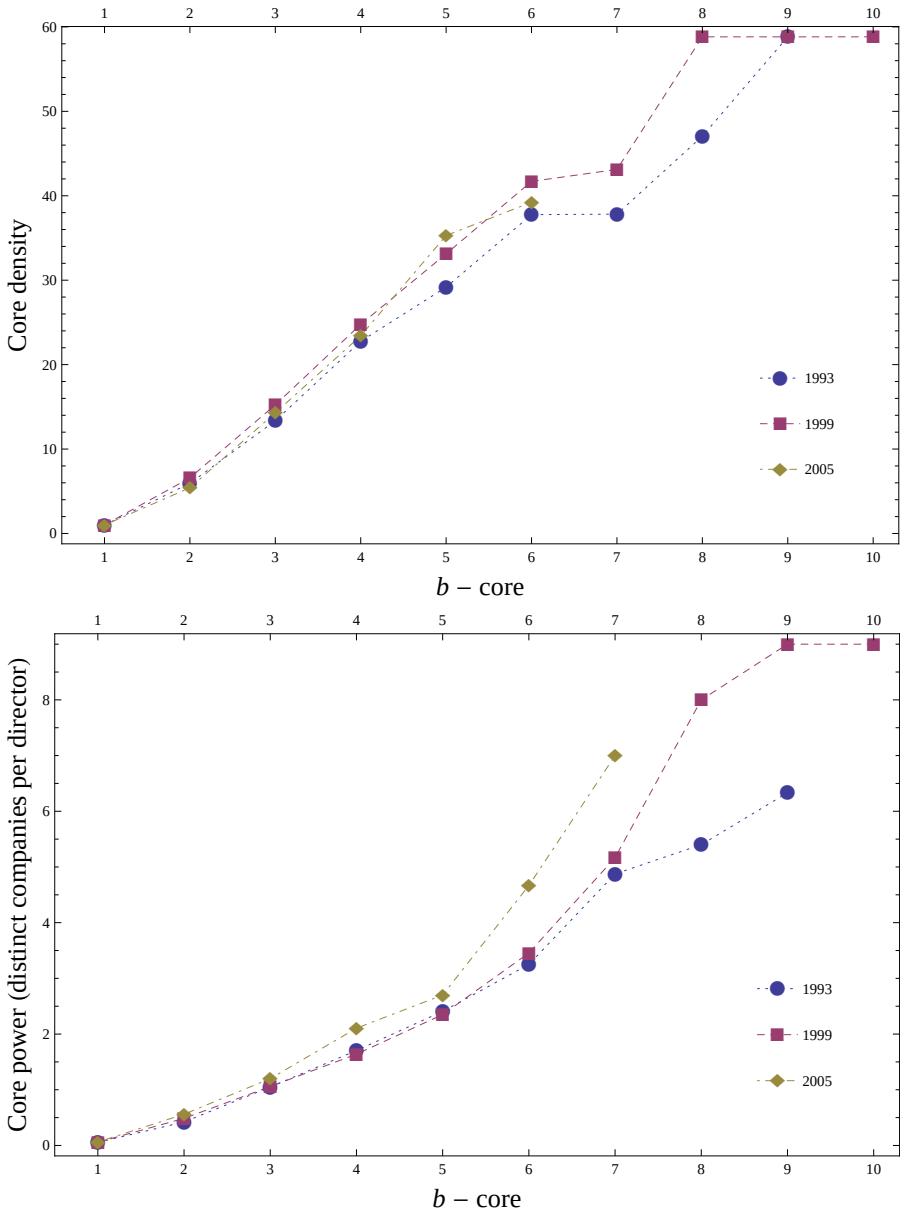

Fig. 3.5: Core companies and core directors

The (normalized) density of b-cores (top panel) remains fairly stable over time, as well as the ratio of distinct core companies to core directors (bottom panel). If anything, core density and core power increase despite the decrease in the average number of mandates over time.

which is by construction confined to the interval $[0, 1]$. The top panel of Figure 3.5 illustrates that (i) the density of b-core sub-graphs increases with b, and that (ii) the density of the respective b-cores remains fairly constant over time in spite of decreasing b-core size. In addition, we can assess the corporate reach per core director by the ratio of distinct core companies to the number of core directors, the rationale being that a core of densely connected directors probably yields the more institutional power the fewer individuals constitute the core, and the more companies they span. It is noteworthy that this measure of core power, shown in the bottom panel of Figure 3.5, actually increases over time, so the recent decline in the number of board memberships does not necessarily mean that core directors in Germany's corporate board network also become less influential.

3.3.3 Centrality

A complementary approach to measuring the importance or influence of directors is to consider their centrality in the overall network of director interlocks. Let $\mathbf{C}$ denote the respective adjacency matrices of the large connected components of $\mathbf{D}$ in the respective years, and let V denote the set of directors contained in C. A shortest path between two directors $u, v \in V$ is known as a graph *geodesic*, which is not necessarily unique, and the length of the geodesic $d_C(u, v)$ is known as the graph *distance* between the pair (u, v). The first centrality measure we consider is *closeness centrality*, which measures the distance of a node to all other nodes in the network, and is typically defined as the reciprocal of the sum of geodesics to all other nodes in the network,

$$\text{closeness}_u = 1/\sum_{v \in V} d_C(u, v)\,. \tag{3.2}$$

Since we would like to compare the centrality of directors across years, we divide by the closeness score of the director with maximal closeness centrality in each year in order to normalize the scores. Directors who are more central in this sense should in principle be better able to reach out into the entire network or be faster in doing so.

Another measure of the centrality of node u is *degree centrality*, constructed by summing the number of links that each node has, $\text{degree}_u = \sum_{v \in V} \mathbf{C}_{uv}$. Intuitively, directors who have many links compared to their peers are in an advantageous position if they are able to influence many of their peers, or if they have better access to resources through their many links. But degree centrality only takes immediate ties of directors into account, and lacks information about the distance to directors that

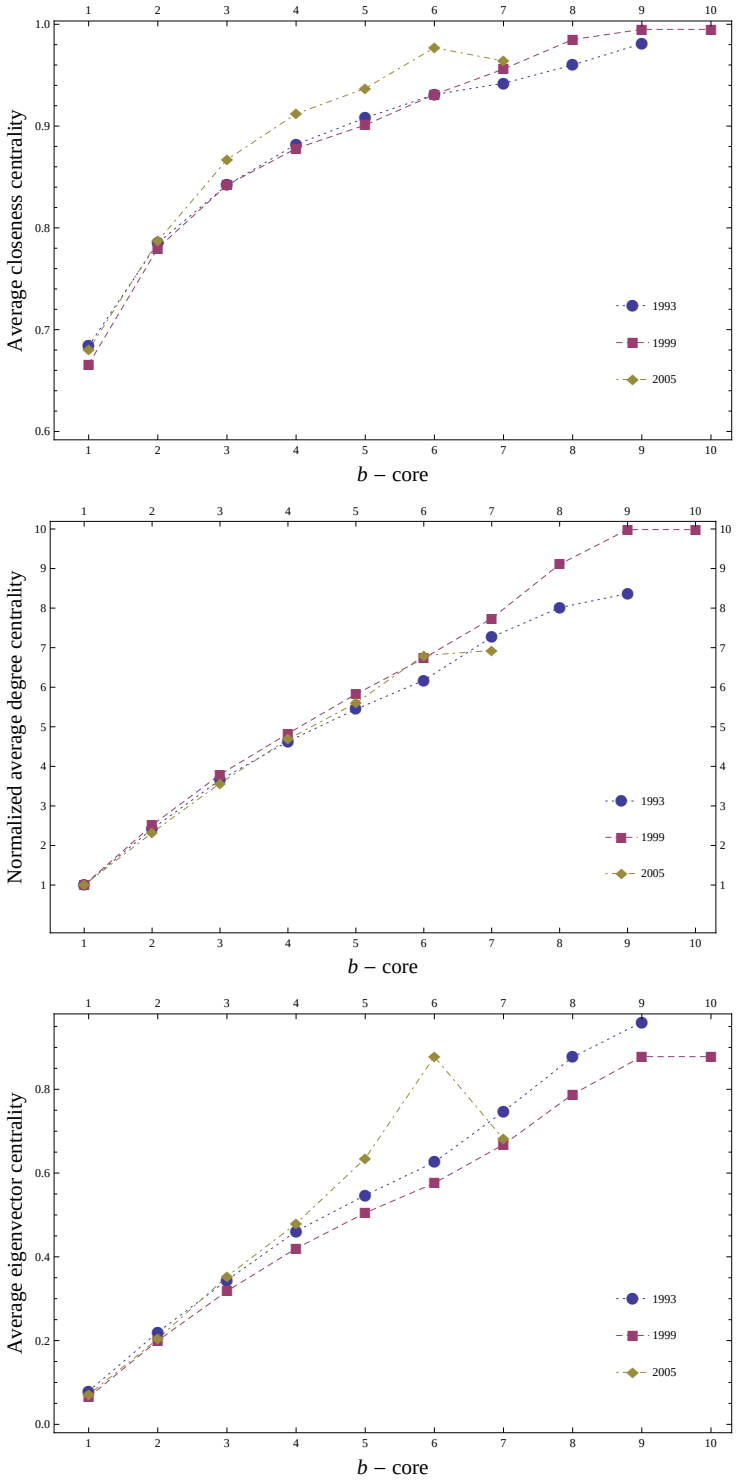

Fig. 3.6: Centrality of directors

Normalized average centrality measures of b-core directors in the respective years: closeness (top), degree (center) and eigenvector (bottom) centrality remain fairly stable over time.

are not immediate neighbors. Moreover, directors with many board memberships have a relatively large degree by construction since the board size distribution has a characteristic scale that is well captured by its mean.

Therefore, we also compute the eigenvector centrality (see Bonacich, 1972) for all nodes in V. *Eigenvector centrality* assigns scores of relative importance to directors in the network, based on the principle that connections to high-scoring directors contribute more to a director's score than equal connections to low-scoring peers. Hence the idea behind eigenvector centrality is that the quality of links is important, because directors who are connected to many influential peers can be expected to be important themselves. Suppose the eigenvector centrality score of node u, denoted e_u, is proportional to the centrality score of its neighbors,

$$e_u = \frac{1}{\lambda} \sum_{v \in V} C_{uv}\, e_v \,, \tag{3.3}$$

where λ is a constant. Then we can write the vector of centrality scores in matrix notation as $\lambda \mathbf{e} = \mathbf{C} \cdot \mathbf{e}$, which shows that $\mathbf{e}$ is an eigenvector of $\mathbf{C}$ with corresponding eigenvalue λ. It is convenient to consider the eigenvector corresponding to the largest eigenvalue of $\mathbf{C}$ since its elements are all non-negative according to the Perron-Frobenius theorem. Again, we divided all scores by the maximum score in each year to normalize the data. Figure 3.6 shows that core directors are not only densely connected among themselves, but that they are also increasingly central in the entire network, which is another characteristic that one intuitively expects in the definition of a network core.

3.4 Core Persistence and Individual Turnover

We have argued that the structural characteristics of director interlocks are stable over time in spite of changes in corporate governance and a decrease in the average number of mandates. Motivated by the persistence in network structure, we want to investigate whether or how the core structure depends on the destinies of particular agents.

3.4.1 Evolution of Company Links

An important aspect here concerns the links in the company network. Their time evolution over consecutive periods reveals some noteworthy patterns: in 1993 (1999) the company network had 597 (490) unweighted links, 290 (195) of which were with companies that remained in the sample in the next period (and had not merged

in the meantime), while 141 (95) of these links were still in place in the following period. In 78 (62) cases, at least one director was constantly part of both boards. In addition, 24 (10) directors had been recruited to reinforce existing links, then serving on average on 4.38 (4.04) boards. Out of these 24 (10) directors, 18 (7) were already serving on at least one board in the previous period, when they held 2.22 (2.68) appointments on average. In the remaining 63 (33) cases, where an existing link was maintained through the recruitment of new directors, a total of 50 (26) directors was appointed to the 63 (33) positions, and these directors then served on average on 4.04 (3.77) boards. Out of these 50 (26) directors, 34 (20) had at least one mandate in the previous period, when they served on average on 2.68 (2.75) boards. So we observe that about half of the company links are being maintained between periods, which is consistent with earlier findings by Schreyögg and Papenheim-Tockhorn (1995) on the reconstitution of German corporate interlocks.[7] Keeping in mind that a substantial number of links in the (initial) company network might be unintended,[8] and given that the sample periods have been chosen sufficiently far apart to warrant board (re)appointment decisions, the observed reconstitution of links would certainly seem to indicate planned or strategic connectivity among German corporations.

Secondly, these figures suggest that companies seem to prefer the appointment of directors who already serve on several other boards, which is particularly true for the maintenance of institutional links over time. It is rather doubtful that these directors were appointed for purely supervisory purposes since the effort involved in monitoring a handful of DAX companies is surely considerable, and in all likelihood becomes increasingly prohibitive if one of the appointments is an executive position. The frequency distribution of executives' supervisory board memberships in Table C.2 nevertheless shows that some executives additionally served on up to ten other boards.

3.4.2 Director Survival

Since multiple board memberships seem to be essential for both the existence and the persistence of a core network, we also investigate the survival of directors over

[7] The percentage of reconstructed ties among German companies is four to five times higher than previously observed in the US (see Stearns and Mizruchi, 1986). From a network core perspective, it would be interesting to clarify whether the percentage of reconstituted ties among the very largest (core) corporations in the US is substantially higher than in the original Stearns and Mizruchi sample.

[8] Imagine a director with three mandates and suppose that she is on the board of company A, which manages to place her on the board of company B for strategic reasons, e.g. to oversee A's interests. If she also serves on the board of a third company C, we consider the link between A and B intentional, while the links AC and BC are unintentional byproducts.

time. Out of a total of 1517 directors in the 1993 sample, 518 are still present in 1999, which is a survival rate of 34%. For the 1999-2005 transition, this figure is 32%. During the first (second) transition period, 12.6% (13.1%) of the surviving directors gained mandates, while 12.4% (11.3%) lost at least one mandate. But these percentages conceal that directors with multiple memberships have a markedly higher survival probability than the vast majority of directors with a single mandate: the survival probability conditional on the number of existing mandates is 31% (28%) for board members with a single mandate, it increases to 51% (47%) for directors with two mandates, 69% (76%) for those with three mandates, and 70% (78%) for those with four or more mandates.[9] It seems fair to say that the persistent structure of Germany's corporate network is driven by the recruitment decisions of large companies, which are characterized by a process of "selective replacement" that expresses itself in the figures on the maintenance of links among companies and the conditional survival of directors. While the vast majority of directors enters and exits the corporate network without ever being particularly central in it, a small number of highly connected key directors warrants a persistent network core over time. Moreover, fluctuations in the destines of key players are mitigated by the reconstitution of ties among large corporations, who favor directors with multiple memberships. To corroborate this claim, we consider the turnover in the centrality of companies and directors between periods.

3.4.3 Turnover in Company and Director Centrality

We start by calculating the change in each of the three centrality measures for surviving nodes in the connected component. Table 3.2 illustrates that about two thirds of the companies but only one third of the directors survive consecutive periods. The life span of directors is biologically limited while the same is obviously not necessarily true for corporations, thus the fact that about 70% of directors but less than 40% of companies drop out between periods is by itself not unexpected. In spite of the expected difference, we find that the *mean absolute change in centrality*, as a measure of variability among survivors, has the same level of magnitude for both companies and directors, and that absolute changes in centrality are rather small in both cases.[10]

In order to properly compare the turnover activity between companies and direc-

[9] These figures are easily calculated from the transition matrices in Appendix C.3.

[10] All three measures of centrality exhibit a slight decrease in *average centrality* between 1993 to 1999, and an increase between 1999 to 2005, as reported in Table 3.2. This is in line with the visual inspection of the network structure in Figure 3.1, which shows an increasing number of peripheral nodes in 1999, and denser cores in 2005.

			companies		directors	
			$1993-1999$	$1999-2005$	$1993-1999$	$1999-2005$
	survivors		91	89	1645	1562
	dropouts		34	38	1087	1081
average centrality	closeness	out	0.5034	0.4438	0.4950	0.4450
		in (t)	0.7789	0.7317	0.7014	0.6850
		in $(t+1)$	0.7521	0.7497	0.6845	0.7082
	eigenvalue	out	0.0023	<0.001	0.0513	<0.001
		in (t)	0.2766	0.2339	0.1040	0.0926
		in $(t+1)$	0.2458	0.3301	0.0866	0.0978
	normalized degree	out	0.0250	0.0270	0.0313	0.0207
		in (t)	0.3636	0.3121	0.1509	0.1358
		in $(t+1)$	0.3295	0.3431	0.1352	0.1857
change in centrality	closeness	avg. $\lvert\Delta\rvert$	0.0547	0.0730	0.0521	0.0684
		avg. Δ	-0.0268	0.0100	-0.0169	0.0233
		benchmark	0.1348	0.1598	0.1057	0.1208
	eigenvalue	avg. $\lvert\Delta\rvert$	0.0883	0.1161	0.0513	0.0571
		avg. Δ	-0.0308	0.0962	-0.0175	0.0052
		benchmark	0.2702	0.2912	0.1174	0.1199
	normalized degree	avg. $\lvert\Delta\rvert$	0.0953	0.1039	0.0543	0.0855
		avg. Δ	-0.0341	0.0310	-0.0157	0.0499
		benchmark	0.2651	0.2838	0.0954	0.1143

Tab. 3.2: Turnover activity in company and director networks

The notation for average centrality measures refers to averages for dropouts ("out"), and the centrality of survivors in the current ("in (t)") and next ("in $(t+1)$") period. The benchmark values for the changes in centrality have been calculated according to the procedure described in this section.

tors, we need to scale the absolute changes in centrality with a benchmark measure of persistence in centrality that accounts for the different scales of the company and director networks. In our benchmark case, we assume that each node's centrality could change to every observed centrality in next period's sample with equal probability, corresponding to a uniformly random rewiring of nodes. Thus the average absolute change in centrality would be zero in the case of a perfect conservation of the relative position of nodes, and would be equal to the benchmark value in case of a completely random rewiring of surviving nodes. For all centrality measures, we observe that the ratio of the benchmark to the observed value is larger for companies than for directors (about 3:1 vs 2:1), showing that surviving companies exhibit significantly less churning in their centrality than surviving directors. Comparing dropouts with survivors, both for companies and directors, we find that survivors are always substantially more central than dropouts (also reported in Table 3.2), and that the normalized degree is about one order of magnitude higher for survivors than for dropouts. Moreover, the very low average eigenvector centrality of dropouts further implies that the importance of the dropouts' few neighbors is also very low on average. In summary, both highly central companies as well as directors tend to stay central, while dropouts are located in more peripheral positions of the network. Company networks exhibit less turnover activity than director networks both in the share of surviving nodes but also in the centrality changes among survivors.

3.4.4 Identifying Company Groups

Finally, we would like to identify cliques among the companies in our dataset. There are essentially two streams of literature which deal with the detection of groups in networks (see, e.g., Newman, 2010, pp. 345–391). The traditional approach is called *graph partitioning* and splits the network into a fixed number of subgraphs, e.g. by spectral decomposition of the so-called Graph Laplacian (see, e.g., von Luxburg, 2007).[11] Graph partitioning algorithms can become very time consuming, but the more serious concern is conceptual because the number of useful partitions is generally not known. *Community detection* therefore has developed algorithmic procedures that endogenize the number of subgraphs in the partitioning process, for instance by iterative edge removal based on the calculation of betweenness scores (see, e.g., Newman and Girvan, 2004). We employ a mixture of these two approaches here, starting from a principal component analysis (PCA) and combining it with a scoring algorithm that creates groups based on the largest components without

[11] The Laplacian is a special form of the adjacency matrix of the network, where the trace of the Laplacian corresponds to the number of links between nodes.

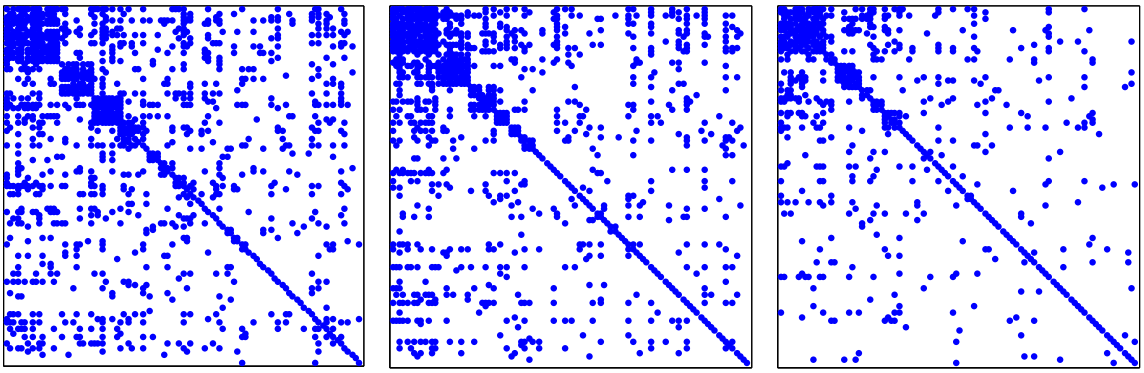

Fig. 3.7: Resorted adjacency matrices for 1993, 1999, and 2005
The network is getting sparser over the years. The number and size of identified cliques is decreasing.

predefining the number of subgraphs. A combination of PCA and some matching algorithm represents a reasonable alternative to community detection algorithms in the social sciences, because the size of datasets is generally smaller than in the natural sciences.[12]

First we take the adjacency matrix of the firm network and standardize its columns by subtracting the column-wide mean and dividing by the standard deviation of column entries. This new adjacency matrix is denoted $\hat{\mathbf{B}}$. The column entries can now be interpreted as the relative weights of the companies' links, while the row entries resemble the relative attention a firm receives through links from other firms. We measure the correlations of link patterns by calculating the empirical correlation matrix $\mathbf{R} = c^{-1}\hat{\mathbf{B}}^T\hat{\mathbf{B}}$, allowing us to infer which firms have similar relative weights in their link patterns. Based on this correlation matrix we compute our new variables, the principal components $\mathbf{F}$, which are linear combinations of the original variables such that $\mathbf{F} = \mathbf{Y}\hat{\mathbf{B}}$. The column vectors in $\mathbf{Y}$ carry the weights for each new variable, and it can be shown that the solution to this problem amounts to solving for $\mathbf{F} = \mathbf{V}\hat{\mathbf{B}}$, where $\mathbf{Y} = \mathbf{V}$ contains the eigenvectors of the correlation matrix $\mathbf{R}$ ordered by descending eigenvalues (see, e.g., Jobson, 1991). The eigenvectors with the highest eigenvalues account for a large amount of the variance in the data, while low eigenvalues stand for eigenvectors and components that contribute very little to the variance and are consequently neglected.

To illustrate the principles that we use to form groups, assume that based on some decomposition we have approximated the adjacency matrix $\mathbf{B}$ by a dimensionally reduced matrix $\hat{\mathbf{E}}$, where both matrices would contain ones for links and zeros otherwise, and $\hat{\mathbf{E}}$ being of lower rank than $\mathbf{B}$ due to the dimensional reduction. To

[12] The benefit of this method is that PCA is more parsimonious and transparent than community detection algorithms, and perhaps also better known among social scientists than the latter. The foundations of our subsequent analysis can be found in Reichardt (2009).

decide whether $\hat{\mathbf{E}}$ is a good representation of the original network, we essentially have to compare and score by rewarding the correct matching of links (and non-links) in $\mathbf{B}$ and $\hat{\mathbf{E}}$, and symmetrically by punishing the matching of links to non-links in either direction. A weighting scheme will be helpful for the comparison because the adjacency matrices of our corporate networks are sparse, therefore actual links are more informative than non-links. These considerations result in a *scoring (or error) function* of the form

$$s(\hat{\mathbf{E}}|\mathbf{B},\Omega_{1\ldots4}) = \underbrace{\sum_{i=1}^{c}\sum_{j=1}^{c}\Omega_{1,ij}\hat{\mathbf{E}}_{ij}\mathbf{B}_{ij}}_{\text{links to links}} - \underbrace{\sum_{i=1}^{c}\sum_{j=1}^{c}\Omega_{2,ij}(1-\hat{\mathbf{E}}_{ij})\mathbf{B}_{ij}}_{\text{non-links to links}} \tag{3.4}$$
$$- \underbrace{\sum_{i=1}^{c}\sum_{j=1}^{c}\Omega_{3,ij}\hat{\mathbf{E}}_{ij}(1-\mathbf{B}_{ij})}_{\text{links to non-links}} + \underbrace{\sum_{i=1}^{c}\sum_{j=1}^{c}\Omega_{4,ij}(1-\hat{\mathbf{E}}_{ij})(1-\mathbf{B}_{ij})}_{\text{non-links to non-links}}$$

where $\Omega_{1\ldots4}$ represent weighting matrices. It is common to focus on the matching of links in the reference matrix $\mathbf{B}$ by equally weighting the (mis)matching of original links, $\Omega_{1,ij} = \Omega_{2,ij} > \Omega_{3,ij} = \Omega_{4,ij}$ (see Reichardt, 2009).

The algorithmic procedure that we employ here to visualize the groups in the network follows exactly the principles illustrated above. The only difference is that instead of comparing two (binary) adjacency matrices, we compare the adjacency matrix with the principal components (which are not binary) in column-wise fashion. The groups to which we want to match firms are given by the largest components resulting from the PCA. Since $\hat{\mathbf{B}}$ describes links, the components in $\mathbf{F}$ describe those links in which companies differ. If we normalize the column vectors in $\mathbf{F}$ and allow for a sign change in every column, we get a new matrix of *link profiles* $\hat{\mathbf{F}}$ with dimensions $c \times 2c$, where each even column contains the entries of the previous (i.e. original, now odd) column with reversed signs. This sign change is necessary since the principal components describe only a new axis within the variable space, but do not inform us of the direction. As detailed below, we will only use the first few columns of $\hat{\mathbf{F}}$ and calculate a similarity score for each group (represented by a column in $\hat{\mathbf{F}}$) and each firm (represented by a column in $\mathbf{B}$). This results in a matrix $\mathbf{S}$ of scores for all firms and groups with dimension $c \times 2k$, where k is the number of included principal components (more on k below). Given the sign change, the number of groups will be $G \leq 2k$. The weights of links and non-links can be approximated by the number of links versus non-links in the original network. Since the graph density is only about 0.03, we set $\Omega_3 = \Omega_4 = 0$. Furthermore, we do not

need to differentiate the weight of each single link as it is already contained in the respective values of the link profile $\hat{\mathbf{F}}$, hence $\Omega_1 = \Omega_2 = 1$. Notice, however, that in contrast to $\hat{\mathbf{E}}$ the link profile $\hat{\mathbf{F}}$ is not a binary matrix (it contains the relative weights of links), therefore we lastly introduce a matrix $\boldsymbol{\Theta}$ that translates $\hat{\mathbf{F}}$ into a binary form such that $\Theta_{jg} = 1$ if $\hat{\mathbf{F}}_{jg} > 0$ and zero otherwise:

$$\mathbf{S}_{ig} = \sum_{j=1}^{c} \boldsymbol{\Theta}_{jg}(\hat{\mathbf{F}}_{jg}\mathbf{B}_{ji})^2 - \sum_{j=1}^{c}(\boldsymbol{\Theta}_{jg} - 1)(\hat{\mathbf{F}}_{jg}\mathbf{B}_{ji})^2 \tag{3.5}$$

for all $i = 1, \ldots, c$ and $g = 1, \ldots, G$. Thus $\boldsymbol{\Theta}$ ensures that we sum over all positive entries in $\hat{\mathbf{F}}$ in the first sum, and over all negative entries in the second sum. For every correct match, that means if a firm i has a link to company j where the link profile would suggest one, we increase the score that firm i obtains for group g by the squared entry in the link profile. Symmetrically, if the firm has a link where we do not expect one, we deduct this score. Each firm is now assigned to the group for which it has the highest score (by identifying the maxima in each row of $\mathbf{S}$). There are, of course, quite a few firms that score rather poorly in all of the groups, simply because they do not belong to any. These firms either have very few links to begin with, or have a unique link pattern. To filter out such firms, we set a threshold in our scoring procedure, yet it turns out that the grouping is quite robust with respect to the exact value of this threshold.[13]

A critical point in any PCA analysis concerns the question how many components k to include in the first place. In our context, we find it instructive to check how many components will create groups containing at least three firms, representing a rather conservative criterion for defining a group. Our algorithm iteratively increases the number of principal components and stops when the last included component no longer produces an additional group. It turns out that only a fraction of the firms can be mapped to groups, with the greatest eigenvalues accounting for roughly 10 percent of total variance, and the smallest relevant eigenvalues accounting for roughly 3 percent of total variance. We never include more than the five largest eigenvalues to create significant groups, that is to say that the inclusion of more than the largest five eigenvalues leads to groups of size smaller than three. Figure

[13] If the best score of a firm is not greater than the mean plus half a standard deviation of scores within a group, we do not match the firm to the group. The exact tuning of this threshold is of course arbitrary: choosing a much larger threshold level leads to smaller but more homogeneous groups (some firms might not be matched at all because of a single differing link), while a much lower threshold will inflate groups by matching peripheral firms that only show marginal similarity in the link pattern. Since neither group turns out to be large compared to the entire set of firms, our quantile-approach is quite robust, and the exact value of the threshold is not crucial for the overall results. In larger datasets, this parameter could certainly be endogenized.

3.7 shows the resorted adjacency matrices for 1993, 1999, and 2005, where we plot cliques with descending size from left to right, followed by firms that do not exhibit specific connection patterns.[14]

In 1993 it is still possible to divide the core of our network into overlapping subgroups, but this structure seems to be fading away over time. The number of firms that belong to a clique is about 30 in 1993, yet this number as well as the size of identified cliques is shrinking over time. There is, however, a number of mega-cap corporations that persistently show up in one of the big cliques: *Allianz, Bayer, Commerzbank, Deutsche Bank, Hochtief, Linde, Lufthansa, Siemens, Thyssen Krupp,* and *Volkswagen* (see Appendix C.4 for details). This visualization confirms our earlier findings that even if the overall level of connectedness in the corporate network is decreasing, highly central firms tend to remain central in the network.

3.5 Discussion

We have argued that Germany's corporate network exhibits a pronounced core structure that persists over time in spite of changes in corporate governance, and substantial churning and entry-and-exit dynamics among corporate directors. A remaining issue concerns the validity of our findings beyond Germany's one hundred largest publicly traded companies. So can we reasonably expect our results to be representative of the entire German corporate network? Judging from the more recent results by Milaković et al. (2010) for a single year, there is reason for optimism. Considering the largest 284 German companies in 2008 (accounting for more than 95% of that year's market capitalization of Germany's stock exchange *Deutsche Börse*), they observe very similar magnitudes in the maximum number of board memberships, and in the density and average centrality of successive b-cores. Second, and more importantly from the viewpoint of the present study, they find that the pronounced core structure in Germany's corporate network is clearly formed by mega-cap companies, thereby justifying our focus on the one hundred largest companies here. Since they examine the corporate network in a single year, however, they lack information on the time evolution of the network.

As our results illustrate, it is exactly the largest three to four dozen mega-cap corporations that are responsible not only for the existence but also the *persistence* of a core over time. While the presence and persistence of a core originate from the appointment decisions of the very largest German corporations, our findings

[14] The source code of the algorithm can be found in Appendix C.1.

leave little room for the relevance of individual directors from a macroscopic point of view: the churning and entry-and-exit dynamics of individual directors in our sample instead emphasize the (seemingly exclusive) importance of the number of mega-cap board appointments that a director has managed to accumulate at a given point in time.

If policymakers were to aim for a reduction of pressure group influence, these types of questions would be crucial for the corresponding policy design, particularly in light of the fact that existing legal restrictions on the number of simultaneous board appointments and the maximum term of service before potential reappointment are obviously not sufficient to decrease the influence of the core network, much less prevent its existence.

To be clear, the main contribution of this paper is certainly of a descriptive nature. We have not performed any confirmatory statistical exercises in the traditional sense, so there is very little (if anything) we can say here about how or whether a corporate core influences the destinies of individual firms over time, but these are questions that could surely be addressed in future research. Nevertheless, we would like to believe that the existence and persistence of a core is interesting in its own right, and goes well beyond concerns regarding pressure group influence, particularly in light of the systemic implications already mentioned at the end of the introduction: the system-wide coordination of opinions, expectations, or even animal spirits is enormously facilitated by the existence of a network core, and could very well make a system more fragile exactly because of that. Think, for instance, of the large-scale coordination of trading positions in financial markets that precede every financial crisis. From our perspective, it is rather noteworthy that financial markets also exhibit a core network structure, at least in the few instances for which data have been available so far (see, e.g., Soramäki et al., 2007).

4. EVOLVEMENT OF UNIFORMITY AND VOLATILITY IN THE STRESSED GLOBAL FINANCIAL VILLAGE

This is a reprint of an article whose final and definitive form has been published as: Kenett D.Y., Raddant M., Lux T., Ben-Jacob E. (2012) Evolvement of Uniformity and Volatility in the Stressed Global Financial Village. PLoS ONE 7(2): e31144.

4.1 Introduction to Stock Market Correlations

Has the world become one small financial global village? Coupling between the world's different markets has become stronger and stronger over the past years, as is evidenced by the financial difficulties, which are affecting many markets around the globe, especially since late 2008. The growing financial integration allows capital to flow rather freely between countries and markets. Investments in stocks can be diversified into global portfolios, consisting of multiple assets from a large number of markets. As a result, stock markets have turned into an extended and strongly coupled complex system, in which large movements in price and volatility are likely to be transferred from one market to the other due to portfolio readjustments. Engle et al. (1990) have shown that volatility clusters are likely to occur jointly in different markets. This fact and other evidence of the interdependencies between the world's economies emphasize the need to understand the coupling and integration of stock markets around the world. As the financial crisis of 2008 was not even considered a possibility by the leading economic theories (see, e.g., Lux and Westerhoff, 2009), it is necessary to rethink and reformulate the understanding and quantification of the coupling between different markets.

When it comes to the analysis of individual markets, a wealth of different measures have been devised and used to analyze similarity between financial time series. These include Pearson's correlations (see Kenett et al., 2011,0; Mantegna and Stanley, 2000; Shapira et al., 2009), co-movement measures like in Harmon et al. (2011), recurrence patterns (see Goswami et al., 2011), and regime switching approaches (see, e.g., Preis et al., 2011; Preis and Stanley, 2010). There are also studies of the co-movement of different stock markets. Forbes and Rigobon (2002) have shown

that a high level of dependence is visible between most markets and that changes in correlation are coupled to volatility changes. However, there are mixed results about the driving forces of the amount of co-movement and of financial integration. While King et al. (1994) did not clearly identify the reasons for changes in the correlation, Beile and Candelon (2011) found evidence that increased trade and financial liberalization go hand in hand with a synchronization of stock markets. Furthermore, Ahlgren and Antell (2010) found that markets are linked closer in times of crisis which significantly hampers the possibility to diversify investments and thus risks. Additional studies looked at correlation structures in particular markets, like Tumminello et al. (2005), or at the correlation between the indices of different markets (see, e.g., Song et al., 2011).

Recently, Kenett et al. (2011) investigated the dynamics of correlations between stocks belonging to the S&P 500 index, and the residual (partial) correlations after removing the influence of the index . To this end, the Index Cohesive Force (ICF), which is the ratio between the average stock correlation, and average stock partial correlation, was introduced. Studying the dynamics of these quantitative measures, a transition in the dynamics of the U.S. market at the end of 2001 was observed. Here we expand these previous analyses to the investigation of other markets. We further extend the scope of the analysis by studying the markets intra and inter correlations. First, we study correlation structures on the level of single markets, the market intra-correlation. Next, we study the correlation between different market pairs, according to three measures - the market index correlation, market meta-correlation, and market ICF correlation.

4.2 Methods

The similarity between stock price changes is commonly calculated via the Pearson's correlation coefficient. The raw stock correlations (see Mantegna and Stanley, 2000) are calculated for time series of the log of the daily return, given by:

$$r_i(t) = log[P_i(t)] - log[P_i(t-1)], \tag{4.1}$$

where $P_i(t)$ is the daily adjusted closing price of stock i at day t. The raw stock correlations are calculated using Pearson's correlation coefficient between every pair of stocks i and j, where

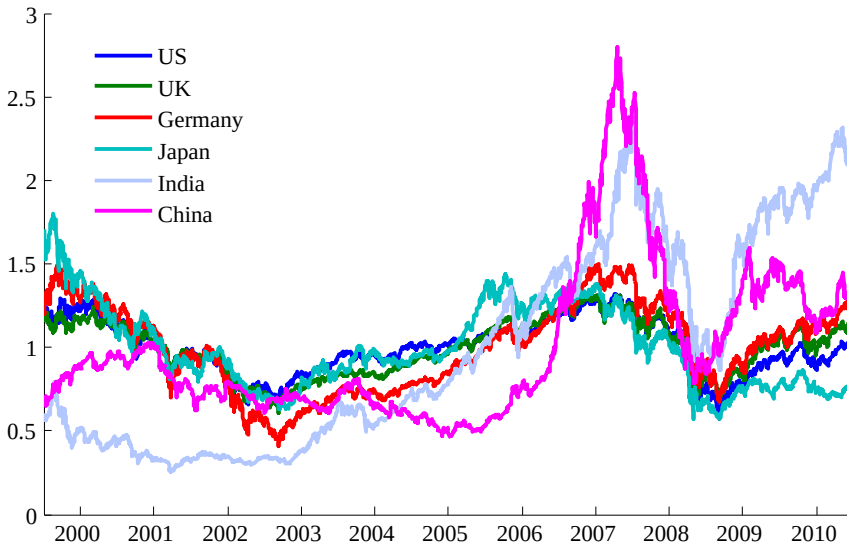

Fig. 4.1: Normalized stock price indices

Normalized stock price indices; S&P 500 (U.S.), FTSE 350 (U.K.), DAX 30 Performance (Germany), NIKKEI 500 (Japan), BSE 100 (India), and SSE Composite (China). All indices have been normalized by their mean. The indices of the U.S., U.K. and Germany (blue, green and red line) appear almost as if they are shifted parallel, which is a sign of their high correlation. Note that all price indices are based on stock prices in local currency.

$$C(i,j) = \frac{\langle (r_i - \langle r_i \rangle)(r_j - \langle r_j \rangle) \rangle}{\sigma_i \sigma_j}, \tag{4.2}$$

$\langle\rangle$ denotes average, and σ_i are the standard deviations (STD).

Partial correlation is a powerful tool to investigate how the correlation between two stocks depends on the correlation of each of the stocks with a third mediating stock or with the index as is considered here. The residual, or partial, correlation between stocks i and j, using the index (m) as the mediating variable is defined by, see Shapira et al. (2009); Kenett et al. (2009); Baba et al. (2004).

$$\rho(i,j|m) = \frac{C(i,j) - C(i,m)C(j,m)}{\sqrt{(1 - C^2(i,m))(1 - C^2(j,m))}}. \tag{4.3}$$

Note that according to this definition, $\rho(i,j|m)$ can be viewed as the residual correlation between stocks i and j, after subtraction of the contribution of the correlation between each of the stocks with the index.

To investigate the dynamics of correlations in capital markets, we make use of a

running window analysis. We use a short time window, of 22-trading days, which is equivalent to one work month, with a full overlap. Thus, for example the first window will be days 1-22, the second window day 2-23, etc. At each window we calculate stock correlation and partial correlation matrices, and average them. This results in a value of correlation (partial correlation) for each stock, representing its average correlation (partial correlation) to all other stocks. This is defined as

$$\overline{C(i)} = \frac{1}{N-1}\sum_{j\neq i}^{N} C(i,j) \tag{4.4}$$

$$\overline{PC(i)} = \frac{1}{N-1}\sum_{j\neq i}^{N} \rho(i,j|m). \tag{4.5}$$

Finally, we calculate the average of average correlations (partial correlations), which represents the total average correlation (partial correlation) in the market,

$$C^{intra} = \frac{1}{N}\sum_{i=1}^{N} \overline{C(i)} \tag{4.6}$$

$$PC^{intra} = \frac{1}{N}\sum_{i=1}^{N} \overline{PC(i)}. \tag{4.7}$$

We denote this variable as the intra-correlation (intra partial correlation), as it represents the average correlation of stocks belonging to one given market.

Next, we investigate the synchronization of two given markets. To this end, we calculate correlation and lagged cross correlation between the intra correlations of each market. The correlation of market correlations is denoted as market meta-correlation (MC), given by

$$MC(d) = \frac{\sum_{t=1}^{N-d}\left(\overline{C^i(t)}-\left\langle\overline{C^i}\right\rangle\right)\left(\overline{C^j(t)}-\left\langle\overline{C^j}\right\rangle\right)}{\sqrt{\sum_{t=1}^{N-d}\left(\overline{C^i(t)}-\left\langle\overline{C^i}\right\rangle\right)^2}\sqrt{\sum_{t=1}^{N-d}\left(\overline{C^j(t)}-\left\langle\overline{C^j}\right\rangle\right)^2}} \tag{4.8}$$

$$d = 0, \pm 1, \pm 2, ..., \pm N-1, \tag{4.9}$$

where d is the lag.

Shapira et al. (2009) and Kenett et al. (2011) have shown that the market index has a cohesive effect on the dynamics of the stock correlations. This refers to the observed effect the index has on stock correlations, where we have found that larger changes of the index result in higher stock correlations, and as such more cohesive

force. The Index Cohesive Force is defined as $ICF(\tau)$ – calculated over a time window τ, as a measure of the balance between the raw and residual correlations given by,

$$ICF(\tau) = \frac{\overline{\langle C(i,j)\rangle_\tau}}{\overline{\langle \rho(i,j|m)\rangle_\tau}} = \frac{C_\tau^{intra}}{PC_\tau^{intra}}, \tag{4.10}$$

where τ is the time window, during which the average correlation and average residual correlation are calculated. $\overline{\langle C(i,j)\rangle_\tau}$ and $(\overline{\langle \rho(i,j|m)\rangle_\tau})$ are the mean of average correlation and average partial correlation.

4.3 Data

For the analysis reported in this paper we use data of the daily adjusted closing price from stocks in six different markets, all downloaded from Thomson Reuters Datastream. The markets investigated are the U.S., U.K., Germany, Japan, India and China. These include the four main stock markets as well as two less developed markets for comparison of the results. For each market we aimed for a sample as broad as possible, without any ex ante selection of branches. See Table 4.1 for details on the used stocks. The number of stocks finally used in our analysis shrinks down significantly, because we only consider stocks that are active from January 2000 until December 2010. Volume data was used to identify and eliminate illiquid stocks from the sample. Here, this corresponded to filtering for stocks which had no movement in the price for more than 6 percent of the 2700 trading days.

Market	Stocks used	Index used	# before	# filtered
U.S.	S&P 500	S&P 500	500	403
U.K.	FTSE 350	FTSE 350	356	116
Germany	DAX Composite	DAX 30 Performance	605	89
Japan	Nikkei 500	Nikkei 500	500	315
India	BSE 200	BSE 100	193	126
China	SSE Composite	SSE Composite	1204	69

Tab. 4.1: Sample statistics for stock data

It should be noted that the correlations measured have some explanatory limitations, which are mainly due to structural differences of the markets and to selection issues of the stocks. First of all, the dataset is by construction biased towards long-lived stocks. Secondly, the intra-market correlations have been calculated on the basis of a market index, which composition is undergoing changes over time. How-

ever, we are pretty certain that the exact composition of the index used for the normalization does not have significant influence on the results.

When we compare time series from different markets, some adjustments must be made, mostly due to differences in trading days. To this end, we either only used data from days in which trading was done in both markets, or we replaced missing data with that of the observation of the last trading day. These two methods yield very similar results for the correlation analysis. When comparing all markets together, we used the joint trading period of the London (U.K.) and Frankfurt (Germany) stock exchange (the bilateral pair which has the most overlap with all other markets) and again replaced missing observations for all other markets with last day observation. For comparisons of the U.S. and Japan one should be aware that it makes sense to consider observations of day t for the U.S. and $t + 1$ for Japan (the date barrier is in the Pacific), since these observations are closer to each other in terms of trading hours. Similar considerations can be taken for China and India, although the effect here is much weaker. In general the calculated correlations might also be influenced by the amount of overlap in daily trading hours, the amount of overlap in trading days, and general economic differences (as mentioned in the discussion). Also, the results depend on the time scale. Here we are interested in the medium run (a few weeks). A different kind of analysis of short-run effects, including a more detailed look on volatility, could be done with high-frequency (tick) data.

4.4 Results

4.4.1 Dynamics of the Individual Markets

A first proxy to the dynamics of the different world's economies is the dynamics of their leading market indices. Here we focus on six of the world's largest economies, representing western markets – U.S., U.K., and Germany – and eastern markets - Japan, India and China. The stock price indices of these countries are presented in Figure 4.1, showing mostly very similar dynamics.

Investigating the index volatility, rather than the index price reveals meaningful hidden information. Studying Figure 4.2, a similarity is observed between the three 'western' markets, while the volatility peaks of the 'eastern' markets only coincide for some time periods. Thus, it is reasonable to ask whether such uniformity between some markets, and multiformity between others, can be quantified.

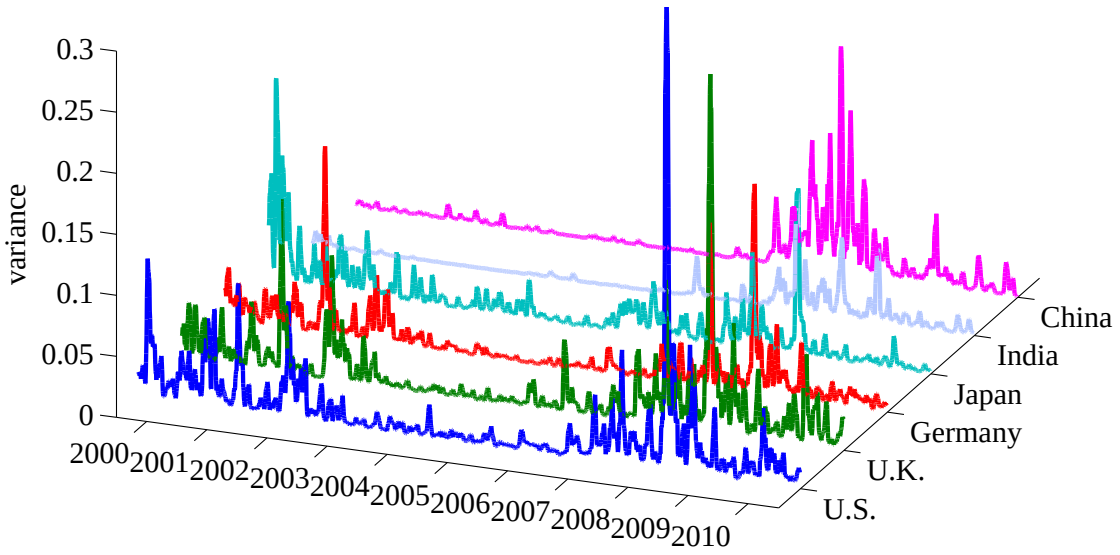

Fig. 4.2: Relative volatility in different markets

Relative volatility in the markets within a 22-day window. The price indices data was standardized for the 10-year interval (the mean is zero and the variance is 1 for each complete time series). The volatility peaks for the U.S, U.K. and Germany mostly coincide while there is less similarity with Japan. India and China show a very different behavior of volatility, especially until 2007.

4.4.2 Dynamics of Market Intra-Correlations

To understand the dynamics of capital markets, much research has focused on the analysis of correlations (see Mantegna and Stanley, 2000; Gopikrishnan et al., 2001; Aste et al., 2010; Plerou et al., 2000). It is standard practice to calculate the correlations between stocks in a given market, and we correspondingly calculate the correlations between the time series of the stock daily returns, for each market separately. To obtain a better understanding of the dynamics of correlations in each market, a sliding window approach is used to calculate the market intra-correlations, using a 22-day window. In Figure 4.3 we present the dynamics of the intra-correlations for each of the six markets (see Figure D.1 in the appendix for the dynamics of the intra partial correlations for each of the six markets).

For each market, a bursting behavior for the intra-correlations is observed. This is consistent with previous findings in Shapira et al. (2009). Furthermore, a similarity in the appearance of intra-correlation bursts is noted for some of the markets as is elaborated in the next section.

Next, we calculate for each of the markets the Index Cohesive Force (ICF, Figure 4.4). High values of the ICF correspond to a state in which the market index dominates the behavior of the market, thus making it stiff and more prone to systematic

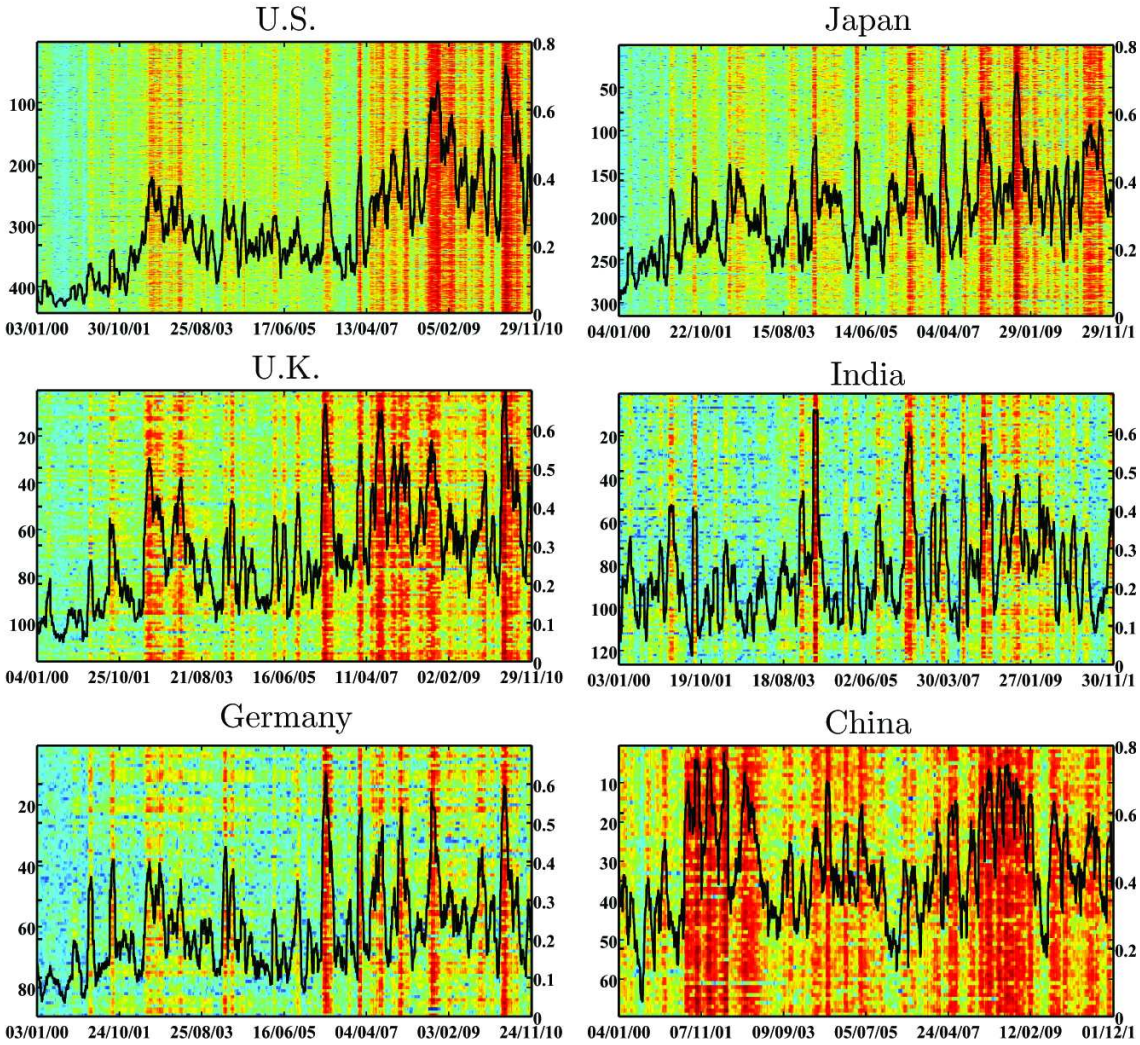

Fig. 4.3: Dynamics of the intra-correlation

Dynamics of the intra-correlation. For each market, we use a 22-day window, and in each window calculate the intra-correlation. This results in the dynamics of the intra-correlation for the period of 2000–2010, for each market separately. Each horizontal line represents the average correlation of one stock (the left y-axis displays the number of the stock). The western markets and Japan show a similar behavior, visualized through vertical stripes at the same time, showing synchronized waves of strong correlations. The black line shows the average of all correlations at a given 22-day window (corresponding to the right y-axis). The trend is increasing for all countries except for China.

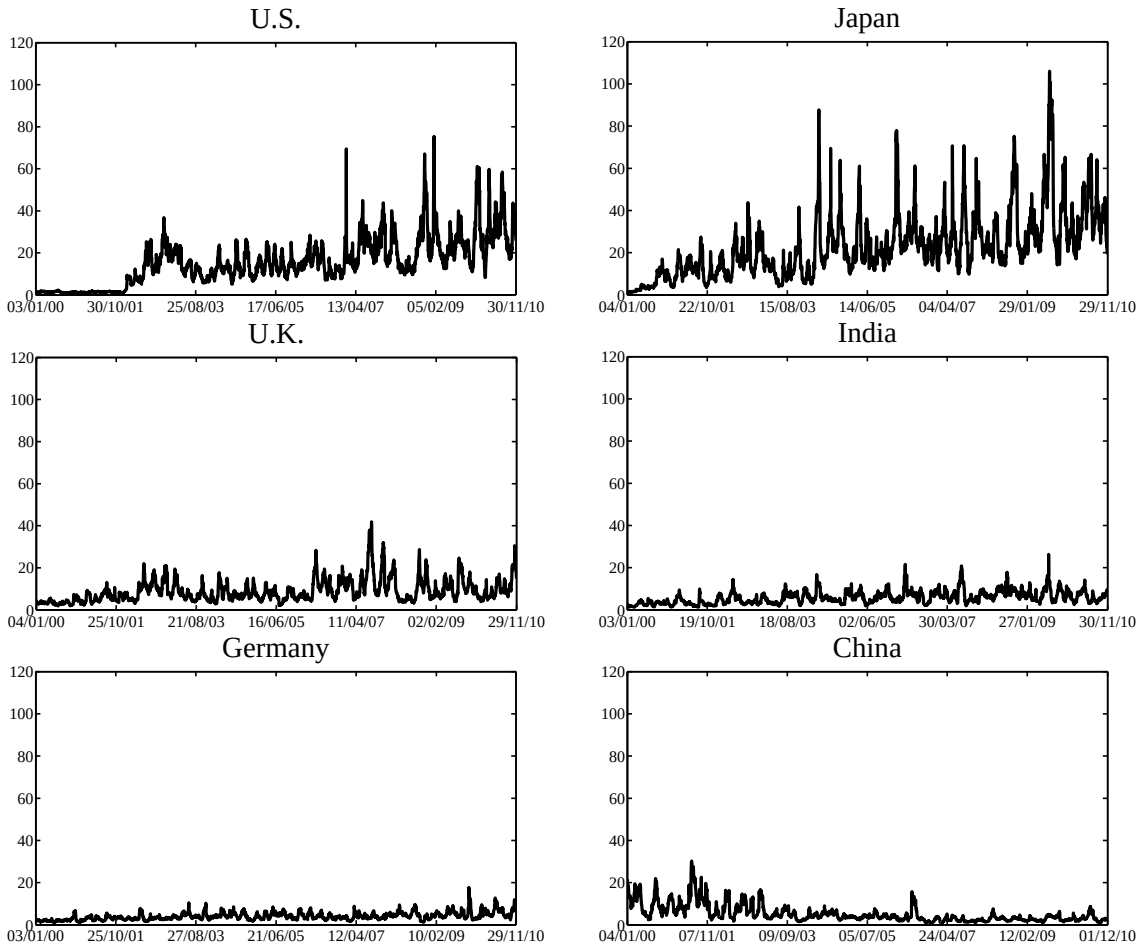

Fig. 4.4: Dynamics of the ICF

The dynamics of the ICF for each market is plotted for the period of 2000–2010. The ICF is increasing in the western markets, especially since 2002. In China we observe a decreasing trend.

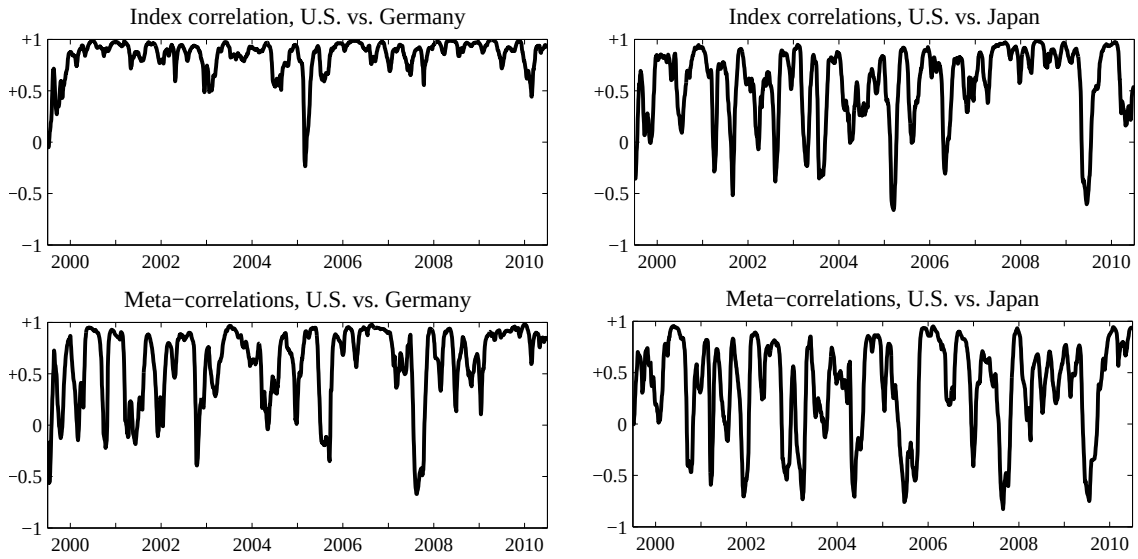

Fig. 4.5: Index correlations and meta-correlations
Index correlations (top) and Meta-correlations (bottom) for the U.S vs. Germany (left) and Japan (right). Both calculated using a 66-day window. The U.S. and Germany show a higher similarity for both measures than the U.S. and Japan. While both measures fluctuate over time, we observe that high correlations do not necessarily show jointly in the top and the bottom figure. We can thus differentiate between times of identical price movements (high index correlation) and global stress (high index correlation and high meta-correlation)

failures. By studying Figure 4.4, it is possible to observe that some markets are similar in their dynamics of the ICF. Some similarities can be observed for the U.S., U.K., Germany, and Japan, whereas China shows a significantly different behavior. The ICF of the U.S. and Japan displays similarity in trend and magnitude, whereas U.K., India and Germany have a similar trend but much lower magnitude. Finally, China shows very different behavior than all other markets.

Markets featuring similar values of the ICF will have a similar dependency on the market index. Thus, if the indices of these markets are highly correlated, these markets should be strongly coupled. As such, the ICF provides new important information on these couplings.

4.4.3 Inter-market Correlations in the Global Financial Market

The observed similarities of indices and correlation patters leads to the question of how synchronized stock markets are with respect to changes in these measures. Thus, we computed the meta-correlations – the correlations between the intra-correlations, using a 66-day window. The index correlations, the index volatility correlations and the ICF correlations were calculated using the same window size.

According to the index correlations the three 'western' markets - U.S., U.K. and Germany - are highly correlated. The index correlations between Japan and India and all other markets are significantly weaker (the difference between these two groups is even more visible for the index volatility). China finally seems rather uncorrelated with the rest of the world, although some upward trend is visible (see a year by year breakdown for the market pair correlations in Appendix D.2). However, index correlations capture only partially the inter relations between different markets.

The introduction of the Index Cohesive Force makes things easier when one is considering the dynamics of a particular market and especially if one is interested in its stability, and provides a valuable measure to assess the state of each individual market. Previous work has shown that in the case of the U.S. market, low values of the ICF (lower than 10) correspond to a relatively healthy state of the market. Specifically, it was found for the U.S. market that the ICF was close to zero, whereas in 2008 it was approaching 60. To further illustrate this point, we have found that the distribution of the ICF values change during times of economic stress, displaying much fatter tails (see for example for the Japanese market in Appendix D.3). However, the ICF has been found to be highly fluctuating, and thus the ICF correlations between markets do not provide a reliable measure of the market inter relations.

Much better results are obtained using the meta-correlations. Using this measure, we found that the three 'western' markets have a high level of uniformity. The Japanese market appears to be significantly more influenced by the 'west' than the Indian market, the Chinese has the lowest correlations. The latter is in line with what was expected for example given the capital controls and regulations in China and limitations for foreign investors, see also Chen et al. (2010). Using a cross-correlation analysis, it is possible to further investigate the level of synchronization between the different markets. Typically, the lag (the time delay for maximum cross correlation) is 0 for high correlations and it fluctuates for low correlations (see Figure 4.5 for the correlations of the U.S., Germany and Japan, and the Figures in Appendix D.4 for the meta and index correlations for all markets, see Appendix D.5 for an alternative visualization for the U.S. market only). Generally speaking, we observe that the magnitude of inter market correlations fluctuates similarly like the magnitude of the intra-market correlations of the different market pairs.

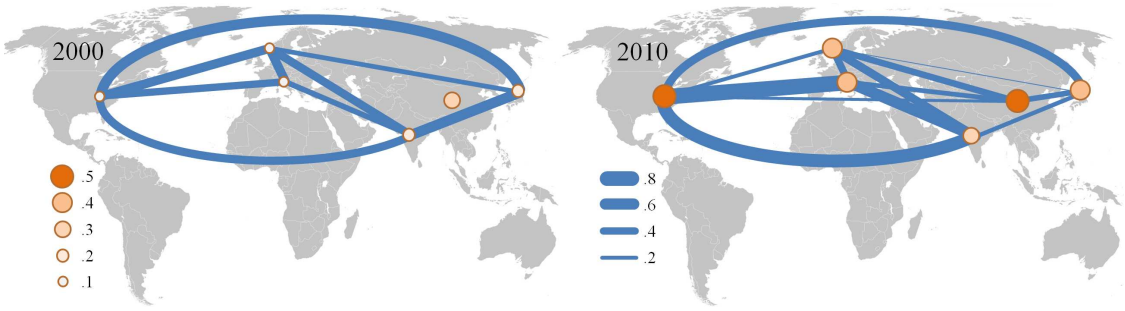

Fig. 4.6: The global financial village
The global financial village for the years 2000 (left) and 2010 (right). The width of the edges of the graph is proportional to the meta-correlation between the markets it connects (right legend). The node size is proportional to the inter-correlations (left legend). For 2000 we observe markets with low intra-correlations and inter-correlations of similar magnitude, excluding China. For 2010 we observe much higher intra-correlations in all markets and a denser network of interdependencies. (The nodes for the U.K. and Germany are further away from each other than their geographical position)

4.4.4 Dynamics of the Global Financial Village

The coupling of markets, as quantified by the meta-correlation, changes over time. The Japanese market switches between following the 'western' and following the 'eastern' worlds: for some time intervals it behaves very similar to the U.S. market (which is also similar to the U.K. and Germany markets), and at other times, the intra-correlations of Japan behave more similar to that of the Asian countries. Similar observations can be made for U.K. and Germany and their similarity to the U.S. vs. Asia. The interdependencies between India and China and the more developed markets are very volatile over time and show maxima in years with important global events (2001: 9/11-attacks, 2003: Iraq war, SARS, etc.). To illustrate the general development, we show the differences in coupling between markets during 2001 and 2010 (see Figure 4.6). The line strength is proportional to the level of the meta-correlations. The world's financial markets show a higher uniformity in the later years of our analysis.[1]

4.5 Discussion

This paper presents a new framework for quantitative assessments of the coupling and interdependences between different markets in the global financial village. The

[1] A video visualizing the development of market interdependencies is available online: http://dl.dropbox.com/u/16978699/globalmarket.mp4

new approach also provides the means to study feedback between the micro (intra market) and the macro (inter markets) levels. More specifically, the stock-stock correlations in the individual markets represent local market dynamics, whereas the meta-correlations represent global market dynamics. Thus, the methodology presented here of intra and meta correlation analysis provides the means to study the bottom-top and top-down feedback mechanisms which take place in the world's economies.

Our results provide new information about the uniformity preset in the world's economies. We find significant uniformity for the three western markets, whereas Japan and India display a greater extent of multiformity; however, this multiformity is time dependent, and periods of significant uniformity with the western markets are observed. Unlike these, the case of China is significantly different. For all our measures it shows an amount of segmentation that is not in line with China's important role in the world economy, especially the huge trade flows we observe.

Earlier studies hint that the sole legal possibility to invest in emerging markets is not sufficient for their full integration with other markets. Investment funds and other institutional investors need accompanying financial products (i.e. country funds, depository receipts, and other derivatives), which are only gradually becoming available in emerging markets. Country specific risks, taxes and holding time requirements can further dampen cross-border investments (see Carrieri et al., 2007; Bekaert and Campbell, 1995). In China, significant parts of the economy are still state-owned. Furthermore, the Chinese stock market is differentiated into one for foreign investors and one for domestic investors. The amount of share holdings for private and foreign investors is still subject to substantial governmental restrictions (see, e.g., Zhu and Pan, 2011). These restrictions are obviously an effective and significant measure to deter foreign investors, and cause a partial de-coupling from other markets. Nevertheless, the methods presented here provide the means to quantify functional differences between developed and emerging markets. Further research is required to expand on this, especially by means of studying many more developed and emerging markets, and their coupling and interdependencies.

Finally, some interesting observations can be made about the general development of financial markets. It has been much debated that markets have become more coupled over the last years, and that we are observing the downside of this development right now during the debt crisis within the Eurozone and the U.S., expressed in pronounced synchronized movements of stock markets. From our analysis it becomes evident that this uniformity does not only stem from an increase of correlation between markets, but that there has also been an ongoing simultaneous

shift towards uniformity in each single market.

In conclusion, using new specially devised analysis methods, we provide the means to investigate and quantify uniformity and multiformity in the global market, and changes in these measures. In the current era, when the global financial village is highly prone to systemic collapses which can sweep the entire village, our approach can provide a sensitive "financial seismograph" to detect early signs of global crises.

5. STRUCTURE IN THE ITALIAN OVERNIGHT LOAN MARKET

5.1 Introduction to Bank Networks

In this chapter we investigate the lending behavior of banks in the Italian overnight loan market. Unlike in most other European countries in Italy, most of the overnight loans are settled by a central trading platform called E-mid. For our analysis we use tick data from this platform from the period 1999–2010. Although loans with different maturities are dealt over this system we focus on overnight loans, which are by far the biggest part of all transactions.

Since the 2008 financial crisis the overall interest in the linkages between banks has risen. Only little research was carried out before, some European markets have been analyzed for example by Iori et al. (2008), Boss et al. (2006), Furfine (2003), Hartmann et al. (2001) and Cocco et al. (2009). The U.S. money market system, Fed-wire, has been analyzed for example by Ashcraft and Duffie (2007).

The risen interest in these markets is twofold. On the one hand it stems from the observation of the partly collapse of interbank markets itself, the other reason is the increasing need for risk assessment in the bank network in general. The contagious effects that played a big role in the events after the Lehman default[1] showed that a micro-prudential analysis of banks' exposures does not capture the systemic risks that the default of a bank can have.

Banks are of course connected through many different financial products, the analysis of overnight loans which we perform here is thus only a first step in understanding the networks of banks.

Until 2008 all bigger banks could relatively easy manage their short and medium run liquidity with various trading partners in different interbank markets. Since then the behavior of banks in the interbank market has changed dramatically. The volume in the interbank markets has fallen sharply, see, e.g., Gabrieli (2009) for

[1] The U.S. investment bank Lehman Brothers Inc. defaulted on 15th September 2008, marking the highpoint of the subprime mortgage crisis. It was followed by a sharp drop of all major stock price indices and financial market distress that necessitated massive bailout programs for banks around the world.

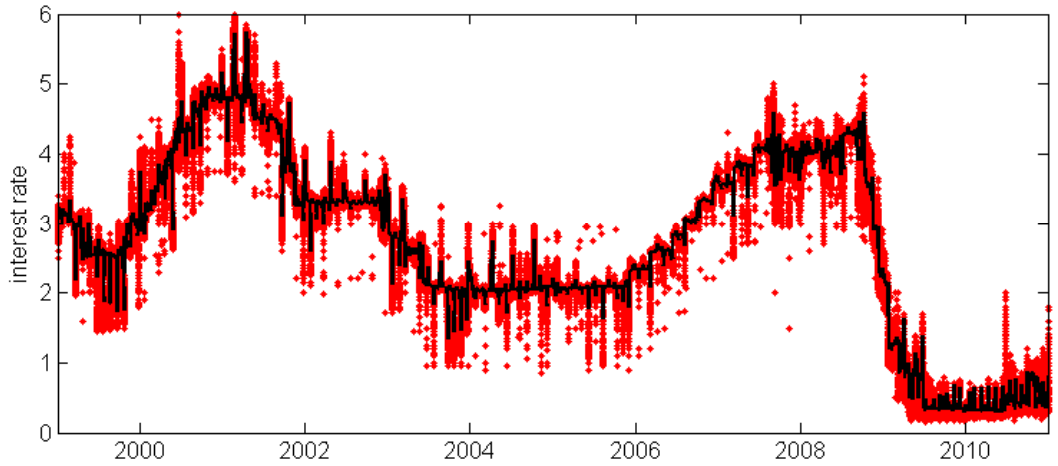

Fig. 5.1: Interest rates in the E-mid market
The plot shows the daily mean rate in the black and every individual trade as a red dot. Cyclical peaks are visible at each end of the month. Overall most of the average rates are very close to the EURIBOR rate.

the E-mid case, instead of a rise of spreads that would compensate for grown credit risks, we observed a shift from interbank market funding to funding by central banks. Very recent studies nevertheless show that interbank markets are still important, but that the trading activity has changed noticeably. These studies include Afonso et al. (2011) and Bech et al. (2011) for the Federal Funds market and Angelini et al. (2009) for the Italian market.

The earlier studies on the Italian market have already shed light on a number of statical regularities of trading behavior in the market. Also, we know that no pronounced clusters exit in the Italian market when conditional trading volume is analyzed, see Fricke and Lux (2012). The structure of the market can at best be described as a core-periphery structure, similar to the findings by Craig and von Peter (2010) for the German market.

Relatively little interest has been devoted to the analysis of interest rates from individual contracts. Hence, this paper will try to add some insights into the structure of this market by looking for preferential lending relationships between banks. Further we will look at how lending conditions and trading volumes developed over time and in which respect the market of today differs from the market as it was before the financial crisis. However, as a starting point we will have a look at the more general statistical patterns of trading activity.

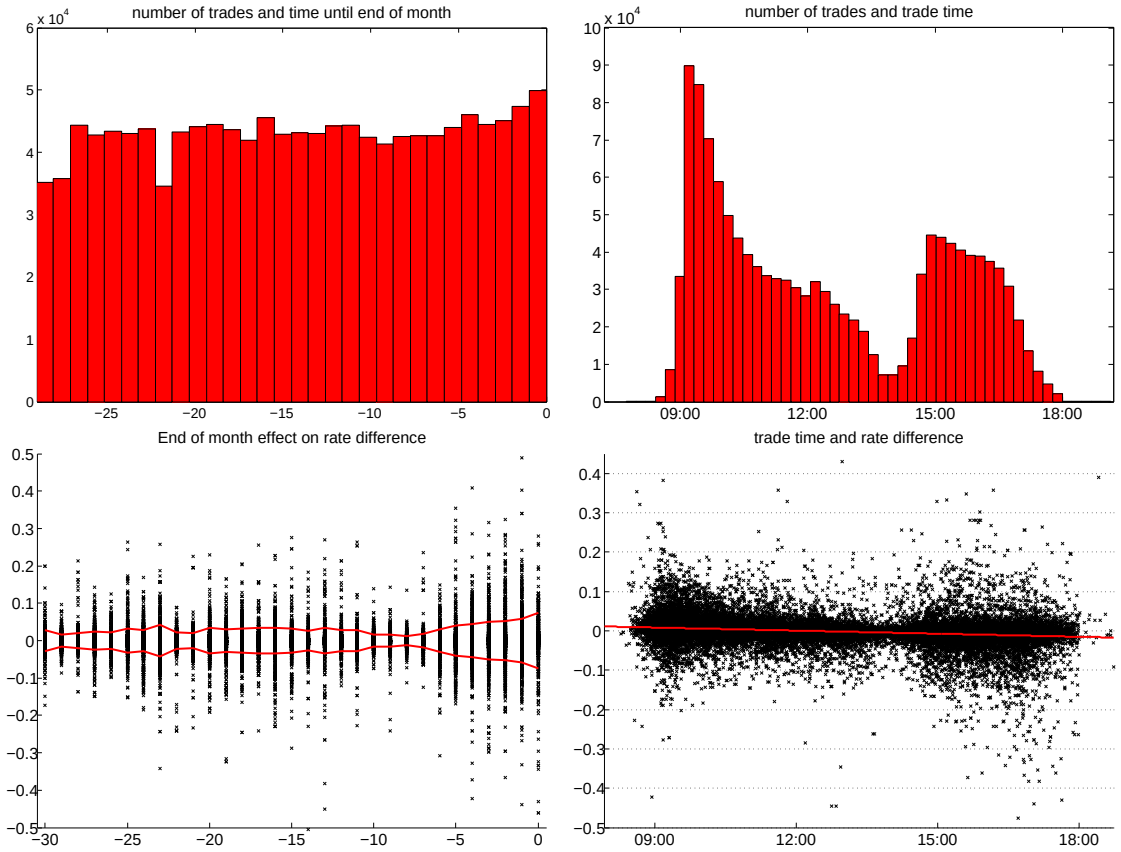

Fig. 5.2: Regularities in trading behavior and rates during the day and month
Top left: the trading activity shows a slight increase at the end of the month, Bottom left: the standard deviation of the average daily rate (red) is increasing at the end of the month, Top right: trading activity shows regular maxima in the morning and afternoon, Bottom right: the deviations from the average daily rate become negative during the day, as shown by the linear fit of the red line.

5.2 Regularities in Trade Behavior

Figure 5.1 gives a first overview of the rates that are paid in the market. The average volume weighted daily mean is given by the solid black line. It follows very closely the EURIBOR rate. Periodic peaks occur on and before every 24th of each month, when the banks balance their positions and report to the supervisor. Each single trade is marked by a red dot, the resulting red area shows the effective range of interest rates being paid. Almost all observations are within the band of the European Central Bank's deposit facility and marginal lending facility rate (for example for the period from June 2003 until December 2005 these rates were at 1% and 3%).

The daily and monthly patters of trading behavior are shown in Figure 5.2.

Within the month we observe a slight increase in trading volume when we approach the 24th. The top left plot shows the number of trades for the days preceding the 24th with descending distance. The bottom left plot shows the dynamics of rate volatility. For comparable results we calculate the difference of each trade's rate from the average weighted daily mean and plot rates for the separate days. The red line indicates the standard deviation for each day. We observe the highest volatility of loan rates at the end of the month.

The daily trading patterns are very regular and are summarized by the top right plot. Pronounced peaks of trading activity are visible around 9 a.m. and 3 p.m. and a smaller one at 12:30 p.m., these can be explained first by office hours and secondly by the regular liquidity in and outflow that stems from the settlement of last day's E-mid trades and settlement from other trading platforms including the cash leg of securities. In general we can confirm the results of Iori et al. (2008).

At last we can look at the development of the average rates during the day. The right bottom panel shows a scatter plot, the average rate is slightly decreasing towards the end of the day, just as the maturity of any initiated contract is effectively decreasing by a few hours.[2] For a detailed analysis of the intraday development of loan rates see Baglioni and Monticini (2008).

5.3 Volatility and Trade Flows

An inspection of the interest rates over time reveals that trading behavior has changed significantly over the last years. Figure 5.3 shows a massive increase of volatility in September 2008 after a transition period that starts in early 2007. For this reason we start with looking at the market for the period from 1999 until 2006, to see how the market is organized in "normal" times and turn to an analysis of the dynamics until 2010 in Section 5.5

As a starting point we have a look at the number of trades and trade volumes for all market participants. We can plot the relationships between all banks as color coded values in a adjacency matrix. Every row in the plots in Figure 5.4 symbolizes one bank i and the entries in the columns give us information about the trades with every other bank j. The rows and columns in all plots are ordered first by nationality of the banks (first foreign banks, then Italian banks) and second by trade volume in ascending order. By definition an entry in row i column j can be interpreted as a relationship where bank i is the borrower in a contract with bank j.

[2] For better visibility the two bottom scatter plots only show a random subsample of the dataset.

[3] The UK bank Northern Rock was faced with severe liquidity problems in September 2007 which finally lead to the bank becoming state owned to prevent a possible default.

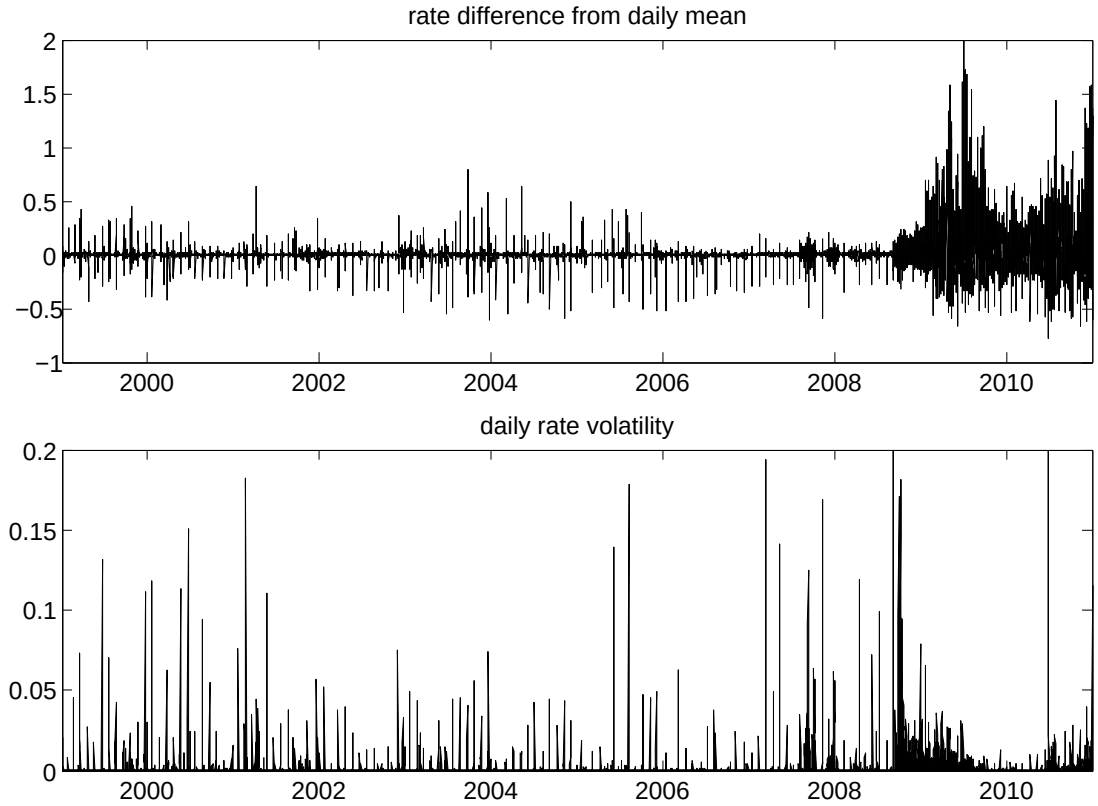

Fig. 5.3: Interest rates and volatility over time

The top panel shows the difference from the mean daily rate for all trades. The bottom panel shows the daily volatility of loan rates. While for the period until early 2007 there are no permanent volatility increases, we see a change in late 2007, when with the Northern Rock bank run[3] *volatility increases slightly, before in late 2008 we observe a drastic change in the market.*

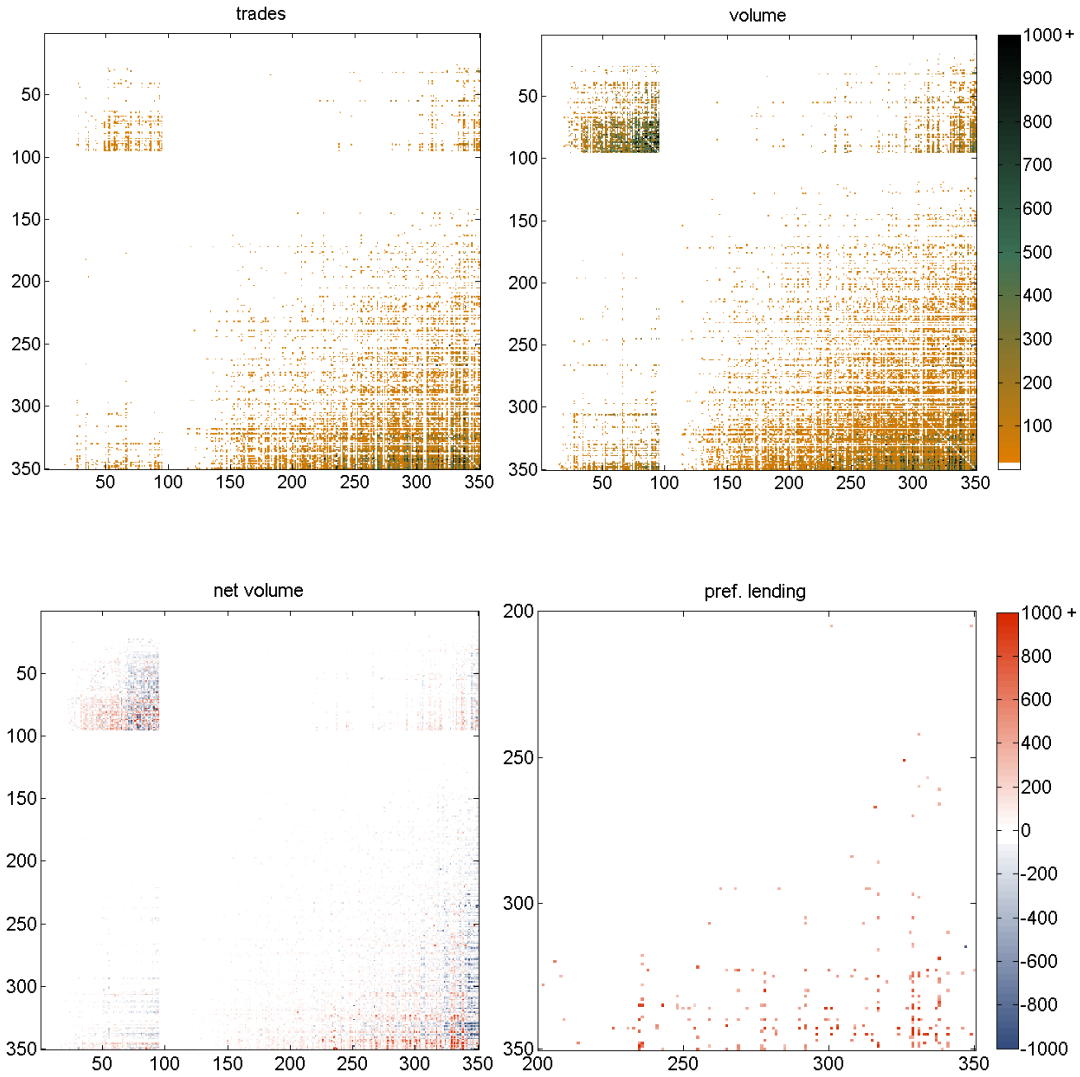

Fig. 5.4: Trade flows, volume and net volume, 1999–2006
Top left: Number of trades, Top right: aggregate volume, identical values for the color coding of number of trades and volume in millions of Euro, Bottom left: Net volume, Bottom right: Net volume for preferential lending relationships from the estimation in Section 5.4. The rows and column are ordered: first into foreign and Italian banks, then by total trade volume. Row entries are borrowing transactions, column entries resemble lending. The plots show the asymmetry in lending, the banks with the highest trade volume are large net borrowers.

From the two top panels we can infer two regularities of the market. First of all, the foreign banks are much more visible in the right plot of aggregate trade volume than in the left plot showing the number of trades. The explanation is that the average volume per trade for foreign banks is significantly larger than for Italian banks. Obviously only larger foreign banks take part in the E-mid market. Secondly, the volume plot is far from symmetric. For the large banks at the bottom of the plot we observe pronounced borrowing activity which is not offset by an equal amount of lending, that should show as dark entries in the rightmost columns. To clarify this issue, the bottom left plot shows the net amounts that result from all trades. This plot is symmetric by construction. We observe that the banks with the largest trading volume are mostly net borrowers in the market.

The loan transactions that we have just seen expressed by a plot of the adjacency matrices can of course be interpreted as a network between the banks in this market. Two problems arise when one wants to map these relationships into a meaningful graph. For very short periods of time aggregation the resulting networks are very volatile and show a high level of randomness. Since thousands of transactions take place on a single day, the aggregation of trades over a longer time span will result in network representations where every bank with some activity will be connected to a very large share of the market participants. From the economic view point there is nothing wrong with this finding. It shows that the market is efficient in the sense that excess liquidity is distributed in the absence of noticeable market segmentations.

A resulting network representation is shown in Figure 5.5. To get an impression of the most important ties in the lending network from 1999–2006 we only consider links that correspond to a minimum of 250 borrowing transactions. As a result we see the strongly connected cluster of (mostly) Italian banks. Some hubs are visible in the core of this network, most of them are characterized by a high in-degree, which reflects the lending asymmetries discussed above.[4]

[4] The visualizations of the networks was performed using the software Pajek and the algorithm by Kamada and Kawai (1989) which produced a planar representation of the graph by minimizing the length of the edges.

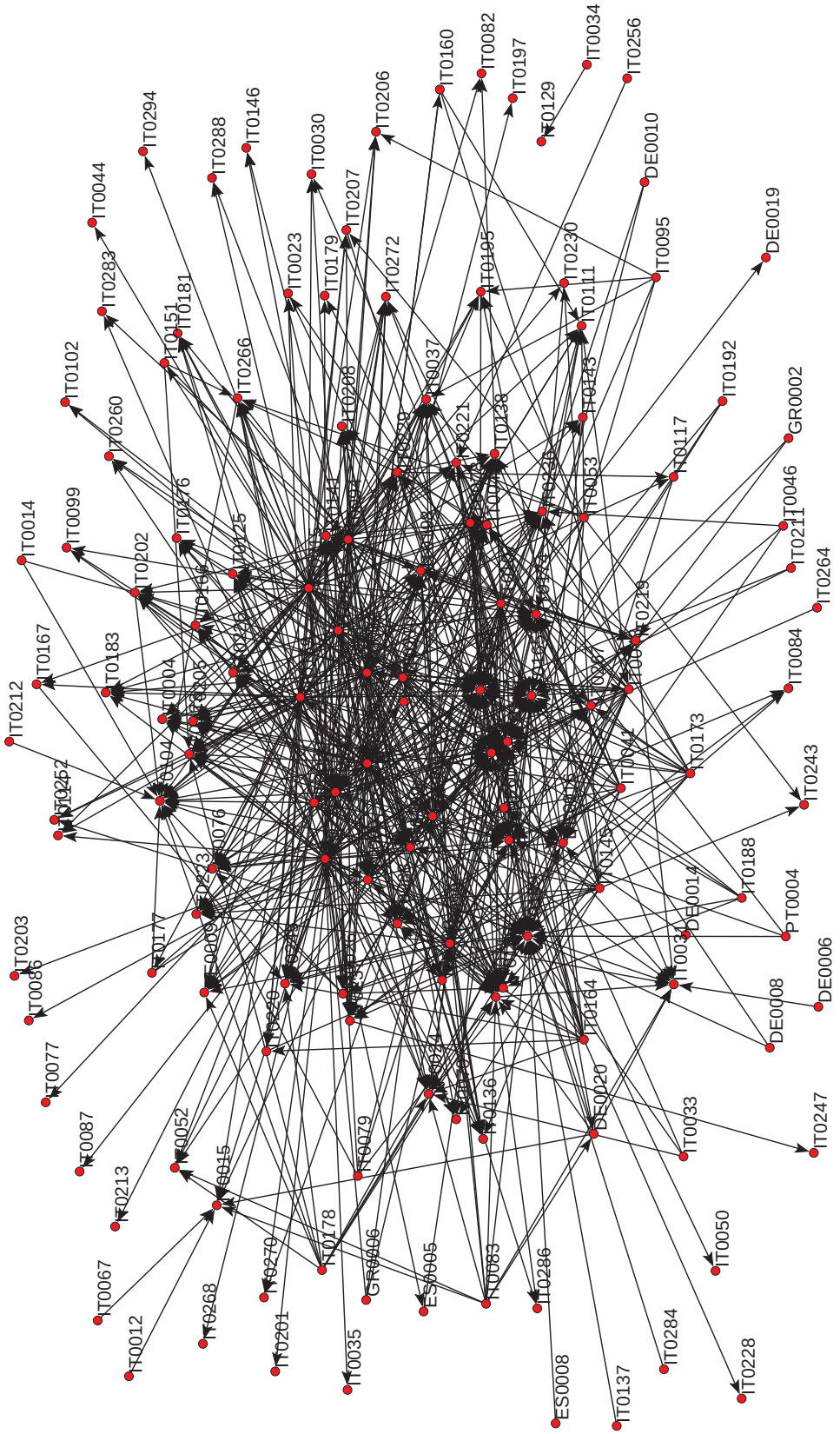

Fig. 5.5: Network of Italian banks 1999–2006

The figure shows a dense network with some noticeable hubs characterized by a high in-degree. Arrows point at the borrower in a lending relationship with at least 250 transactions.

5.4 Estimation of Credit Spreads and Preferential Lending Relationships

5.4.1 What Loan Rates Can Tell

The relatively large dataset with about 1.3 million observations allows us not only to investigate trading patters, we can of course also investigate if banks trade at loan rates that differ significantly from the mean. For the years until 2006 the spreads for overnight loans cannot be expected to be very large since the counterpart risks for a one day loan are rather meaningless. Nevertheless, the range of banks that trade in the market is large, we have some global players but also some very small institutions, hence, some difference in risk should be priced in at least in a long run average.

In case that banks trade with each other very often, we can also analyze if the trading for this pair results in loan rates that differ from the average, conditional on the individual spreads and some other control variables. Significant deviations for pairs of trading partners can then be interpreted as a situation where preferential lending takes place between couples of banks. This analysis of "friendly" relationships could help to distinguish "random" trading relationships from those where institutional or personal ties play a role.

5.4.2 Estimation

The varying volatility in the market is of course a problem for the estimation, thus, similar to Cocco et al. (2009) we use the daily volatility to normalize the basis point interest rate differences that is our dependent variable. The remaining intraday volatility fluctuations are rather unsystematic. To obtain values that can be interpreted similar as interest rates we multiplied the standardized rate differences by the average of daily volatilities. The resulting variable is *bpd*. Further we discard the observations from the last day of each month and single days with an extremely high volatility, since trading behavior here differs noticeably from "normal" days and is of no help for our estimation.

As in most high frequency financial data we observe strong dependence. In contrast to stock markets, where the squared price changes show long lasting autocorrelation as a consequence of long memory in volatility (see, e.g., Engle and Russell, 2010), our data shows this feature even in the raw price changes. Since we are only interested in effects that happen on top of some autoregressive process, we estimate different versions of our model and compare the results to check for robustness

In the "simple" model we account for autocorrelation in the data by taking a weighted average of the last 8 trades, denoted $\overline{ar}$ to filter for autocorrelation[5]. We can then further estimate the bid ask spread in the data, ba, the influence of the log traded amount am, the influence of trading time tm, and the day, given by the difference until the end of the month EoM (the last three all as deviations from their mean values, day and time measured in units of days). For all the roughly 180 banks with at least 250 loan contracts we can estimate their spread by adding a matrix of dummy variables B. This matrix then has 180 columns with entries in B_{ti} if bank i is the borrower in contract t. Similar we can estimate pairwise relationships and add the dummy matrix $P_{ty(i,j)}$, where P has as many columns y as we have couples of banks i and j where bank i is borrowing at least 250 times from bank j. This results in estimating

$$bpd_t = \beta_0 + \beta_1 \overline{ar}_t + \beta_2 ba_t + \beta_3 am_t + \beta_4 tm_t + \beta_5 EoM_t + \gamma B_t + \eta P_t + \epsilon_t \qquad (5.1)$$

In order to get an idea of the influence of the standardization procedure we also estimate this model with a filtered version of the raw loan rate differences. The sample here gets smaller, because we filter all trading days where the volatility is larger than 0.0005, a value that produces a time series where the heteroskedasticity seems not too bad. Further we estimate the model also without P to make sure the estimation of bank fixed effects and preferential lending are independent.

The simple model actually works very well for the short run autocorrelation but for longer horizons some remains visible. In the "extended" model the autoregressive process is specified in a bit more detail. Similar to the so-called HAR model by Corsi (2009) we model the autoregressive process with variables that cover different parts of the lag structure. In addition to the $\overline{ar}$ term, which reflects the current market price, we introduce $\overline{ar}^q$ and $\overline{ar}^h$ which reflect the average price differences from the last 15 minutes and the proceeding hour of trading. The extended model can be written down as

$$bpd_t = \beta_0 + \beta_1 \overline{ar}_t + \beta_2 \overline{ar}^q_t + \beta_3 \overline{ar}^h_t + \beta_4 ba_t + \beta_5 am_t + \beta_6 EoM_t + \gamma B_t + \eta P_t + \epsilon_t \qquad (5.2)$$

In this model the effect of time tm cannot be estimated since this would conflict with the long run rate variable $\overline{ar}^h$. When we test this specification of the model and

[5] The weights were derived from the coefficients when estimating the model with 8 lags. Hence the result is the same as estimating the model with 8 separate lag terms, but a weighted average has shown to be more stable when adding all other variables.

regress only on the *ar* variables, we see that it removes the autocorrelation better than the simple model, not to say perfectly. However, when we add all our dummy variables we see from the DW statistics that the filtering is acceptable but not as good. The likely reason for this is that also our dependent variables show some autocorrelation which might lead to a slight underestimation of $\overline{ar}$. This effect can be dampened by removing trades from the dataset where one bank is the borrower in successive trades. Essentially this mean that we remove trades that are likely to result from order splitting.

In general one should keep in mind that the micro-structure of this loan market differs from, for example, stock markets in two decisive ways. First of all, unlike stocks, loans are not a perfectly homogeneous good; if a lender wants to make a loan contract depends on the credit quality of the borrower and possibly on his already existing exposure to this borrower. Secondly, the market is not anonymous, the counterparts of a trade know each other, and might negotiate about a trade before settling it on the E-mid platform (see also Beaupain and Durré, 2008). This is likely to lead to a sluggish reaction to price movements. While new prices are quoted several times within a minute in busy trading periods, the effective time it can take to negotiate and process a trade is likely to be a bit higher, say, in the order of minutes.

5.4.3 Results

Table 5.1 shows the OLS estimation results for four versions of the model. A constant is needed because the volume weighted average daily mean rate differs from the unweighted average over all trades. The coefficients β_1 to β_6 are all significant (mostly on the 99% level) and have the expected sign. The difference of the results for the models using raw data versus the standardized data are visible but they still yield comparable results. Since more volatile trading days have been filtered from the raw data sample the coefficient for the autoregressive term is still a bit larger than for the standardized data model. The same effect might explain the difference in the coefficients for time tm. The influence of the day EoM seems to be limited on the volatility pattern we saw in the previous section, from the table we see that the influence is very small and the exact result seems to depend on details of the model specification and the filtration of the dataset.

The estimation results are stable when adding the preferential lending fixed effects P, none of the other variable changes sign, changes in the coefficients are negligible, given that we triple the number of variables in this step.

In the extended model most of the split orders, which come predominantly from

indep. variable	raw data	std. data	std. data	ext. model
$const$	.2367	.2162	.2290	.1135
	(31.5)	(28.3)	(30.8)	(18.2)
$\overline{ar}$	.6506	.6698	.6662	.4302
	(689.9)	(867.2)	(882.9)	(277.3)
$\overline{ar}^q$				.3034
				(159.7)
$\overline{ar}^h$				.1172
				(74.2)
ba	.4909	.4686	.4422	.5472
	(272.5)	(333.3)	(313.1)	(318.4)
am	.0707	.0654	.0498	.0496
	(83.1)	(97.2)	(67.8)	(62.3)
tm	-.2453	-.1765	-.2239	
	(-30.7)	(-28.2)	(-35.7)	
EoM	-.0015	-.0006	-.0006	.0002
	(-15.9)	(-8.1)	(-8.3)	(2.2)
B	#172	#189	#189	#176
P			# 755	#412
obs.	660,155	949,013	949,013	663,264
DW	1.98	2.00	1.98	1.91
σ^2	.3700	.3336	.3166	.2935
R^2	.6416	.6408	.6590	.6724

Tab. 5.1: Regression results

Results from the OLS regression. The left column contains the results for the raw data model, the two center columns results for the standardized data simple model. The results for the extended model are in the right column. T-values are in parentheses. The number of variables for the borrower fixed effects B and preferential lending P are shown below. The estimation results for these variables are summarized in Figure 5.6 and 5.7.

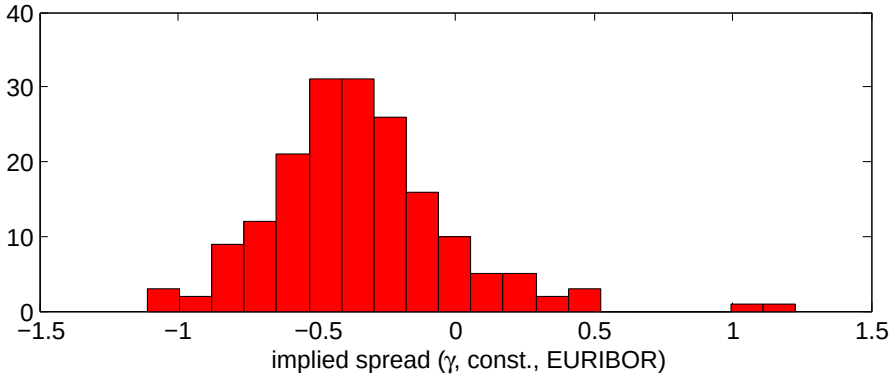

Fig. 5.6: Implied credit spreads
The histogram shows the implied credit spreads for the period 1999–2006. The reference point is the EURIBOR rate. The average rate in the Italian market was on average marginally below the EURIBOR rate, most banks trade within a range of 2 bps.

the larger banks, have been removed. As a consequence the sample contains relatively more trades from small banks, which results in a higher average loan rate. Due to the lower number of observations fever relationships P can be estimated. The DW value is slightly worse than for the simple model, because it only accounts for autocorrelation on lag 1.

To compare the simple and the extended model in a bit more detail we checked if the estimated fixed effects γ and η are similar. In fact the bank fixed effects are almost identical, although the sample size for the extended model is much smaller. The estimation results for preferential lending relationships show some variations, here the absolute values seem less reliable, but the classification into preferential versus non-preferential relationships is rather robust. For details see Figure E.1 in the appendix.

To check for the significance of the results we perform a simple bootstrapping experiment for both, the bank fixed effects γ and the preferential lending relationship fixed effects η. This is done by separately re-shuffling the dummy matrices B and P and repeatedly estimating the model with these randomized dummy matrices. An alternative p-value can than be calculated from the bootstrapped distributions of the resulting γ and η. The results confirm the p-values calculated from the t-statistics.[6]

[6] For η for example, a coefficient value of .059 marks the 95% confidence interval from the bootstapping experiment, while the t-statistics suggest a value of .058 (assuming the same average variance). Alternatively the dummy variable P can be shifted in time, which conserves the autocorrelation. In this case the bootstrapped distribution of η becomes slightly assymetric and the bounds for the 95% interval are -.07 and .06. To summarize, this indicates that the significance of the estimates are (if at all) most likely only slightly overstated by the regular t-statistics.

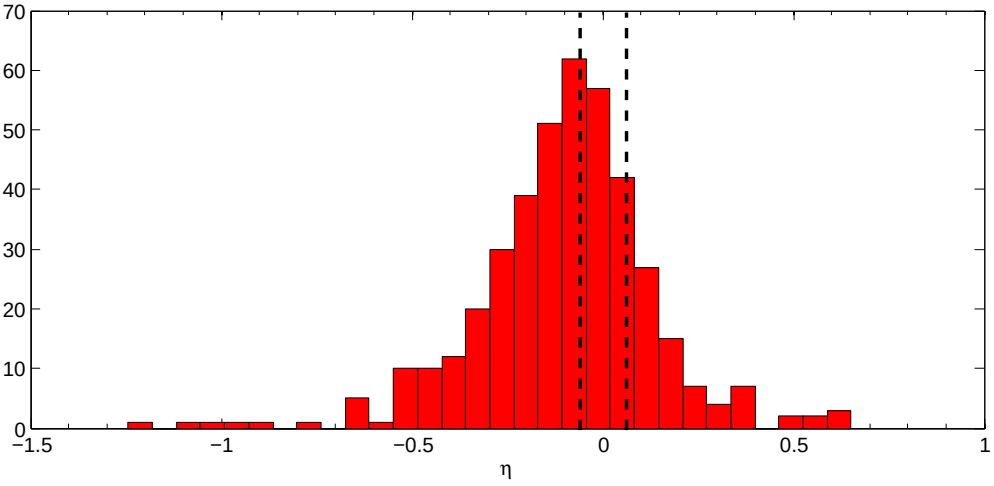

Fig. 5.7: Estimated coefficients for frequent trading relationships
The histogram shows the estimated deviations of the interest rate for trading relationships with at least 250 trades. The 95% confidence interval is indicated by the dashed line. The distribution is biased towards negative values which means that the majority of frequent trading relationships comes with a slightly lower loan rate. Values derived from the extended model.

The distribution of borrower fixed effects γ, which can be interpreted as credit spreads are shown in Figure 5.6. Here we show them as the difference from the EURIBOR rate. Obviously most of the banks borrow within a band of 2 bps, which is not much. However it is important to account for these effects before we turn to the pairwise bank relationships, which would otherwise be overshadowed.

The influence of preferential lending finally is shown in Figure 5.7. The distribution of preferential lending effects is biased towards negative values. This is not totally unexpected, because in this subsample large banks should be overrepresented, remember that only relationships with a minimum of 250 borrowing transactions are estimated. We can visualize these preferential lending relationships by looking at its adjacency matrix. A plot with all relationships where the loan rate was significantly lower (95% conf. level) than the average is shown in the bottom right panel in Figure 5.4. The plot shows the net volume for these lending relationships (in this plot the bottom right part of the adjacency matrix is magnified). The most frequent lending relationships are characterized by one-sided borrowing activity. Significant deviations from the mean loan rate occur only for Italian banks. Preferential lending, as shown in the plot, happens predominantly when top 30 banks borrow from smaller Italian banks or from other banks with very high market volume.

We can also show the network of these preferential lending relationships in Fig-

Fig. 5.8: Network of preferential lending relationships

The network of preferential lending relationships has about half as many links as the trade network. The maximum degree is significantly reduced and the links of the central hubs are limited to the most important trading partners. Links derived from the extended model.

ure 5.8. The network is dominated by unidirectional links to big hubs, these banks steadily absorb the excess liquidity from smaller banks, which obviously leads to some kind of preferential relationships. These relationships expressed by slight discounts in the interest rates are small, so they might not be of big economical importance for the single bank, nevertheless they become visible in our data. Lending relationships which are presumably of a more random kind are filtered out in this network representation. Conversely, lending relationships that result in higher then average loan rates result from lending from more peripheral banks. The resulting network of these non-preferential lending relationships does not have a dense core and is much more segmented than the latter network, see Figure E.2 in the appendix.

5.5 Lending Dynamics and Financial Crisis

5.5.1 Development of Credit Spreads and Volume Dynamics

In the following we turn to an analysis of the market dynamics over time and to the changes that have been induced by the ongoing financial crisis. We start with the estimation of credit spreads on a year by year basis.[7] The plots in Figure 5.9 reveal that the number of trades (and volume) has a decreasing trend that even accelerates in 2008. The number of banks for which we can estimate the spread is thus also decreasing. While the range of spreads, measured by the standard deviation of γ, are very low until 2007, we see a sharp increase afterwards and a slightly puzzling dip in 2009.

Since the composition of the sample shows some churning over time we should also look at the sample of 14 banks which are very active throughout the whole time in Figure 5.10. The fixed sample confirms our results, while spreads are relatively low until 2007, 2008 shows a slight amplification. In 2010 we see a much more differentiated picture. This panel also reveals that 2009 is characterized by an slight increase in the spreads (relative to EURIBOR) which affects all banks similarly, and hence leads to a drop in the standard deviation of spreads (see also Figure E.3 in the appendix). The results for 2009 might also suggest that instead of trading at a higher rates, banks choose not to trade if all, if possible, and used the central banks for their refinancing operations (see also Gabrieli (2009) for this issue).

We can also look at how much the positions and trade shares within the network have changed from year to year. Denote by $V_{[N\times N]}$ the matrix of aggregate trade volumes between the N banks in our network, then the share of total volume RV_{ij}^t

[7] We use the simple model since this is more efficient for smaller samples and we have seen that the results for the borrower fixed effects do not differ significantly from the extended model.

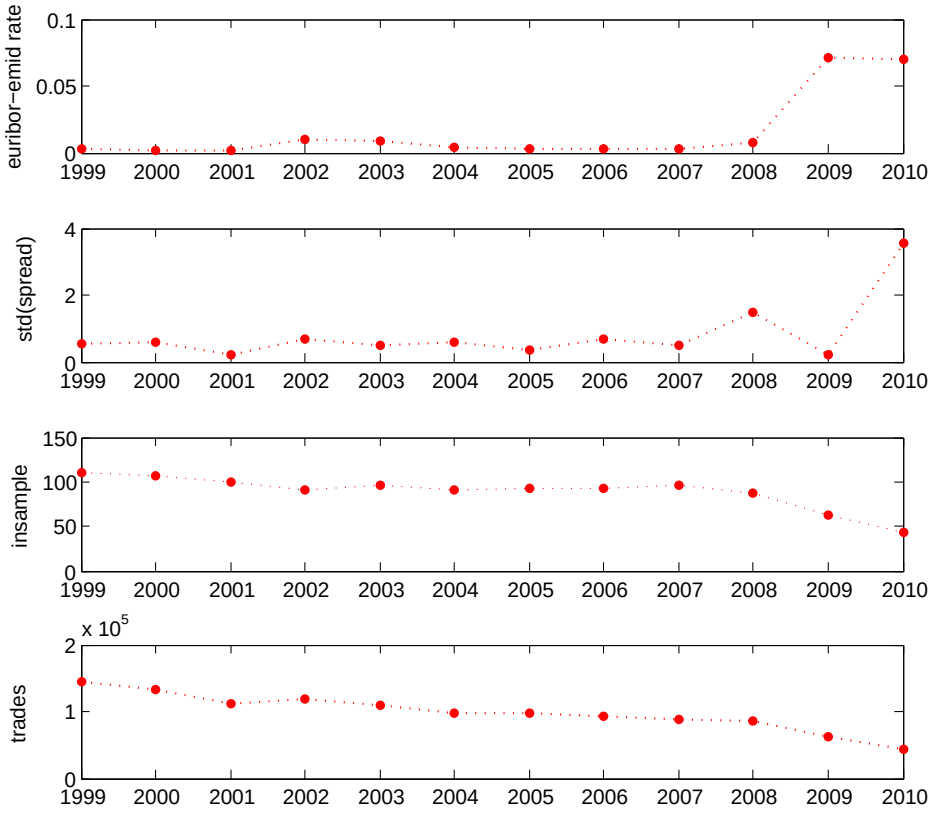

Fig. 5.9: Credit spreads over time

Panel 1: The difference of the average E-mid rate and the EURIBOR rate is rather small, an increase is visible after 2008. Panel 2: The standard deviation of estimated credit spreads is increasing in 2010 after noticeable changes in the spreads in 2008 and 2009. Panel 3: The number of banks with at least 200 trades is decreasing steadily, the process accelerates in 2008. Panel 4: The number of overnight trades on the E-mid platform is declining from around 135,000 in 1999 to 45,000 in 2010.

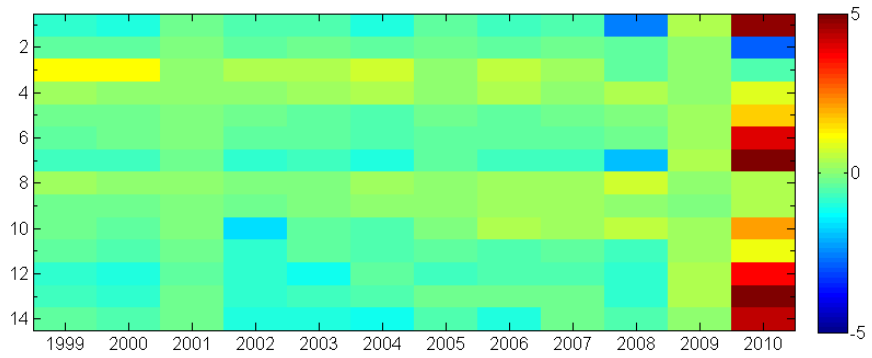

Fig. 5.10: Credit spreads over time, fixed sample
The panel shows the color codes spreads with the EURIBOR as a reference for the 14 banks which are constantly trading on E-mid from 1999 until 2010. In 2008 the spreads become a bit more pronounced, in 2009 we observe an increase of spreads which equally effect all 14 banks. In 2010 spreads are again widening and increasing. We observe a reordered ranking of the implied ranking of banks.

that bank i borrows from bank j in year t can be expressed as

$$RV^t = \frac{V^t}{\sum_{i=1}^{N}\sum_{j=1}^{N} V^t} \tag{5.3}$$

and the change in relative volumes is given by

$$\Delta RV^{t,t-1} = \frac{\sum_{i=1}^{N}\sum_{j=1}^{N} |RV^t - RV^{t-1}|}{2} \tag{5.4}$$

For ΔRV a value of 0 corresponds to a situation where the volume shares have been unchanged, the maximum value is 1 and describes in situation where every bank changed all trading partners.

For the dynamics of the net positions we first have to calculate the net volumes as $NV^t = V^t - (V^t)^T$. Since we only want to compare the net borrowing for banks which were trading with each other in two successive years we filter the net volumes such that we use only those entries from the matrix which were non-zero for both years, hence $NV_{ij}^{F,t+1} = NV_{ij}^{t+1}$ if $V_{ij}^t > 0$ and 0 otherwise, conversely for $NV^{F,t}$. Then the relative net volumes are given by

$$RNV^t = \frac{NV^{F,t}}{\sum_{i=1}^{N}\sum_{j=1}^{N}|NV^{F,t}|} \tag{5.5}$$

and the change in these net volumes can then be calculated as

$$\Delta RNV^{t,t-1} = \frac{\sum_{i=1}^{N}\sum_{j=1}^{N}|RNV^t - RNV^{t-1}|}{2}. \tag{5.6}$$

This measure is also bound between 0 and 1. Changes in total volume from year to year do not have a direct effect on these measures, since we treat all quantities as shares of the annual total amounts.

Finally we can calculate the ratio of net positions to total volume NTV as

$$NTV^t = \frac{\sum_{i=1}^{N}\sum_{j=1}^{N}|NV^t|}{2\sum_{i=1}^{N}\sum_{j=1}^{N}V^t}, \tag{5.7}$$

which tells us how much of the lending volume in the market stems from lending relationships which do not net out within one year.

The top panel of Figure 5.11 shows the volume differences. For most of the time about one half of the relative volume was shifted to other trading partners from year to year, the rate is increasing heavily after 2008. The development of relative net volume changes in the middle panel shows a different behavior. We see a first dip here in 2002. This coincides with the year when more foreign banks entered the E-mid market, see Fricke and Lux (2012). We observe a slight increase from then on until 2008, for 2009 and 2010 we see a slight decline, which is very interesting, because it does not follow the trend of the volume figures. The ratio of net positions to total volume in the bottom panel explains most of this effect. While the market volume in general is shrinking, unidirectional lending is gaining relatively importance in the market, the ratio of net positions to total volume is increasing to over 90% after a small dip in 2007.

5.5.2 Lending in the Post-Lehman Market

Finally we can repeat our analysis of trade flows and preferential lending relationships for the post-Lehman period. Figure 5.12 shows the number of trades, volume and net volume with the color coding similar to Figure 5.4. The number of trades and volume have experienced a noticeable drop, yet the asymmetric lending pattern

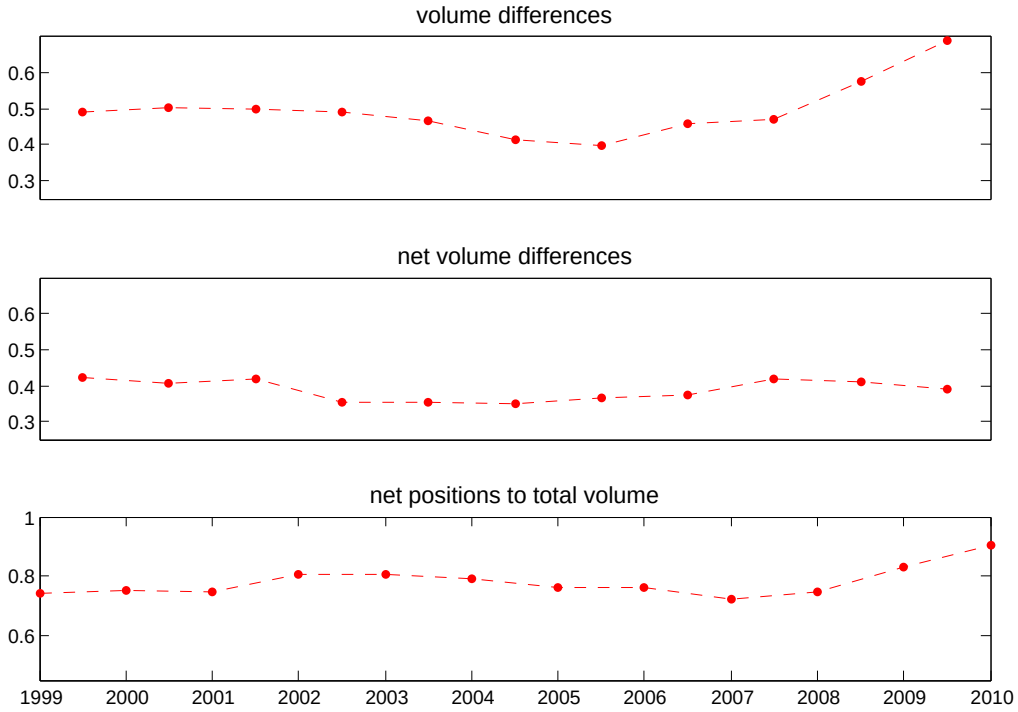

Fig. 5.11: Volume dynamics

Top panel: The share of relative volumes differences in borrowing relationships varies between 0.4 and 0.5 until 2008, after then it increases to 0.7; we observe in increasing change of trading partners. Middle panel: The change in relative net volume differences is relatively stable at around 0.4. We observe a slight decrease in 2002 when more foreign banks enter the market and a slight peak from 2007 to 2008. Bottom panel: The ratio of net positions to total trading volume is increasing to 0.9 after is was between 0.7 and 0.8 until 2008.

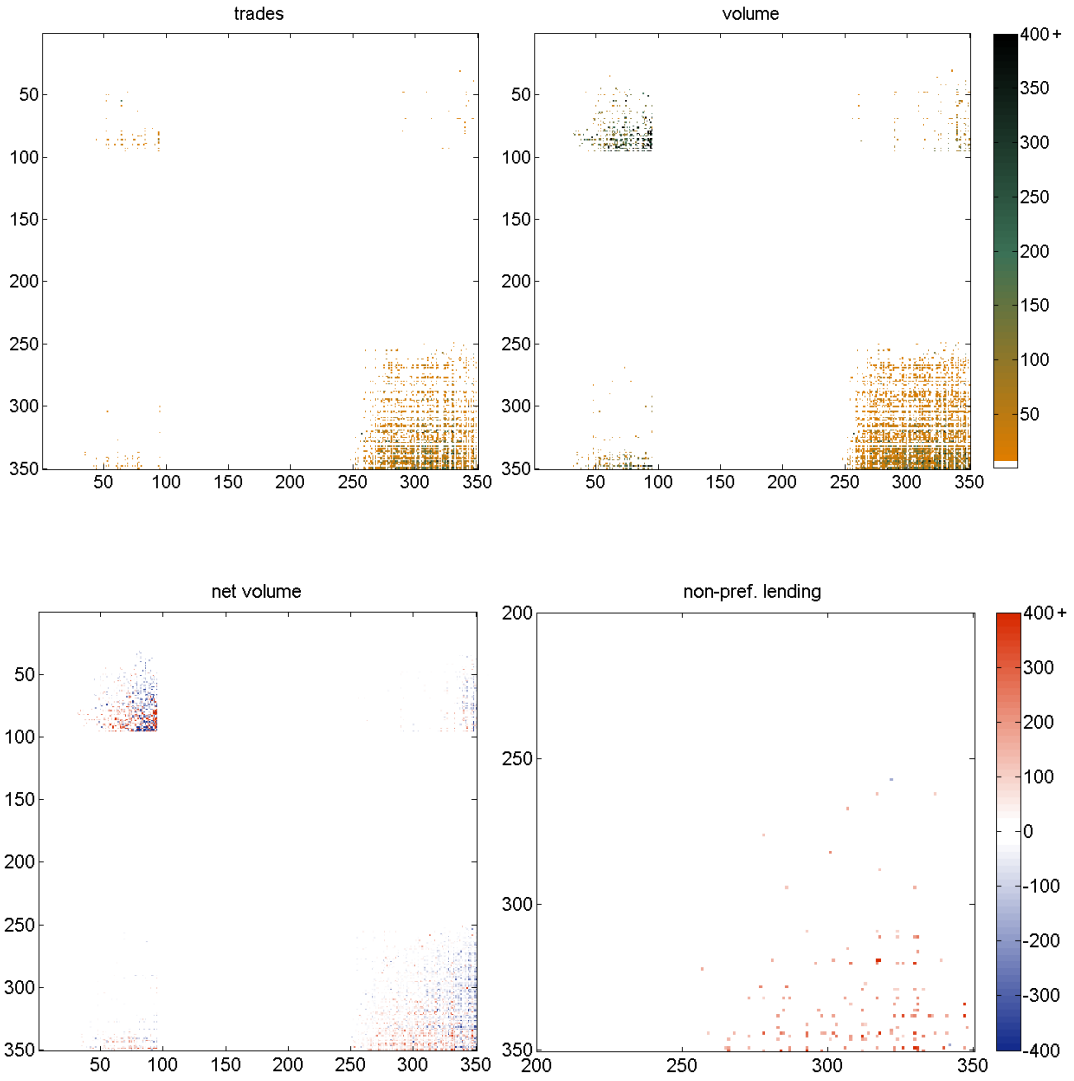

Fig. 5.12: Trade flows, volume and net volume, post-Lehman
Top left: Number of trades, Top right: aggregate volume, Bottom left: Net volume, Bottom right: non-preferential lending relationships. The rows and columns are ordered: first into foreign and Italian banks, then by total trade volume. Row entries are borrowing transactions, column entries represent lending. The trade volume has decreased, some banks have left the market.

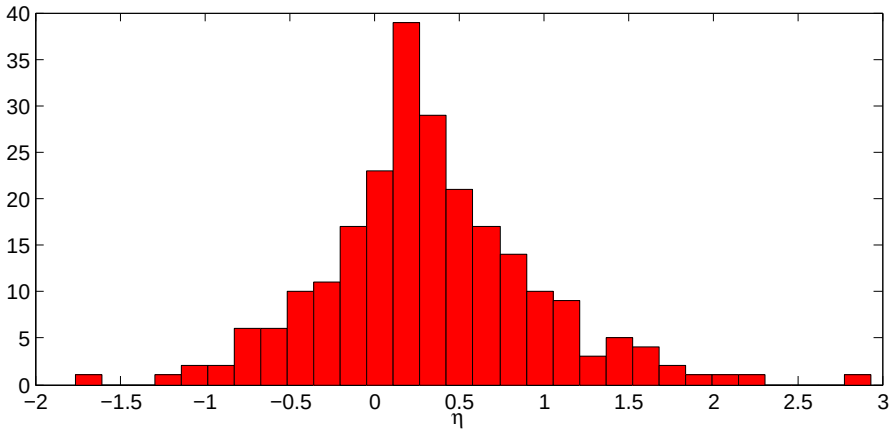

Fig. 5.13: Distribution of η for the post-Lehman period
The histogram of η shows that for the past Lehman period lending relationships with at least 80 trades have a bias for rate premia. The threshold is scaled down to account for the shorter time horizon and the smaller average number of trades.

among the Italian banks is still visible.

We have already discussed the estimation of credit spreads on a year by year basis, thus we can now directly turn to the estimation of preferential lending relationships for the entire period of August 2008 – December 2010. The distribution of η, the coefficients from the estimation of frequent lending relationships is shown in Figure 5.13. For this period the histogram is biased towards positive values, which is in sharp contrast to the results for the period from 1999 until 2006.

The nature of the transition that took place in the market becomes more clear when we again plot the adjacency matrix of these relationships. Instead on focusing on the lending relationships that result in lower rates, we have a look at those which result in slightly higher rates, the "non-preferential" lending. The bottom right plot of Figure 5.12 shows that now many of the one-sided borrowing relationships, which until 2008 lead to slight discounts in the loan rate, trade at a small premium (see Appendix E.4 for a network representation). The interpretation of this change is straightforward, the basic pattern of the market is that we have some large banks with a huge net liquidity (refinancing) demand and large group of relatively smaller banks with some excess supply. As long as the economic situation was stable and counterparty risks were negligible, the small banks were reluctant to lend to the big banks. After 2008 the basic situation of excess demand and supply was the same but most likely the risk assessment has changed. Lending relationships with a permanent net position of one of the parties now tendencially lead to slightly increased loan

rates.

5.6 Discussion

The Italian interbank market has undergone significant changes during the last 12 years. After its start it could attract not only Italian banks but also a number of foreign banks joined the market. Some smaller banks have left the market, this might be a result of merges and acquisitions activity, some of them might also have transfered the refinancing and liquidity management to larger affiliated banks.

The trading volume in the market went down significantly, especially since interbank markets became stressed in 2008. A noticeable change is that we can observe economically significant spreads in the market since 2010. After Angelini et al. (2009) have already observed a widening of spread for loans with a longer maturity, this could be a signal for a changing risk assessment of banks also in the overnight market. One could draw the conclusion that until 2007 banks would be willing to lend to anyone on the overnight market with some reputation and that in 2008, when a day-to-day monitoring of the counterparts became necessary, because there was suddenly a much higher risk of default, they were not capable of this monitoring, or it was too costly.

A changing behavior is also observed for the very frequent trading relationships. While we see slight discounts from these relationships until 2006, the reverse happens from 2008 until 2010. The net exposure to a borrower is now something that is associated with an additional risk that is priced into the loan rate, additional to the overall borrower specific spread.

Methodologically we have seen that it is possible to combine approaches from network science, like the analysis of flows and network structure, with approaches from empirical economics, the analysis of interest rates, in a complementary way.

6. CONCLUSIONS

This thesis deals with topics which – at least superficially – are rather diverse. The overarching element is that an analysis of dependencies and thus of network structure was applied for all of them. In Chapter 2 we have seen network structures which represent different levels of influence of market participants. Such systems, in which a large number of agents are involved, but only a factually much smaller core of agents drive the outcome of a system, are clearly opposed to conventional economic models where agents are indistinguishable.

One might argue that in this model reasonable features that can stabilize markets and dampen volatility are blinded out. The reason for this is that we want to focus on the interaction effects that arise from these structures, since it has already been shown in the literature that herding effects will also happen if a reasonable number of rational agents or 'fundamentalist' are present.

As a result we have seen that the hierarchical pattern that we introduced has significant influence on the volatility of the opinion index in this herding model. This was most pressing in the scenario where both, the degree distribution of the network, and the distribution of the weights of the top-level agents, followed a power law. From the modeling point of view this might seem very stylized, but in fact, social, economic, and political systems often show settings where influence and connectivity is concentrated on smaller sub-groups. This can happen through delegation, vote, or just as consequence of economies of scale and efficiency. A logical step in further research would be to show, how these structures arise endogenously in such a model.

In Chapter 3 we have shown the development of a real network over time. The network of German corporate boards is at least one small example for a system where we can clearly identify a group of agents, in this case real managers, who are far more connected and very likely more influential than others. We have argued that despite a certain decrease in overall connectivity, structural patterns of the network are maintained over time. While certain properties of the degree distribution might be persistent by construction, it would be hard to explain that distinct links between companies should show persistence only by chance. The replacement of overly central managers with other overly central managers hints at some amplification effect.

While one can argue that this might result from the promotion of very experienced and successful managers to even more prestigious posts, it also means that connectivity might be self-enforcing. If we evaluate this network structure in the light of our herding model from the first chapter, we can suppose that the core of this network could be quite susceptible to collective opinions swings, which might have economic implication if connectivity goes hand in hand with influence. Unfortunately this hypothesis might never be testable. What is encouraging is the fact that the number of studies on similar networks has increased (see, e.g., Vitali et al., 2011), which is likely to lead to a better understanding of the map of the real economy. In general, as we gain access to more data of complex network structures in the economy, new opportunities for simulations emerge. This might bring especially agent-based modelers very close to the forecasting community, and is likely to lead to more policy related research in this field.

It is not very obvious why the content of Chapter 4 is network science. On a first glance we deal with time-series data of stock prices and with its correlations. These correlations can be used to derive a dependency network. Hence, we can derive a network in which the links describe the relationships between the stocks equivalent to correlations coefficients. One reason for why a network approach to this field is interesting is that the classical portfolio models do at some point rely on the spectral decomposition of some correlation matrix, and that for this to work efficiently we need at least as many observations as we have stocks in your sample. As a logical consequence a dimensional reduction is necessary if we want to have a look at many stocks at the same time on shorter time horizons.

Our results do of course not allow us to manage any portfolio, but they do allow us to quantify market behavior. We can identify if markets are stressed and if this stress is local or global. This research is likely to be extended, covering two important issues. First, this methodology needs to be put on firmer statistical foundation, which means that measures for significance have to be derived. Secondly, not only complete markets but also single stocks should be analyzed. This could happen either jointly for all stocks of all markets, or in some hierarchic setting, where first the relationships between functional groups of stocks are analyzed, and single stocks follow at a second level. Such a setting could possibly also be extended to work with different asset classes and more countries, such that the whole model could work as a global financial seismograph.

The last chapter deals with a topic which has gained a lot of interest especially since the last (still current?) financial crisis. The contagious effects that we have seen during this crisis did not happen specifically on the interbank loan market, but

rather trough asset backed securities and credit default swaps. Still, as a result the interbank markets broke down, which was a sign of the loss of trust and showed the awareness of the banks about immanent contagions effects.

The results from Chapter 5 show that the effect on interbank markets is a lasting one. We observe a widening of spreads and most likely a changing behavior towards large net exposures to counterparts. The very low market volume clearly indicates that the central banks are still needed to keep the refinancing process running. The way back to money markets that rely on the central bank only as a backup facility seems rather long and bears opportunities for further research. The extension of the bank network analysis to other markets and products is pressing but the availability of data is still rather poor.

In general, the impact that this crisis had on policy seems a little bit disappointing, at least to the author. We have learned that this kind of financial contagion – or cascade effects, as the physicist would say – can happen. The basic theoretical foundations for its analysis have been laid, see, e.g., Watts (2002), and economists have applied them to different markets. The response of the policy makers are marginal changes to capital requirements of banks and the building up of massive rescue facilities for the worst case. If we want to tackle these contagious risks more seriously, there might be two approaches: Either we systematically account for this risks as part of some new 'Basel' framework, or we need incentives that remind the banks to distribute and share risk in our economy such that they no longer become systemic.

To exonerate the policy makers a little bit it is fair to say that economists did not prepare them very well for this crisis. As mentioned in the introduction, the appearance of crisis is not very much favored in the setup of the mainstream macroeconomic models. There is some hope that the ongoing academic debriefing of this crisis will have a ripple effect.

REFERENCES

Afonso, G., Kovner, A., and Schoar, A. (2011). Stressed, not frozen: The Federal Funds market in the financial crisis. *Journal of Finance*, 4:1109–39.

Ahlgren, N. and Antell, J. (2010). Stock market linkages and financial contagion: A cobreaking analysis. *The Quarterly Review of Economics and Finance*, 50:157–166.

Albert, R., Jeong, H., and Barabási, A.-L. (1999). Diameter of the world-wide web. *Nature*, 401:130–131.

Alfarano, S. and Lux, T. (2007). A noise trader model as a generator of apparent financial power laws and long memory. *Macroeconomic Dynamics*, 11(S1):80–101.

Alfarano, S., Lux, T., and Wagner, F. (2005). Estimation of agent-based models: The case of an asymmetric herding model. *Computational Economics*, 26:19–49.

Alfarano, S., Lux, T., and Wagner, F. (2008). Time-variation of higher moments in a financial market with heterogeneous agents: An analytical approach. *Journal of Economic Dynamics and Control*, 32:101–136.

Alfarano, S. and Milaković, M. (2009). Network structure and N-dependence in agent-based herding models. *Journal of Economic Dynamics and Control*, 33:78–92.

Alfarano, S., Milaković, M., and Raddant, M. (2012). A note on institutional hierarchy and volatility in financial markets. *The European Journal of Finance*, forthcoming.

Alfi, V., Cristelli, M., Pietronero, L., and Zaccaria, A. (2009). Minimal agent based model for financial markets I. *European Physical Journal B*, 67:385–397.

Allen, F. and Gale, D. (2001). Financial contagion. *Journal of Political Economy*, 108:1–33.

Angelini, P., Nobili, A., and Picillo, C. (2009). The interbank market after August 2007: What has changed, and why? *Bank of Italy, Working paper*.

Aoki, M. (2008). Thermodynamic limits of macroeconomic or financial models: One- and two-parameter Poisson-Dirichlet models. *Journal of Economic Dynamics and Control*, 32:66–84.

Ashcraft, A. and Duffie, D. (2007). Systemic dynamics in the federal funds market. *American Economic Review, Papers and Proceedings*, 97:221–225.

Aste, T., Shaw, W., and Matteo, T. D. (2010). Correlation structure and dynamics in volatile markets. *Physical Review E*, 12.

Baba, K., Shibata, R., and Sibuya, M. (2004). Partial correlation and conditional correlation as measures of conditional independence. *Australian & New Zealand Journal of Statistics*, 46(4):657–664.

Baglioni, A. and Monticini, A. (2008). The intraday price of money: Evidence from the e-mid interbank market. *Journal of Money, Credit and Banking*, Vol. 40(7):1533–1540.

Bala, V. and Goyal, S. (2000). A non-cooperative model of network formation. *Econometrica*, 68:1181–1230.

Banerjee, A. V. (1992). A simple model of herd behavior. *Quarterly Journal of Economics*, 107(3):797–817.

Barabási, A.-L. and Albert, R. (1999). Emergence of scaling in random networks. *Science*, 286:509–512.

Baruchi, I., Grossman, D., Volman, V., Shein, M., Towle, V., and Ben-Jacob, E. (2006). Functional holography analysis: Simplifying the complexity of dynamic networks. *Chaos*, 15:015112.

Battiston, S. and Catanzaro, M. (2004). Statistical properties of corporate board and director networks. *European Physical Journal B*, 38:345–352.

Beaupain, R. and Durré, A. (2008). The interday and intraday overnight market: Evidence from an electronic platform. *ECB working paper*, No. 998.

Bech, M. L., Bergstrom, C. T., Garratt, R. J., and Rosvall, M. (2011). Mapping change in the Federal Funds market. *Federal Reserve Bank of New York, Staff Reports*, no. 507.

Beile, M. and Candelon, B. (2011). Liberalization and stock market co-movement between emerging economies. *Quantitative Finance*, 12(2):299–312.

Bekaert, G. and Campbell, R. (1995). Time-varying world market integration. *The Journal of Finance*, 50(2):403–444.

Beyer, J. and Höpner, M. (2003). The disintegration of organized capitalism: German corporate governance in the 90s. *West European Politics*, 26:179–198.

Bikhchandani, S., Hirshleifer, D., and Welch, I. (1992). A theory of fads, fashion, custom, and cultural change as informational cascades. *Journal of Political Economy*, 100(5):992–1026.

Bonacich, P. (1972). Factoring and weighting approaches to status scores and clique identification. *Journal of Mathematical Sociology*, 2:113–120.

Borgatti, S. P. (2005). Centrality and network flow. *Social Networks*, 27:55–71.

Borgatti, S. P. (2006). Identifying sets of key players in a social network. *Computational and Mathematical Organization Theory*, 12:21–34.

Borgatti, S. P. and Everett, M. G. (1999). Models of core/periphery structures. *Social Networks*, 21:375–395.

Borgatti, S. P. and Foster, P. C. (2003). The network paradigm in organizationl research: A review and typology. *Journal of Management*, 29(6):991–1013.

Bornholdt, S. (2001). Expectation bubbles in a spin model of markets: Intermittency from frustation across scales. *International Journal of Modern Physics C*, 12:667–674.

Boss, M., Elsinger, H., Summer, H., and Thurner, M. (2006). Network topology of the interbank market. *Quantitative Finance*, 4(6).

Brass, D. J., Galaskiewicz, J., Greve, H. R., and Tsai, W. (2004). Taking stock of networks and organizations: A multilevel perspective. *Academy of Management Journal*, 47(6):795–817.

Brock, W. A. and Hommes, C. H. (1997). A rational route to randomness. *Econometrica*, 65:1059–1095.

Caldarelli, G. and Catanzaro, M. (2004). The corporate boards networks. *Physica A*, 338:98–106.

Carrieri, F., Errunza, V., and Hogan, K. (2007). Characterizing world market integration through time. *Journal of Financial and Quantitative Analysis*, 40(2):915–940.

Chamley, C. P. (2004). *Rational Herds*. Cambridge University Press, New York.

Chang, S.-K. (2007). A simple asset pricing model with social interactions and heterogeneous beliefs. *Journal of Economic Dynamics and Control*, 31:1300–1325.

Chen, Z., Jiang, H., and Sim, A. (2010). Regulation change and volatility spillovers: evidence from China's stock markets. *Emerging Markets Finance & Trade*, 46(6):140–157.

Cocco, J., Gomes, F., and Matins, N. (2009). Lending relationships in the interbank market. *Journal of Financial Intermediation*, 18:24–48.

Cont, R. (2001). Empirical properties of asset returns: Stylized facts and statistical issues. *Quantitative Finance*, 1(2):223–236.

Cont, R. and Bouchaud, J. P. (2000). Herd behaviour and aggregate fluctuations in financial markets. *Macroeconomic Dynamics*, 4:170–196.

Conyon, M. J. and Muldoon, M. R. (2006). The small world of corporate boards. *Journal of Business Finance & Accounting*, 33(9):1321–1343.

Corsi, F. (2009). A simple approximate long-memory model of realized volatility. *Journal of Financial Econometrics*, 7(2):174–196.

Craig, B. and von Peter, G. (2010). Interbank tiering and money center banks. *Deutsche Bundesbank Discussion Paper, Series 2*, 12/2010.

da Rocha, L. (2011). *Exploring patterns of empirical networks, PhD Thesis*. Department of Physics, Umea University.

Davis, G. F., Yoo, M., and Baker, W. E. (2003). The small world of the American corporate elite, 1982–2001. *Strategic Organization*, 1(3):301–326.

Dunne, J., Williams, R., and Martinez, N. (2002). Food-web structure and network theory. *PNAS*, 99:20:12917–12922.

Egenter, E., Lux, T., and Stauffer, D. (1999). Finite-size effects in Monte Carlo simulations of two stock market models. *Physica A*, 268:250–256.

Engle, R., Ito, T., and Lin, W. (1990). Meteor showers or heat waves? Heteroskedastic daily volatility in the foreign exchange market. *Econometrica*, 58:525–542.

Engle, R. and Russell, J. (2010). Analysis of high frequency financial data. In Ait-Sahlia, Y. and Hansen, L., editors, *Handbook of Financial Econometrics, Vol. 1*. Elsevier.

Erdös, P. and Renyi, A. (1959). On random graphs. *Publicationes Mathematicae*, 6:290–297.

Eubank, S., Guclu, H., Kumar, V. A., Marathe, M., Srinivasan, A., Toroczkai, Z., and Wang, N. (2003). Modelling disease outbreak in realistic urban social networks. *Nature*, 429:180–184.

Forbes, K. and Rigobon, R. (2002). No contagion, only dependence: Measuring stock market comovements. *The Journal of Finance*, LVII(5):2223–2261.

Freeman, L. (2004). *The Development of Social Network Analysis*. Empirical Press, Vancouver.

Fricke, D. and Lux, T. (2012). Core-periphery structure in the overnight money market: Evidence from the e-mid trading platform. *Kiel Working Papers*, No. 1759.

Furfine, C. (2003). Interbank exposures: quantifying the risk of contagion. *Journal of Money, Credit and Banking*, 35(1).

Gabaix, X., Gopikrishnan, P., Plerou, V., and Stanley, H. E. (2006). A theory of power-law distributions in financial market fluctuations. *Quarterly Journal of Economics*, 121(2):461–504.

Gabrieli, S. (2009). The functioning of the European interbank market during the 2007-08 financial crisis. *CEIS Research Paper Series*, Vol. 7(7), No. 158.

Galaskiewicz, J. (2007). Has a network theory of organizational behaviour lived up to its promises? *Management and Organization Review*, 3(1):1–18.

Garibaldi, U., Penco, M. A., and Viarengo, P. (2003). An exact physical approach to market participation models. In Cowan, R. and Jonard, N., editors, *Heterogeneous Agents, Interactions and Economic Performances*, Lecture Notes in Economics and Mathematical Systems, pages 91–103. Springer, Berlin.

Gopikrishnan, P., Rosenow, B., Plerou, V., and Stanley, H. (2001). Quantifying and interpreting collective behavior in financial markets. *Physical Review E*, 64:035106.

Goswami, B., Ambika, G., Marwan, N., and Kurths, J. (2011). On interrelations of recurrences and connectivity trends between stock indices. *arXiv*, page 1103.5189.

Granovetter, M. (1973). The strength of weak ties. *American Journal of Sociology*, 81:1287–1303.

Harmon, D., Aguair, M. D., Chinellato, D., Braha, D., and Epstein, I. (2011). Predicting economic market crises using measures of collective panic. *arXiv*, 1102.2620.

Hartmann, P., Manna, M., and Manzanares, A. (2001). The microstructure of the Euro money market. *Journal of International Money and Finance*, 20(6):895–948.

Heemskerk, E. (2007). *Decline of the Corporate Community*. Amsterdam University Press.

Hoffman, G. (1975). A theory of regulation and self-nonself discrimination in an immune network. *Eur. Journal of Immunology*, 5:638–647.

Holme, P. (2005). Core-periphery organization of complex networks. *Physical Review E*, 72:046111.

Holme, P. and Saramaki, J. (2012). Temporal networks. *Physics Reports*, forthcoming.

Hommes, C. H. (2006). Heterogeneous agent models in economics and finance. In Tesfatsion, L. and Judd, K. L., editors, *Handbook of Computational Economics*, volume 2, pages 1109–1186. North-Holland, Amsterdam.

Hong, H., Kubik, J. D., and Stein, J. C. (2005). Thy neighbor's portfolio: Word-of-mouth effects in the holdings and trades of money managers. *Journal of Finance*, 60:2801–2824.

Iori, G. (2002). A micro-simulation of traders' activity in the stock market: the role of heterogeneity, agents' interactions and trade friction. *Journal of Economic Behavior and Organization*, 49:269–285.

Iori, G., de Masi, G., Precup, O., Gabbi, G., and Caldarelli, G. (2008). A network analysis of the Italian overnight money market. *Journal of Economic Dynamics & Control*, 32:259–278.

Irle, A., Kauschke, J., Lux, T., and Milaković, M. (2011). Switching rates and the asymptotic behavior of herding models. *Advances in Complex Systems*, 14(3):359–376.

Jackson, M. and Wolinsky, A. (1996). A strategic model of social and economic networks. *Journal of Economic Theory*, 71:44–74.

Jackson, M. O. (2008). *Social and Economic Networks*. Princeton U.P.

Jobson, D. J. (1991). *Applied Multivariate Data Analysis*. Springer, New York.

Kamada, T. and Kawai, S. (1989). An algorithm for drawing general undirected graphs. *Information Processing Letters*, 31:7–15.

Kenett, D., Shapira, Y., and Ben-Jacob, E. (2009). RMT assessments of market latent information embedded in the stocks' raw, normalized, and partial correlations. *Hindawi Journal of Probability and Statistics*, pages 249370,10.1155/2009/249370.

Kenett, D., Shapira, Y., Madi, A., Bransburg-Zabary, S., and Gur-Gershgoren, G. (2010). Dynamics of stock market correlations. *AUCO Czech Economic Review*, 4(1).

Kenett, D., Shapira, Y., Madi, A., Bransburg-Zabary, S., and Gur-Gershgoren, G. (2011). Index cohesive force analysis of NY market reveal phase transition into stiff market state. *PlosOne*, 6(4):e19378.

King, M., Sentana, E., and Wadhwani, S. (1994). Volatility and links between national stock markets. *Econometrica*, 62(4):901–933.

Kirman, A. (1991). Epidemics of opinion and speculative bubbles in financial markets. In Taylor, M. P., editor, *Money and Financial Markets*, pages 354–368. Blackwell, Cambridge.

Kirman, A. (1993). Ants, rationality, and recruitment. *Quarterly Journal of Economics*, 108:137–156.

Krugman, P. (2009). What went wrong with economics. *The Economist, July*.

Lacasa, L., Luque, B., Ballesteros, F., Luque, J., and Nuno, J. (2008). From time series to complex networks: The visibility graph. *PNAS*, 105(13):4972–4975.

Liljeros, F., Edling, C. R., Amaral, L. A., Stanley, H. E., and Åberg, Y. (2001). The web of human sexual contacts. *Nature*, 411:907–908.

Lorrain, F. and White, H. (1971). Structural equivalence of individuals in social networks. *Journal of Mathematical Sociology*, 1:49–80.

Lux, T. and Schornstein, S. (2005). Genetic learning as an explanation of stylized facts of foreign exchange markets. *Journal of Mathematical Economics*, 41:169–196.

Lux, T. and Westerhoff, F. (2009). Economic crisis. *Nature Physics*, 5(2).

Mantegna, R. and Stanley, H. (2000). *An Introduction to Econophysics: Correlation and Complexity in Finance*. Cambridge University Press, Cambridge, UK.

Milaković, M., Alfarano, S., and Lux, T. (2010). The small core of the german corporate board network. *Computational and Mathematical Organization Theory*, 16(2):201–215.

Mintz, B. and Schwartz, M. (1981). Interlocking directorates and interest group formation. *American Sociological Review*, 46(6):851–869.

Moreno, J. L. and Jennings, H. H. (1938). Statistics of social configuration. *Sociometry*, 1:342–374.

Newman, M. E. J. (2002). Assortative mixing in networks. *Phys. Rev. Letters*, 89:208701.

Newman, M. E. J. (2003). The structure and function of complex networks. *SIAM Review*, 45:167–256.

Newman, M. E. J. (2010). *Networks, An Introduction*. Oxford U.P., New York.

Newman, M. E. J. and Girvan, M. (2004). Finding and evaluating community structure in networks. *Physical Review E*, 4. 026113.

Newman, M. E. J., Strogatz, S. H., and Watts, D. J. (2001). Random graphs with arbitrary degree distributions and their applications. *Physical Review E*, 64:026118.

Pagan, A. (1996). The econometrics of financial markets. *Journal of Empirical Finance*, 3:15–102.

Palla, G., Derényi, I., and Vicsek, T. (2005). Uncovering the overlapping community structure of complex networks in nature and society. *Nature*, 435:814–818.

Plerou, V., Gopikrishnan, P., Rosenow, B., Amaral, L., and Stanley, H. (2000). A random matrix theory approach to financial cross-correlations. *Physica A*, 287(3–4):374–382.

Preis, T., Schneider, J., and Stanley, H. (2011). Switching processes in financial markets. *Proceedings of the National Academy of Sciences*, page doi:10.1073/pnas.1019484108.

Preis, T. and Stanley, H. (2010). Switching phenomena in a system with no switches. *Journal of Statistical Physics*, 138(1):431–446.

Provan, K. G., Fish, A., and Sydow, J. (2007). Interorganizational networks at the network level: A review of the empirical literature on whole networks. *Journal of Management*, 33(3):479–516.

Reichardt, J. (2009). *Structure in Complex Networks, Lect. Notes Phys. 766.* Springer, Berlin.

Robins, G. and Alexander, M. (2004). Small worlds among interlocking directors: Network structure and distance in bipartite graphs. *Computational & Mathematical Organization Theory*, 10:69–94.

Rosvall, M. (2006). *Information Horizons in a Complex World, PhD thesis.* Umea University.

Rosvall, M. and Bergstrom, C. (2008). Maps of random walks on complex networks reveal community structure. *PNAS*, 105(4):1118–1123.

Schnettler, S. (2009). A structured overview of 50 years of small-world research. *Social Networks*, 31:165–178.

Schreyögg, G. and Papenheim-Tockhorn, H. (1995). Dient der Aufsichtsrat dem Aufbau zwischenbetrieblicher Koopertationsbeziehungen? *Zeitschrift für Betriebswirtschaft*, 65:205–230.

Schwarzkopf, Y. and Farmer, J. D. (2008). Time evolution of the mutual fund size distribution. *arXiv/0807.3800.*

Seidman, S. B. (1983). Network structure and minimum degree. *Social Networks*, 5:269–287.

Shapira, Y., Kenett, Y., and Ben-Jacob, E. (2009). The index cohesive effect on stock market correlations. *The European Physical Journal B*, 72(4):657–669.

Song, D., Tumminello, M., Zhou, W., and Mantegna, R. (2011). Evolution of worldwide stock markets, correlation structure and correlation based graphs. *Physical Review E*, 84(2):026108.

Soramäki, K., Bech, M., Arnold, J., Glass, R., and Beyeler, W. (2007). The topology of interbank payment flows. *Physica A*, 379:317–333.

Stauffer, D. and Sornette, D. (1999). Self-organized percolation model for stock market fluctuation. *Physica A*, 271:496–506.

Stearns, L. B. and Mizruchi, M. S. (1986). Broken-tie reconstitution and the functions of interorganizational interlocks: A reexamination. *Administrative Science Quarterly*, 31:522–538.

Travers, J. and Milgram, S. (1969). An experimental study of the small world problem. *Sociometry*, 32:425–443.

Tumminello, M., Aste, T., Matteo, T. D., and Mantegna, R. (2005). A tool for filtering information in complex systems. *Proceedings of the National Academy of Sciences of the United States of America*, 102(30):10421–10426.

Tumminello, M., Matteo, T. D., Aste, T., and Mantagna, R. (2007). Correlation based networks of equity returns sampled at different time horizons. *Eur. Phys J. B*, 55:209–217.

Uzzi, B., Amaral, L. A. N., and Reed-Tsochas, F. (2007). Small-world networks and management science research: A review. *European Management Review*, 4:77–91.

Venkatasubramanian, V., Politis, D. N., and Patkar, P. R. (2005). Entropy maximization as a holistic design principle for complex optimal networks. *Process Systems Engineering*, 52(3):1104–1109.

Vitali, S., Glattfelder, J. B., and Battiston, S. (2011). The network of global corporate control. *PlosOne*, 6(10):e25995.

von Luxburg, U. (2007). A tutorial on spectral clustering. *Statistics and Computing*, 17:395–416.

Wasserman, S. and Faust, K. (1994). *Social Network Analysis*. Cambridge U.P.

Watts, D. (2002). A simple model of global cascades on random networks. *PNAS*, 99(9):5766–5771.

Watts, D. J. and Strogatz, S. H. (1998). Collective dynamics of 'small-world' networks. *Nature*, 393:440–442.

Wermers, R. (1999). Mutual fund herding and the impact on stock prices. *Journal of Finance*, 54(2):581–622.

White, H., Boorman, S., and Breiger, R. (1976). Social structures from multiple networks. *American Journal of Sociology*, 81:730–780.

Zhu, H. and Pan, C. (2011). Conditional constraints and player behavior in china's stock market. In Lilai, X., editor, *China's Economy in the Post-WTO Environment*. Edward Elgar, Cheltenham.

APPENDIX

A. A HOLOGRAPHY OF THE GERMAN STOCK MARKET

A.1 Introduction and Data

This appendix investigates the system of the German stock market. We follow the work by Kenett et al. (2009) who show that normalized correlation of returns show a clearer picture of similarity than Pearson's correlation coefficient. Similar like Kenett et al. (2011) and Baruchi et al. (2006) we then perform a 3-dimensional mapping of the correlations of stock returns of publicly listed German firms. Further we show how to derive the plot of the correlations structures shown in the introduction of this thesis.

The dataset consists of daily closing prices of all publicly listed German firms for a period of two years (2008 and 2009). Thus, the firms in the dataset are largely identical to the firms used in the analysis of board networks by Milaković et al. (2010). After removing firms with incomplete time series and negligible trading volume, a total of 114 firms and 506 trading days remain.

A.2 Correlations

The stock prices are transformed to returns,

$$r_i(t) = \ln(Y_i(t + \Delta t)) - \ln(Y_i(t)). \tag{A.1}$$

One can then calculate stock correlations using Pearsons's correlation coefficient,

$$C(i,j) = \frac{\langle r(i) - \mu(i) \rangle \langle r(j) - \mu(j) \rangle}{\sigma(i)\sigma(j)}. \tag{A.2}$$

We also calculate a normalized correlation matrix. For this normalization we first need the matrix of meta-correlations MC. The meta-correlation measures the similarity of each two stocks i and j and is given by the respective two rows in the

correlation matrix C, leaving out the elements $C(i,i), C(j,j), C(i,j)$ and $C(j,i)$.

$$MC(i,j) = \frac{\sum_{k \neq i,j}^{N} (C_{ik} - \mu c_i)(C_{jk} - \mu c_j)}{\sqrt{\langle \hat{C}_i^2 \rangle \langle \hat{C}_j^2 \rangle}} \tag{A.3}$$

The normalized correlations NC can then by calculated by multiplying the elements of the two matrices,

$$NC_{i,j} = C_{i,j} MC_{i,j}. \tag{A.4}$$

Figures A.1 and A.2 show the raw and normalized correlations of stock return. The stocks are ordered by similarity derived from applying a dendrogram algorithm. The right part of each figure shows the level at which two elements are merged. Both figures show some sectoral grouping (traditional industry on top and remaining blue chips from about row 20). The normalized correlation show a more pronounced grouping than the raw correlation, which is also visible from the less flat dendrogram tree.

A.3 Holography

To visualize the network structure of stock returns we perform a dimensional reduction of the variable space by principal component analysis. Figure A.3 shows all stock in a 3D space given by the leading eigenvectors. The information that was lost by normalization and dimensional reduction is retrieved by plotting colored links between most correlated stocks, the color of each line is determined by the entries in the matrix of raw correlations C.

The Figure shows that the average correlation is increasing along the axis given by the largest eigenvector. The most correlated stocks seem to form a convex hull around stocks with less pronounced correlation. Figure A.4 shows that the decisive subgroups which appear as red squares in Figure A.2 are the main attachment points in 3D-space.

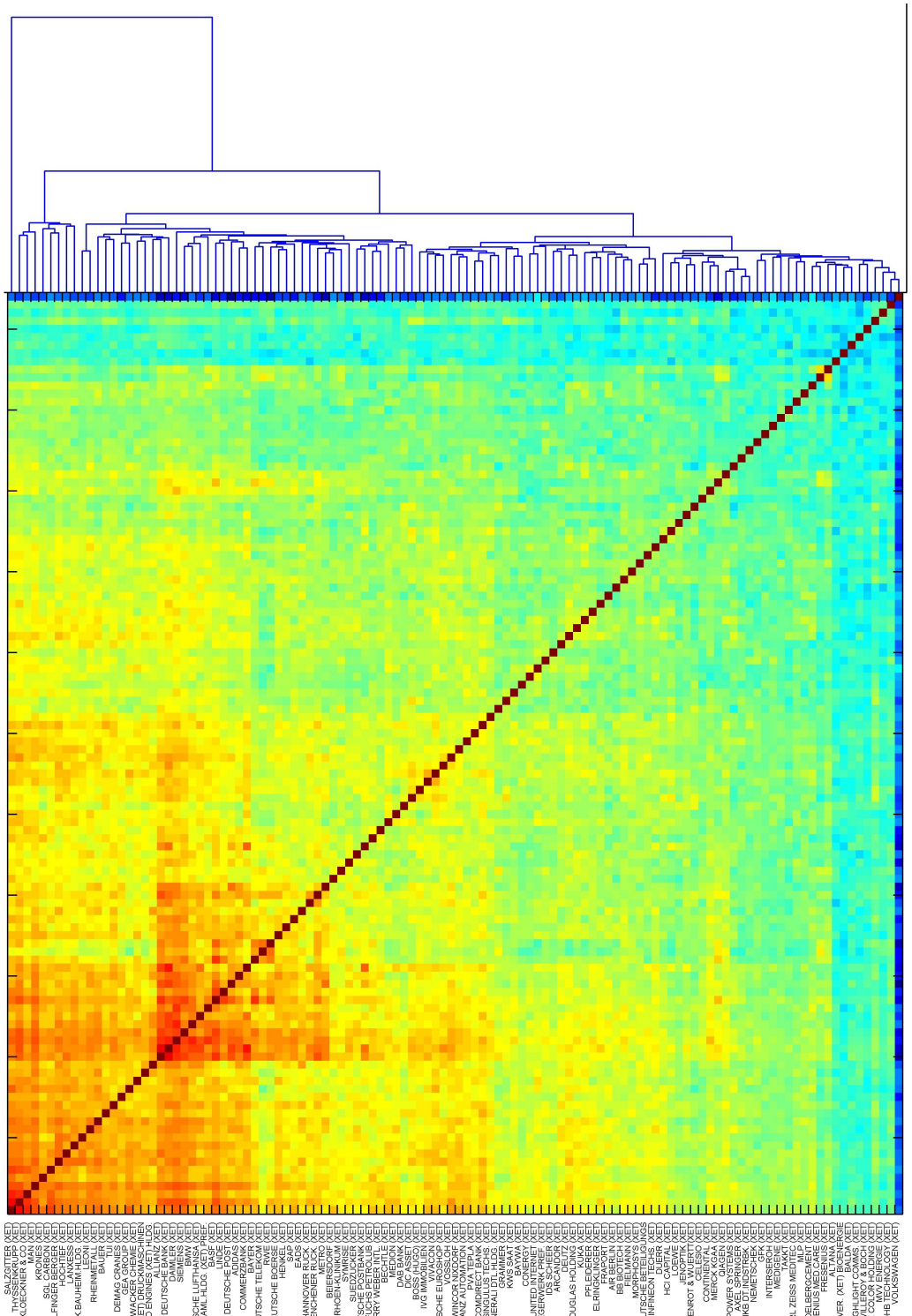

Fig. A.1: Raw correlation of stock returns
The matrix is ordered according to the outcome of the dendrogram clustering algorithm shown on right.

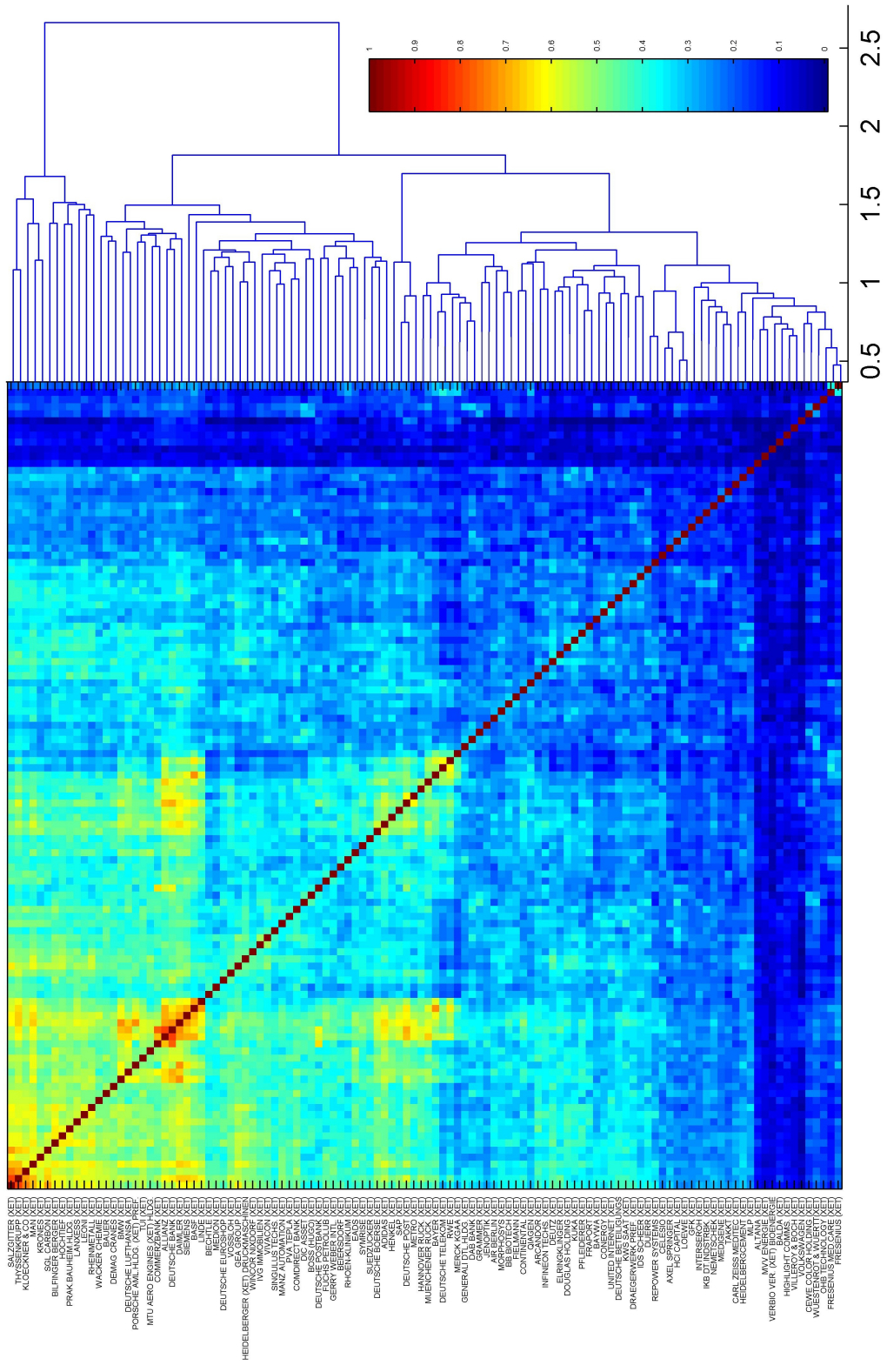

Fig. A.2: Normalized correlation of stock returns
The matrix is ordered according to the outcome of the dendrogram clustering algorithm shown on right.

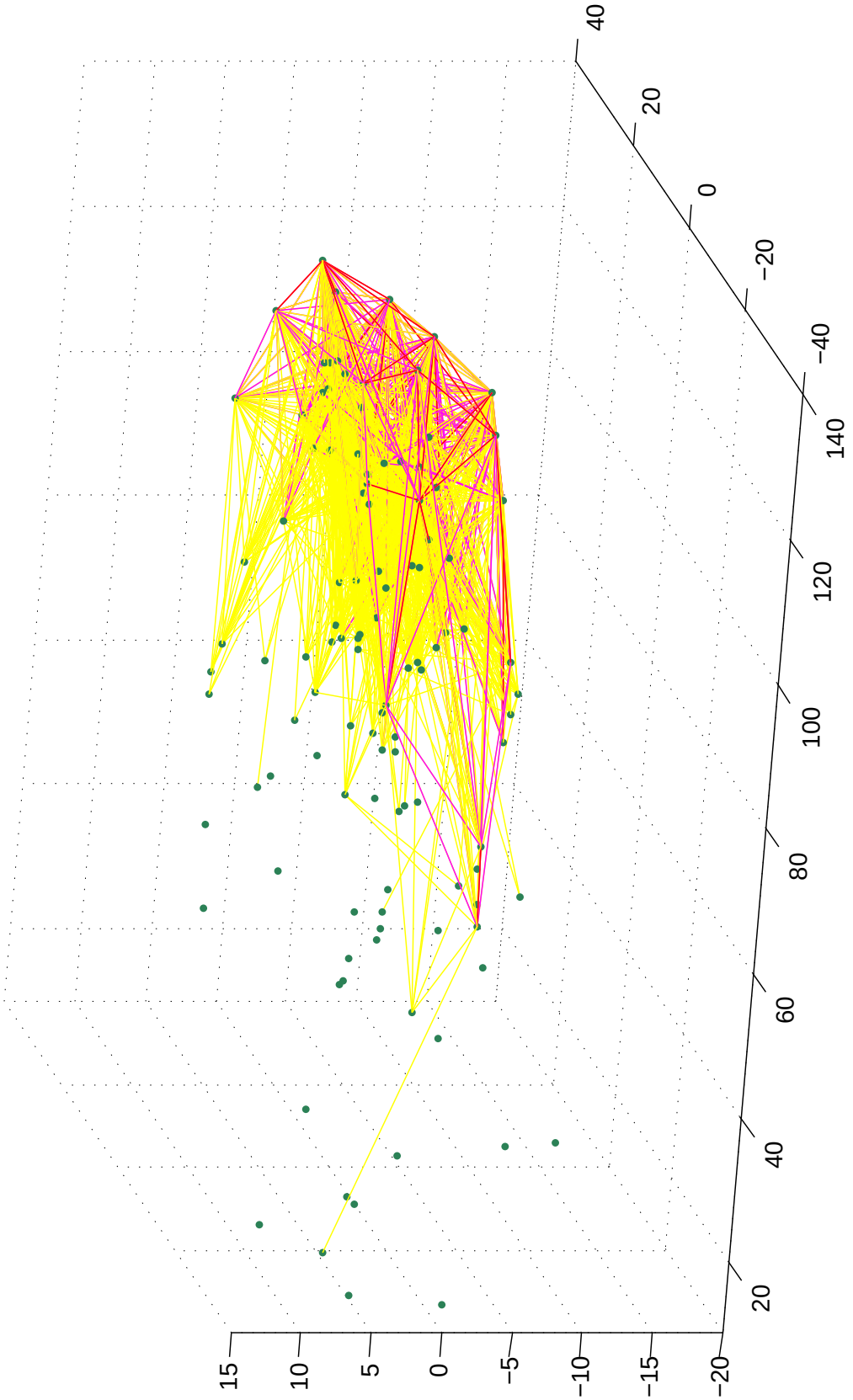

Fig. A.3: Stocks in 3D principal space derived from the normalized correlation matrix *Color-codes lines, correlation* > 0.5 *(yellow),* > 0.6 *(magenta),* > 0.7 *(red).*

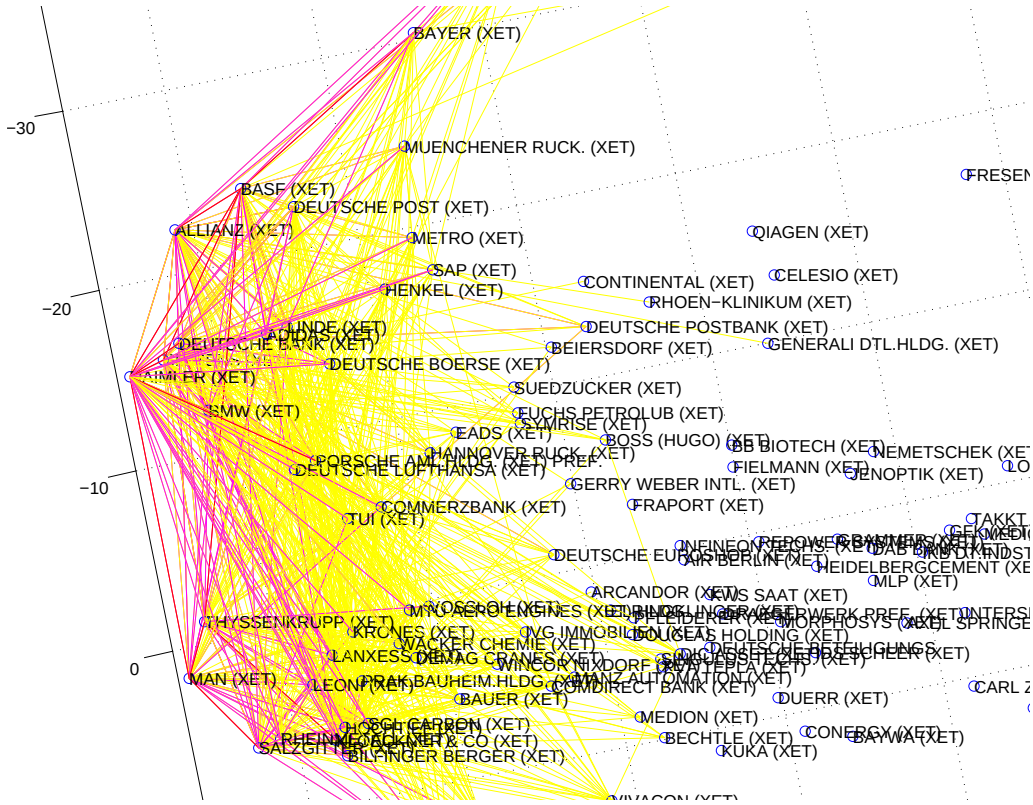

Fig. A.4: Stocks in 3D principal space, top view
Color-codes lines, correlation > 0.5 *(yellow),* > 0.6 *(magenta),* > 0.7 *(red).*

B. THE HERDING MODEL

B.1 Independent One-Leader Benchmark

Let us start by considering an arbitrary agent in the fully connected core who is always in a *fixed* state and does not change opinion. As before, let $1/N < p < 1$ denote the fraction of followers that are connected to the fixed-opinion agent, or *independent leader*, such that the agent has pF followers, and assume that the remaining $(1-p)F$ followers are allocated with equal weight among the remaining core agents, indexed by $i = 1, \ldots, N-1$. When $p = 1/N$, all core agents have the same number of followers, F/N. Conversely when $p \to 1$, the system is almost entirely represented by the leader. For ease of notation, let us write the transition probability as

$$\pi_i = (a + \lambda N F_i/F)\ \Delta t \qquad \text{for} \quad i = 1, \ldots, N-1, \tag{B.1}$$

where F_i now denotes the *system-wide number of followers in the opposite state*, so the $N-1$ equally weighted core agents will obey the transition rate (B.1). As before, we set $\Delta t = 1/(a+\lambda N)$. Furthermore, let β be an indicator function that takes on the values 0 or 1 depending on whether the state of agent i equals or is different from the state of the fixed-opinion agent. Then we can rewrite the herding term in Eq. (B.1), NF_i/F, taking into account the fixed opinion of the leader (say, being optimistic)

$$N\frac{F_i}{F} = \frac{N}{F}\left(Fp\beta + (n-1)\frac{F(1-p)}{N-1}\right)\ , \tag{B.2}$$

which yields the modified version of the transition probability (B.1),

$$\begin{aligned} \pi_i &= \left(a + \lambda N p\beta + \lambda \frac{N}{N-1}(1-p)n\right)\ \Delta t \\ &\approx (a + \lambda N p\beta + \lambda(1-p)n)\ \Delta t \end{aligned} \tag{B.3}$$

for large N. Depending on the value of the indicator function β, the transition probabilities of agent i are either

$$\pi_i = (\varepsilon + (1-p)n)\,\lambda\,\Delta t \qquad \text{or} \tag{B.4}$$

$$\pi_i = (\varepsilon + Np + (1-p)n)\,\lambda\,\Delta t\,, \tag{B.5}$$

where we adapted ε to the definition (2.7) by noting that a fully connected core implies $D = N$.

Fixing the opinion of one agent is equivalent to creating an asymmetry in the autonomous component that stems from the additional term Np in the modified transition rates. Put simply, the system exhibits a tendency towards the fixed opinion that depends on p. A straightforward mean-field argument (see, e.g., Alfarano and Milaković, 2009) results in the following system-wide transition probabilities, analogous to an extensive version of the transition rates (2.4) and (2.5),

$$\pi^- = \frac{n}{N}\,\frac{\varepsilon + (1-p)(N-n)}{\varepsilon + N}\,, \tag{B.6}$$

$$\pi^+ = \frac{(N-n)}{N}\,\frac{\varepsilon + Np + (1-p)n}{\varepsilon + N}\,. \tag{B.7}$$

The equilibrium distribution of such a unary Markov process is (see, e.g., Garibaldi et al., 2003) the *Polya distribution* $R(\varepsilon_1, \varepsilon_2; z)$, with $z = n/N$ and shorthands[1]

$$\varepsilon_1 = \frac{\varepsilon + Np}{1-p}\,, \qquad \varepsilon_2 = \frac{\varepsilon}{1-p}\,. \tag{B.8}$$

Increasing the value of the control parameter p leads to an increasingly asymmetric distribution peaked around the opinion of the leader. Fixing the opinion of one agent, however, yields a very unsatisfactory approximation for the simulations in Section 2.5, where the leader is not in a fixed state but rather switches states as well. Therefore we proceed by assuming that the 'independent' leader switches opinion randomly, without being influenced by other agents, which basically means that the autonomous term in the mean-field transitions (B.6) and (B.7) is now stochastic and time-dependent, hinging on the random realizations of the leader's state.

Such a situation is harder to tackle analytically because it leads to a stochastic differential equation with random coefficients. In order to approximate the full mathematical problem, we employ a so-called *adiabatic* approximation that neglects

[1] The Polya distribution converges to the Beta distribution for large N. The results of this section, however, do not significantly depend on whether we use a continuous or discrete approach (material upon request).

the adjustment of the system to the switching of the leader by assuming that the leader's switches are slow enough in order for the $N-1$ agents to reach statistical equilibrium. Then we can consider the system as being in statistical equilibrium most of the time and, consequently, the resulting equilibrium distribution G_e becomes the superposition of two independent equilibrium distributions, corresponding to the two possible configurations of the leader,

$$G_e = \frac{1}{2}R(\varepsilon_1, \varepsilon_2; z) + \frac{1}{2}R(\varepsilon_2, \varepsilon_1; z) \ , \tag{B.9}$$

which is an average of the previous asymmetric distributions among the two alternative configurations of the leader. The equilibrium distribution is now symmetric (note the interchange of the parameters ε_1 and ε_2) and U-shaped. From Eq. (B.9), the second moment of the equilibrium distribution $M_{2,e}$ is given by

$$M_{2,e} = \frac{1}{2}M_2(\varepsilon_1, \varepsilon_2) + \frac{1}{2}M_2(\varepsilon_2, \varepsilon_1) \ , \tag{B.10}$$

where $M_2(\cdot, \cdot)$ denotes the second moment of the respective asymmetric Polya distribution with parameters $\varepsilon_1, \varepsilon_2$, and the variance of the equilibrium distribution for a given p is

$$\begin{aligned} Var[z]_p &= \frac{1}{2}Var[\varepsilon_1, \varepsilon_2] + \frac{1}{2}Var[\varepsilon_2, \varepsilon_1] \\ &\quad + \frac{1}{2}\left\{M_1^2[\varepsilon_1, \varepsilon_2] + M_1^2[\varepsilon_2, \varepsilon_1]\right\} - \left(\frac{1}{2}\right)^2 \ , \end{aligned} \tag{B.11}$$

where M_1 designates the first moment of the respective asymmetric Polya distribution, and $1/2$ is obviously the mean of the equilibrium distribution G_e. The two variances are equal since they are the same under an exchange of the two parameters $\varepsilon_1, \varepsilon_2$, hence the previous equation can be written as

$$Var[z]_p = Var[\varepsilon_1, \varepsilon_2] + \frac{1}{2}\left\{M_1^2[\varepsilon_1, \varepsilon_2] + M_1^2[\varepsilon_2, \varepsilon_1]\right\} - \frac{1}{4} \ . \tag{B.12}$$

It is possible to show (see, e.g., Garibaldi et al., 2003) that

$$M_1[\varepsilon_1, \varepsilon_2] = \frac{\varepsilon_1}{\varepsilon_1 + \varepsilon_2} \ , \tag{B.13}$$

$$Var[\varepsilon_1, \varepsilon_2] = \frac{\varepsilon_1\varepsilon_2}{(\varepsilon_1 + \varepsilon_2)^2}\frac{\varepsilon_1\varepsilon_2 + N}{N(\varepsilon_1\varepsilon_2 + 1)} \ , \tag{B.14}$$

and utilizing these in Eq. (B.12) yields

$$Var[z] = \frac{1}{4} - \frac{\varepsilon_1 \varepsilon_2}{(\varepsilon_1 + \varepsilon_2)(\varepsilon_1 + \varepsilon_2 + 1)} \,. \tag{B.15}$$

Finally, recalling the shorthands in (B.8), we obtain the variance as a function of the control parameter p,

$$Var[z]_p = \frac{1}{4} - \frac{1 + pN}{(2 + pN)(3 + pN - p)} \,, \tag{B.16}$$

under the parameter choice $\varepsilon = 1$, i.e. $\lambda = 1$ and $a = 1$. For $N \gg 1$, we immediately see that Eq. (B.16) provides boundary values that are consistent with our previous findings: if $p = 1/N$, the variance tends to $1/12$, representing the correct value for the uniform distribution (recall the parameter choice $\varepsilon = 1$); if $p \to 1$, the variance tends to $1/4$, representing a distribution concentrated either in 0 or 1. We simulated the modified model with a randomly switching leader, successively increasing the control parameter p in a fully connected core of size $N = 500$ with a total of $F = 500,000$ followers. As before, we simulated each parametrization with half a million sweeps.

The results, along with the prediction (B.16), are shown in Figure 2.3. For easier comparison with the simulation results in Figures 2.3 and 2.4, we calculate the standard deviation in the number of followers for each parametrization of p, which is

$$\sigma = \sqrt{\frac{1}{N}(pF)^2 + \frac{N-1}{N}\left(\frac{(1-p)F}{N-1}\right)^2 - \left(\frac{F}{N}\right)^2}, \tag{B.17}$$

and invert the relation to obtain

$$p = \frac{\sigma\sqrt{N-1}}{F} + \frac{1}{N}. \tag{B.18}$$

While the independent leader scenario exhibits a quicker convergence to the limiting variance of one-fourth than the one-leader model, both versions are qualitatively similar in the sense that there is sudden and pronounced increase in volatility already for small values of p. The main difference between the independent vs one-leader scenarios is that the independent leader switches randomly (thus independently) between the two states, while the switches of the one-leader in Section 2.5.3 still depend on the interactions with the other core agents, which intuitively slows down the variance amplification relative to the independent leader case. As far as the creation of fluctuations and therefore risk is concerned, the important common feature of both models is that they exhibit a sudden and pronounced increase in system-wide volatil-

ity as soon as a relatively small number of core agents obtains a disproportionately large weight in the core network.

B.2 Source Code of the Herding Simulation

```
tend=19;          % number of loops
T=500000;         % T steps
result=zeros(tend,2);
N=500;            %# of agents
ratio=1000;
draws=zeros(N,1);
delta=ones(N,1);% herding switches
% initialize random number generator
rand('twister',sum(100*clock));
randn('state',sum(100*clock));
%load thes;       % load followers seed if necessary
tic;
% optional parameter setup
%pincrease=-0.2;
%pstartvalue=5.9;
%parameter=zeros(tend,1);
%parameter(1)=pstartvalue;
%for a=2:tend;
%     parameter(a)=parameter(a-1)+pincrease;
%end

for l=1:tend      %start MC loop
A=zeros(N,N);
count=zeros(T,1);
WA=zeros(N,N);
CF=zeros(1,N);    % # connected F
nlinks=zeros(1,N);
S=zeros(1,N);     % # followers

% set up random network      (optional)
%linkprob=1;      % linking "probability"
%threshold=unifrnd(0,1,N,N);  %make matrix of random numbers
%c=2;
%for a=1:N
%     for b=c:N
%          if threshold(a,b)<linkprob
%               A(a,b)=1;
%               A(b,a)=1;
%          end
%     end
%     c=c+1;
%end
```

```
43
44 %A=circle(N,25);      % setup lattice
45
46 A=sfg(N,10,5);        % setup scale free graph
47
48 %list of # of links
49 for a=1:N
50 nlinks(1,a)=sum(A(a,:));
51 end
52
53 % set aut. switching for eps==1
54 aut=mean(nlinks)/(N-1)
55 eps=aut*N/mean(nlinks)
56
57 % homogenous agents scenario
58 %S(1,1:N)=1000;
59
60 %  draw from uniform
61 %S(1,1:N)=round(abs(unifrnd(ratio-parameter(l),ratio+parameter(↘
       l),N,1)));
62
63 % draw followers from pareto
64 %S(1,:)=makemeanpareto(parameter(l),ratio,N);
65
66 % take followers seed
67 tseed;
68 S(1,:)=thes(l,:);
69 mixup;
70
71 F=sum(S);       % calculate total # of followers
72 avgF=F/N;       % calc average f
73
74 for a=1:N       % calculate connected followers
75       xxf=0;
76       for b=1:N;
77       xf=A(a,b)*S(b);
78       xxf=xxf+xf;
79       end
80       CF(a)=xxf;
81 end
82
83 si=round(unifrnd(0,1,1,N));
84 for i=1:N
85       if si(i)==0
86            si(i)=-1;
87       end
88 end
89 S=S.*si;
90
```

```
 91 for a=1:N      % build weighted adj matrix
 92     for b=1:N
 93         WA(a,b)=A(a,b)*S(b);
 94     end
 95 end
 96
 97  for b=1:T    % Switching ...
 98         draws(:,1)=unifrnd(0,1,N,1);
 99         for a=1:N
100             fiplus=0.5*(CF(a)+sum(WA(a,:)));
101             fiminus=CF(a)-fiplus;
102             if S(a)<0
103                 if draws(a)<(aut+delta(a)*fiplus/avgF)/(aut+N);
104                     S(a)=-S(a);
105                     WA(:,a)=-WA(:,a);
106                 end
107             else
108                 if draws(a)<(aut+delta(a)*fiminus/avgF)/(aut+N)
109                     S(a)=-S(a);
110                     WA(:,a)=-WA(:,a);
111                 end
112             end
113         end
114         for a=1:N
115             if S(a)>0
116                 count(b)=count(b)+S(a)+1;
117             end
118         end
119  end
120 share=count./(F+N);  % counting share of agents in each state
121 result(l,2)=var(share);
122 result(l,1)=std(abs(S));
123 toc;
124 end   % end MC loop
125 result
126 save xsfg9 result;
```

C. FURTHER DETAILS ABOUT THE BOARD NETWORK

C.1 Source Code of the Clustering Algorithm

```
% find groups in adj with pca
clear store srepr srepradj numb repradj repr numeig a b lam myA mynames score adjnlist optA corrmat eigval eigvec DDD scorepoints groupvalue groupid lam opt_name stA;
myA=Aoneb;    % read adj matrix
mynames=ycomp(1:length(myA),1);  % read corresponding vector of names
%build standardized adj
myA=myA+diag(ones(length(myA),1)/2);  % fill diag

optA=zeros(length(myA));
adjnlist=(zeros(length(myA),1));
%standardize adj matrix
for a=1:length(myA)
    for b=1:length(myA)
        stA(a,b)=(myA(a,b)-mean(myA(:,b)))/std(myA(:,b));
    end
end

% make corr matrix eigenvales etc.
corrmat=1/length(myA)*stA*stA';
eigval=eig(corrmat);
[eigvec,DDD] = eig(corrmat);
Factor=stA'*eigvec;

a=1;
numeig=0;
while eigval(a,1) > 3.5
    numeig=numeig+1;
    a=a+1;
end

score=zeros(length(myA),2*numeig);

%make scoringmatrix proportial to F
for a=1:numeig
    store(:,a+a-1)=Factor(:,a)/sum(abs(Factor(:,a)));
```

```
35      store(:,a+a)=-Factor(:,a)/sum(abs(Factor(:,a)));
36  end
37
38  if sum(Factor(:,1)) > 0
39      scorepoints(:,1)=store(:,1);
40      scorepoints(:,2:2*numeig-1)=store(:,3:2*numeig);
41  else
42     scorepoints(:,1)=store(:,2);
43      scorepoints(:,2:2*numeig-1)=store(:,3:2*numeig);
44  end
45
46  %scoring
47  for lam=1:2*numeig-1
48      for b=1:length(myA)
49          for a=1:length(myA)
50              if scorepoints(a,lam)>0
51                  if myA(a,b)>0
52                      score(b,lam)=score(b,lam)+scorepoints(a,lam↘
                            )^2;
53                   else
54                       score(b,lam)=score(b,lam)-0*scorepoints(a,↘
                             lam)^2;
55                   end
56              end
57              if scorepoints(a,lam)<0
58                  if myA(a,b)==0
59                      score(b,lam)=score(b,lam)+0*scorepoints(a,↘
                            lam)^2;
60                  else
61                      score(b,lam)=score(b,lam)-scorepoints(a,lam↘
                            )^2;
62                 end
63              end
64          end
65      end
66  end
67
68  %select best fitted group and write into vector groupid
69  for a=1:length(myA)
70          [gval,gid]=max(score(a,:));
71     if max(score(a,:))>mean(score(:,gid))+std(score(:,gid))/2
72          [groupvalue(a),groupid(a)]=max(score(a,:));
73      else
74          groupvalue(a)=-1;
75          groupid(a)=2*numeig;
76      end
77  end
78
79  % remove firms with no good score
```

```
numb=hist(groupid,1:1:2*numeig);
for a=1:length(numb)
    if numb(a)<4
        if numb(a)>0
            for b=1:length(myA)
                if groupid(b)==a
                    groupid(b)=2*numeig;
                end
            end
        end
    end
end

% make sortinglist from groupid
c=1;
for b=1:2*numeig
    for a=1:length(myA)
        if groupid(a)==b
            adjnlist(c)=a;
            c=c+1;
        end
    end
end

% resort adjacency matrix
for a=1:length(myA)
    repr(a,:)=scorepoints(adjnlist(a),:);
end

c=1;
for a=1:length(myA)
    for b=c:length(myA)
        if myA(adjnlist(a),adjnlist(b))>0
            optA(a,b)=1;
            optA(b,a)=1;
            opt_name(a,1)=mynames(adjnlist(a));
        end
    end
    c=c+1;
end
```

C.2 Distribution of Board Membership

	1	**2**	**3**	**4**	**5**	**6**	**7**	**8**	**9**	**10**
1993	1528	136	36	17	11	8	3	2	3	0
1999	1528	113	34	16	9	5	3	1	0	2
2005	1436	107	31	9	7	2	1	0	0	0

Tab. C.1: Overall frequency distribution of mandates

year	executives	# of additional mandates									
		0	**1**	**2**	**3**	**4**	**5**	**6**	**7**	**8**	**9**
1993	565	456	58	21	12	8	5	2	1	2	0
1999	539	469	29	19	9	5	4	1	1	0	2
2005	456	401	37	11	3	4	0	0	0	0	0

Tab. C.2: Frequency of executives' supervisory board memberships

C.3 Transition Matrices for Board Membership

		# of mandates in 1999										
		0	**1**	**2**	**3**	**4**	**5**	**6**	**7**	**8**	**9**	**10**
# of mandates in 1993	**0**	906	911	39	7	4	0	0	0	0	0	0
	1	920	369	30	10	4	1	1	2	0	0	0
	2	59	33	14	4	1	0	0	0	0	0	0
	3	9	8	6	3	1	2	0	0	0	0	0
	4	4	7	2	1	1	1	0	0	0	0	0
	5	4	1	2	0	1	1	1	0	0	0	0
	6	1	0	0	0	0	2	2	1	0	0	1
	7	1	0	1	0	1	0	0	0	0	0	0
	8	0	0	0	0	0	1	0	0	0	0	0
	9	1	0	0	2	0	0	0	0	0	0	0
	10	0	0	0	0	0	0	0	0	0	0	0

Tab. C.3: Transition matrix for board membership during 1993–1999.

# of mandates in 1999	# of mandates in 2005										
	0	**1**	**2**	**3**	**4**	**5**	**6**	**7**	**8**	**9**	**10**
0	977	883	34	10	1	0	0	0	0	0	0
1	961	328	32	6	2	0	0	0	0	0	0
2	49	24	16	3	1	1	0	0	0	0	0
3	6	9	3	4	1	3	1	0	0	0	0
4	4	5	3	1	0	0	0	0	0	0	0
5	3	2	2	0	0	0	0	1	0	0	0
6	0	0	1	1	1	1	0	0	0	0	0
7	0	1	1	0	0	1	0	0	0	0	0
8	0	0	0	0	0	0	0	0	0	0	0
9	0	0	0	0	0	0	0	0	0	0	0
10	0	0	0	1	0	0	0	0	0	0	0

Tab. C.4: Transition matrix for board membership during 1999–2005

# of mandates in 1993	# of mandates in 2005										
	0	**1**	**2**	**3**	**4**	**5**	**6**	**7**	**8**	**9**	**10**
0	662	1125	58	16	4	2	0	0	0	0	0
1	1197	104	25	7	1	3	0	0	0	0	0
2	94	11	4	0	1	0	1	0	0	0	0
3	21	4	4	0	0	0	0	0	0	0	0
4	12	2	0	1	0	0	0	1	0	0	0
5	8	1	0	0	0	1	0	0	0	0	0
6	2	2	1	2	0	0	0	0	0	0	0
7	2	1	0	0	0	0	0	0	0	0	0
8	0	1	0	0	0	0	0	0	0	0	0
9	2	1	0	0	0	0	0	0	0	0	0
10	0	0	0	0	0	0	0	0	0	0	0

Tab. C.5: Transition matrix for board membership during 1993–2005

C.4 Adjacency Matrices Sorted by Cliques

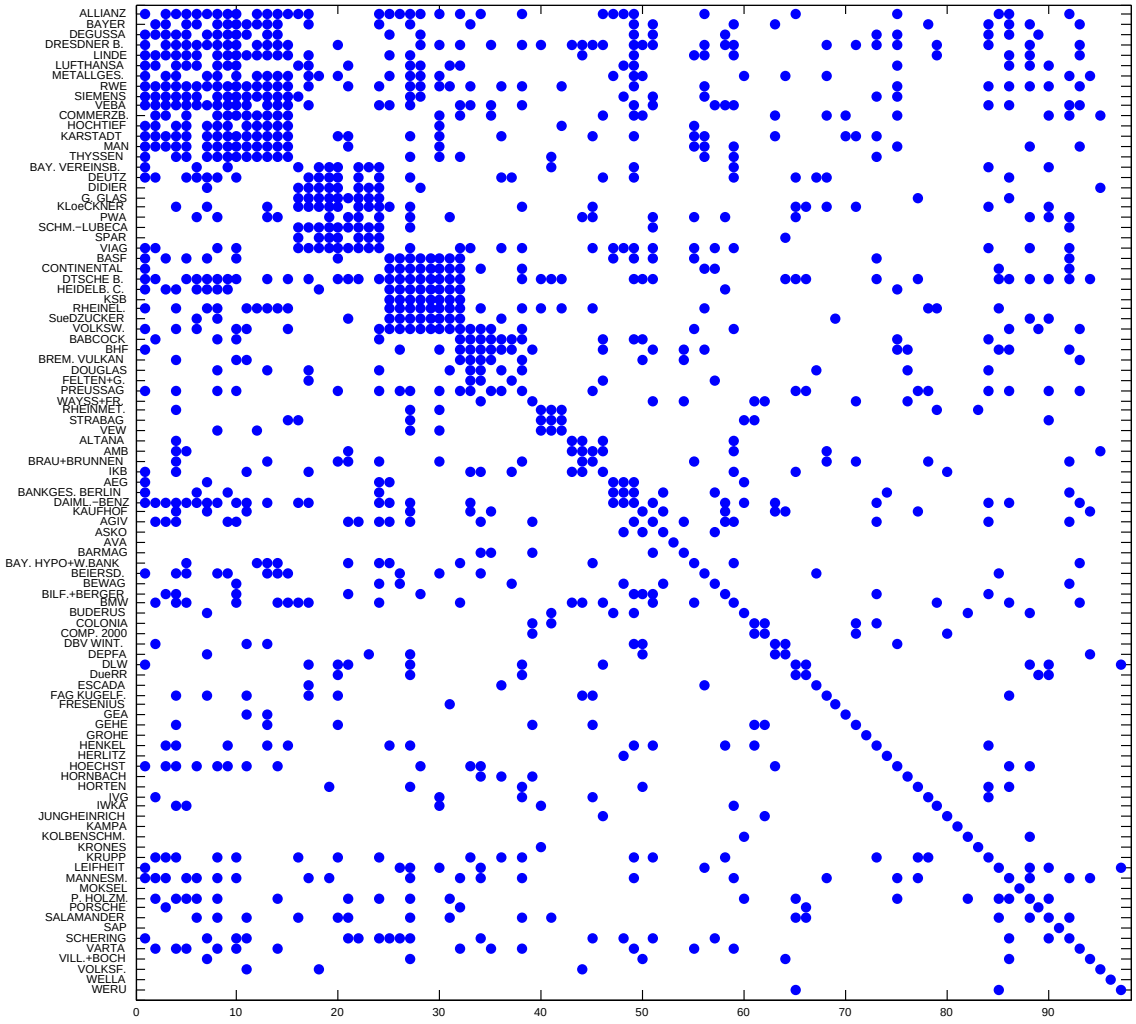

Fig. C.1: Resorted adjacency matrix 1993

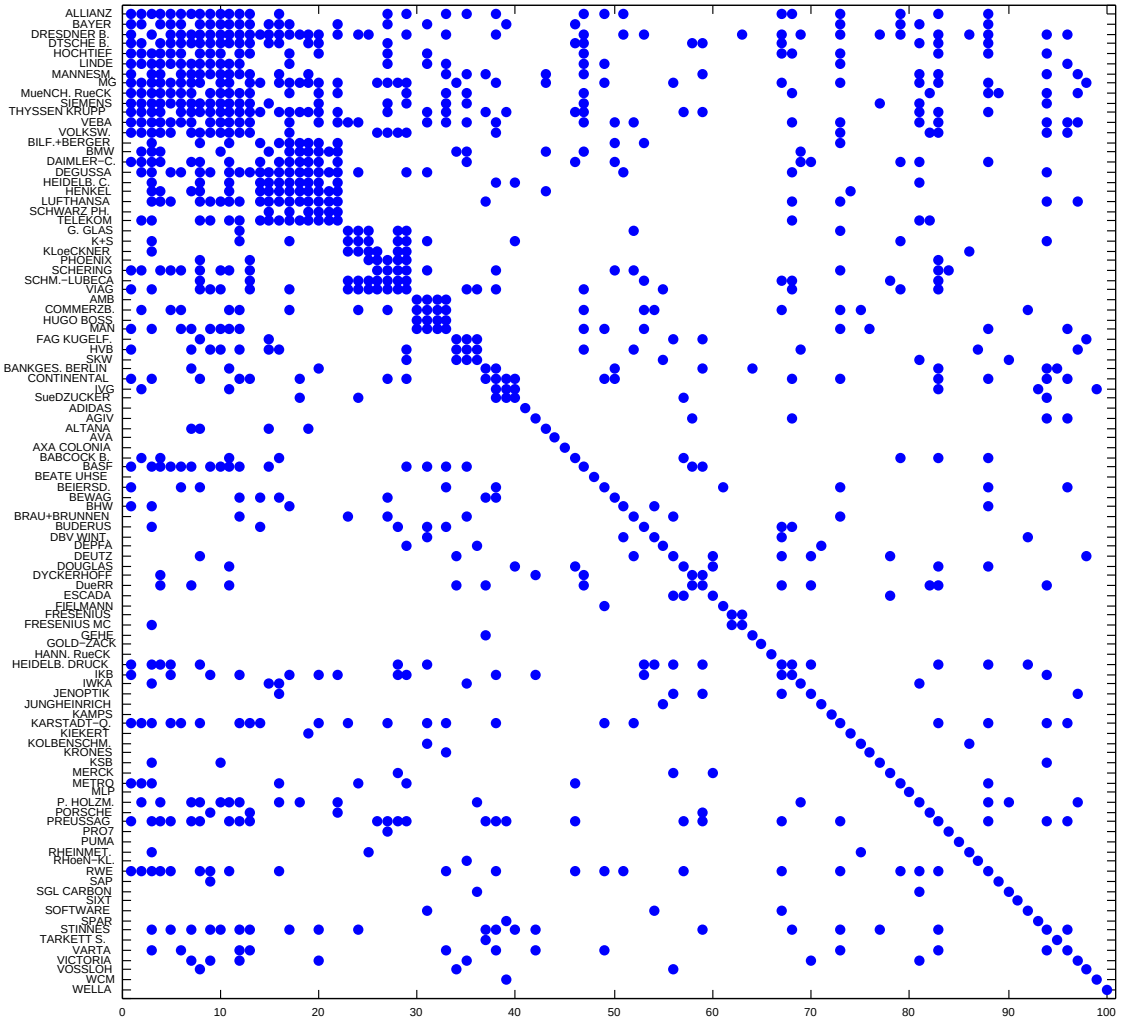

Fig. C.2: Resorted adjacency matrix 1999

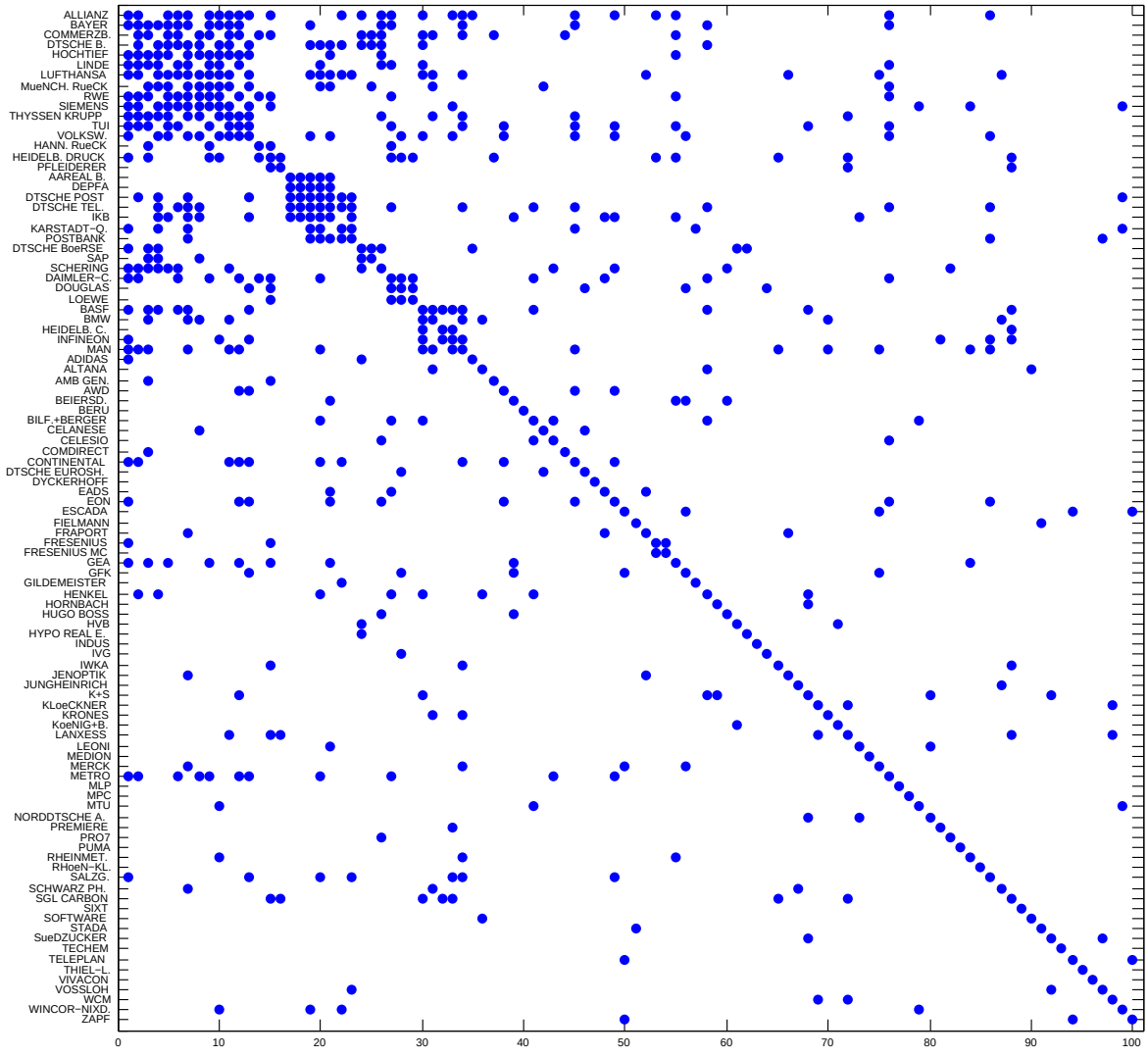

Fig. C.3: Resorted adjacency matrix 2005

D. PLOTS OF THE FINANCIAL VILLAGE

D.1 Partial Correlations

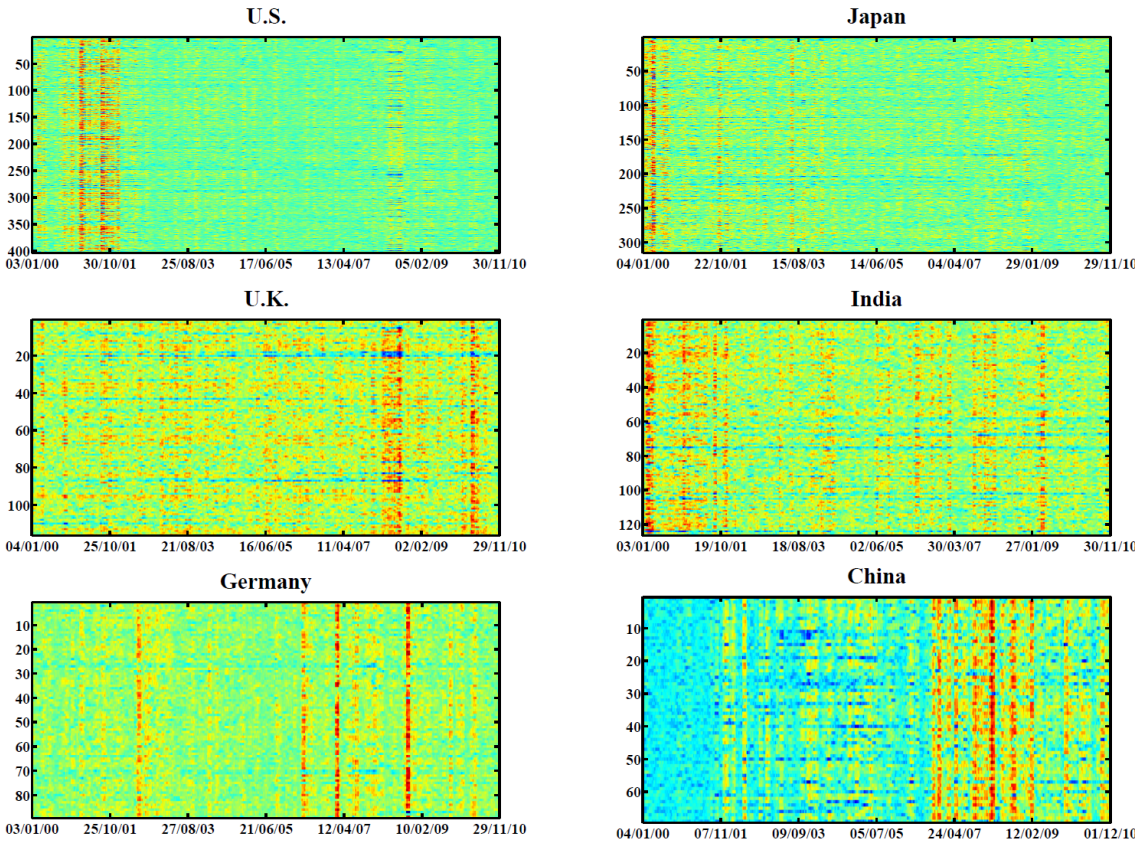

Fig. D.1: Dynamics of the intra partial correlation

For each market, we use a 22-day window, and in each window calculate the intra partial correlation, removing the effect of the index. Each horizontal line represents the average correlation of one stock (the left ordinate displays the number of the stock).

D.2 Pairwise Correlations between Countries

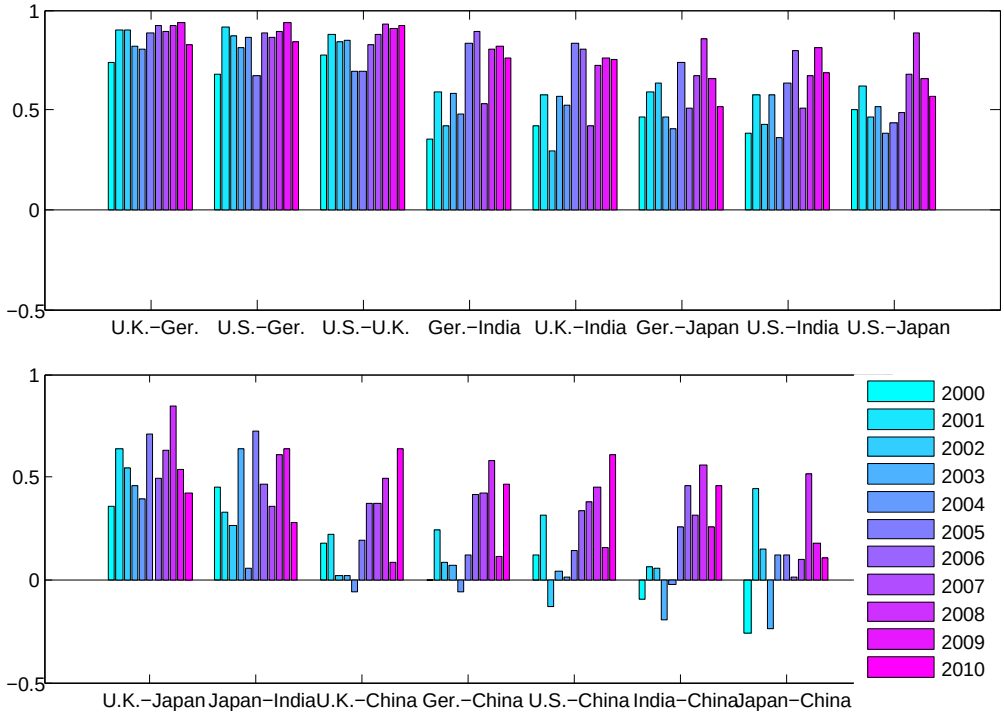

Fig. D.2: Average correlation of price indices

The year-by-year correlations were calculated as the average over all 66 day windows of each year. The pairs are sorted in descending order by total average correlation. Averaging by years allows us to judge on the general – medium to long run – interdependence between markets.

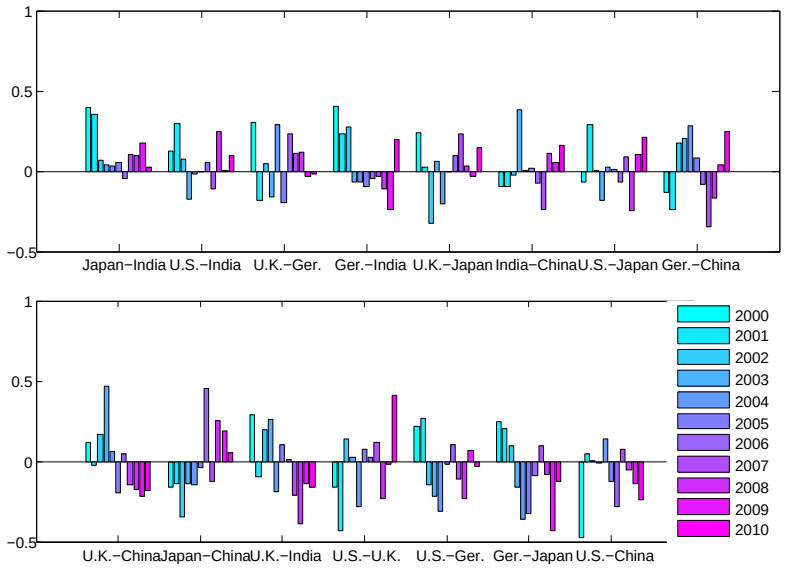

Fig. D.3: Average correlation of ICF

The year-by-year correlations were calculated as the average over all 66 day windows of each year. The pairs are sorted in descending order by total average correlation. Averaging by years allows us to judge on the general – medium to long run – interdependence between markets.

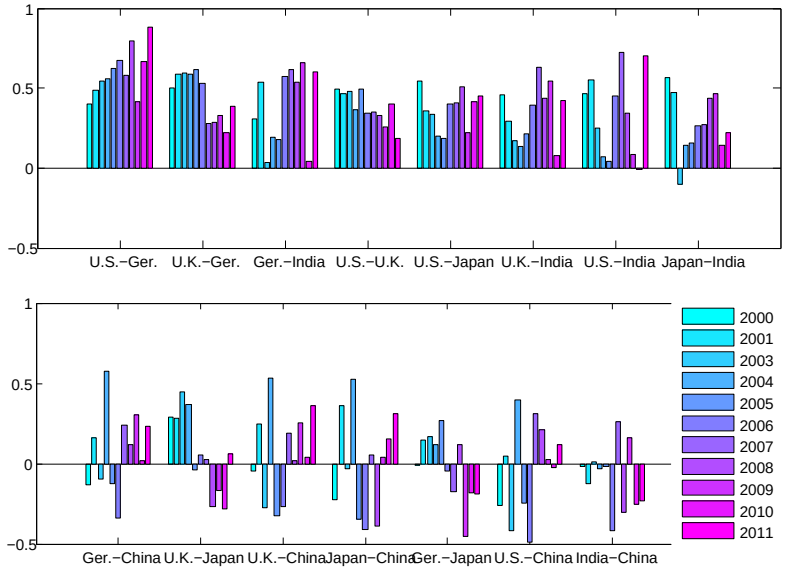

Fig. D.4: Average meta-correlation

The year-by-year correlations were calculated as the average over all 66 day windows of each year. The pairs are sorted in descending order by total average correlation. Averaging by years allows us to judge on the general – medium to long run – interdependence between markets.

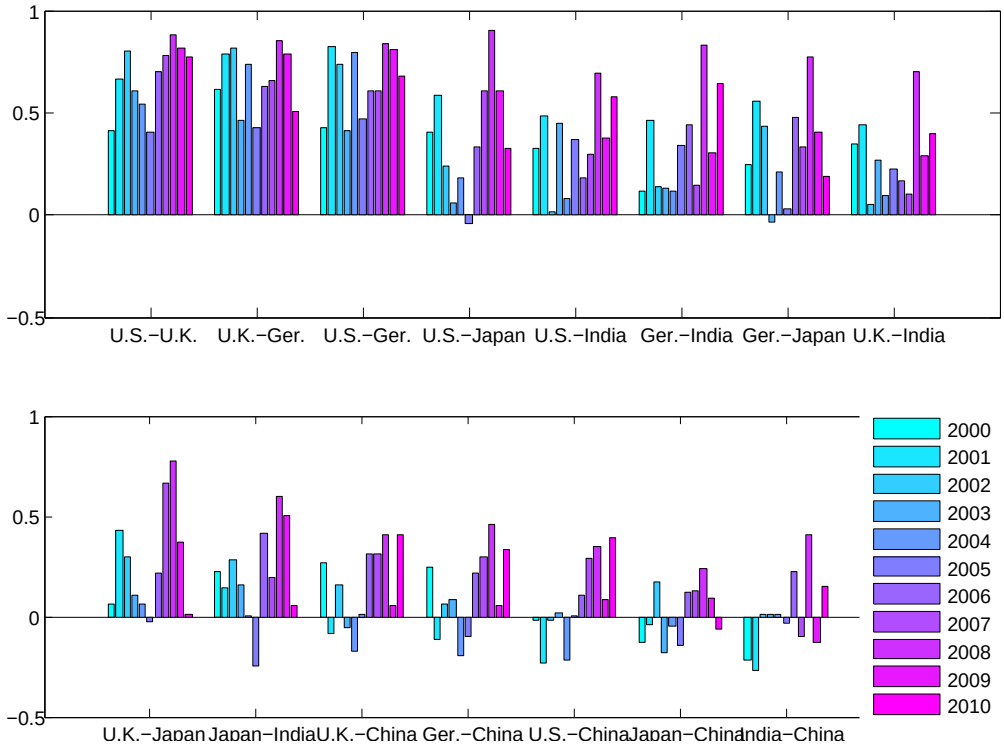

Fig. D.5: Average index volatility correlation

The year-by-year correlations were calculated as the average over all 66 day windows of each year. The pairs are sorted in descending order by total average correlation. Averaging by years allows us to judge on the general – medium to long run – interdependence between markets.

D.3 Dynamics of ICF

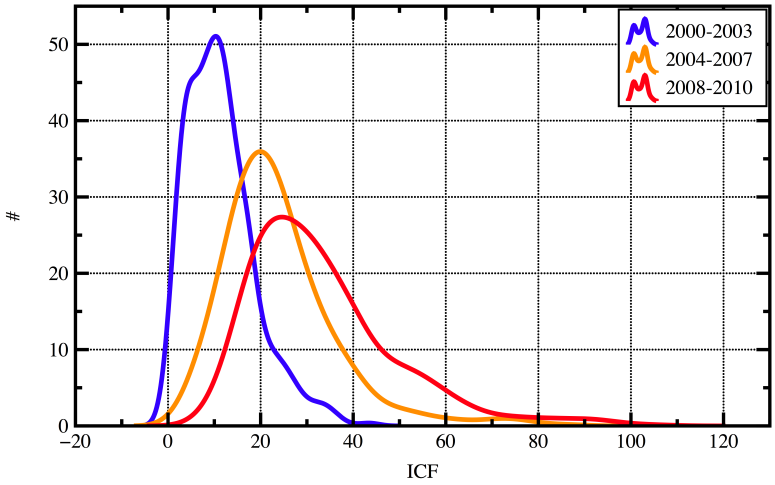

Fig. D.6: Distributions of the Index Cohesive Force
ICF values for the Japaneses market in different periods - 2000-2003 (blue), 2004-2007 (orange), and 2008-2010 (red). It is observable that the distributions are different for the studied periods, and that the ICF values are higher with a fat tail distribution for periods marked by strong economic fluctuations.

D.4 Meta-Correlations

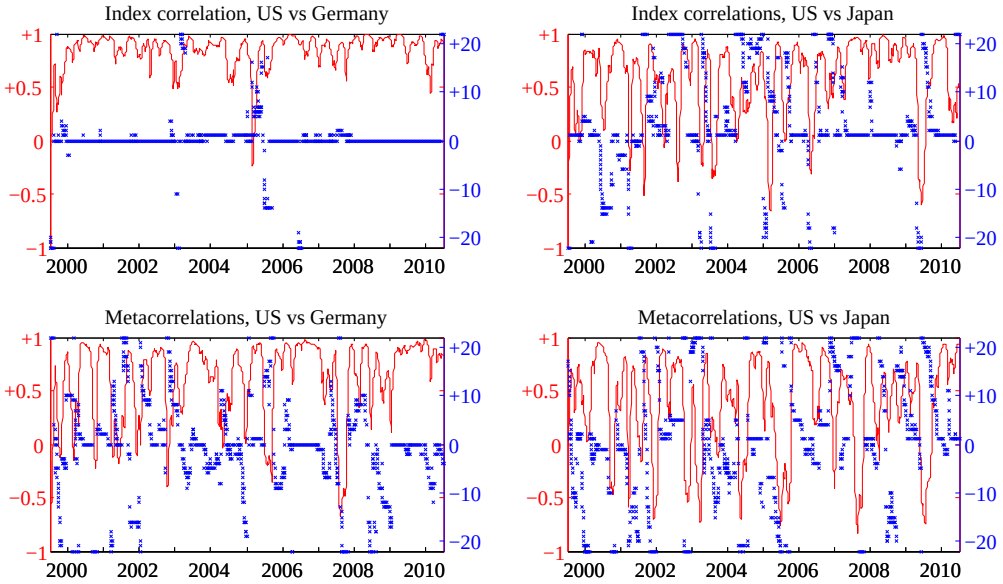

Fig. D.7: Market correlations: US-Germany, US-Japan
Index correlations (top) and meta-correlations (bottom) for US-Germany and US-Japan, Lag with maximum correlation (blue cross) and correlation at lag 0 for the cross-correlation of the indices. Both performed for a 66-day window.

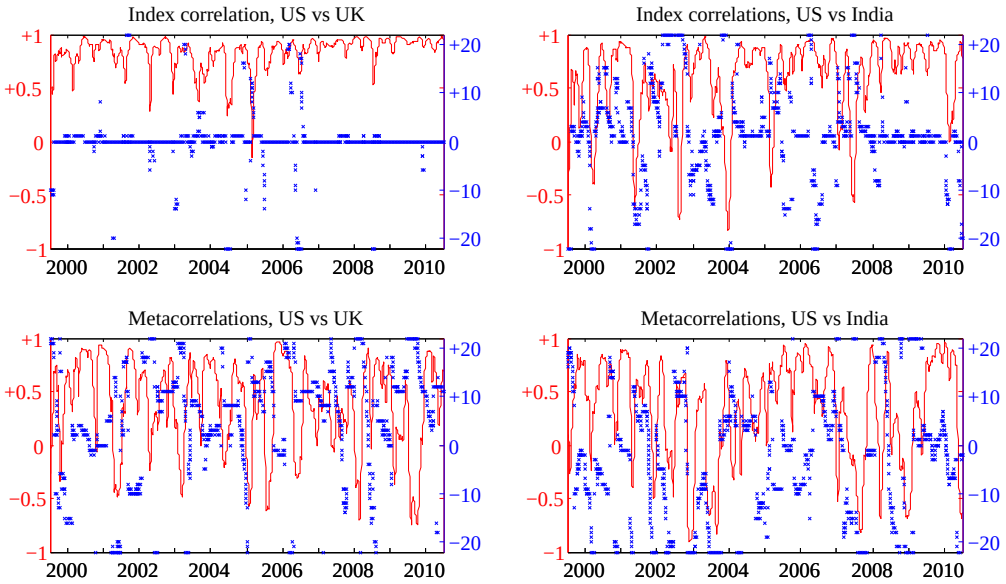

Fig. D.8: Market correlations: US-UK, US-India

Index correlations (top) and meta-correlations (bottom) for US-UK and US-India, Lag with maximum correlation (blue cross) and correlation at lag 0 for the cross-correlation of the indices. Both performed for a 66-day window.

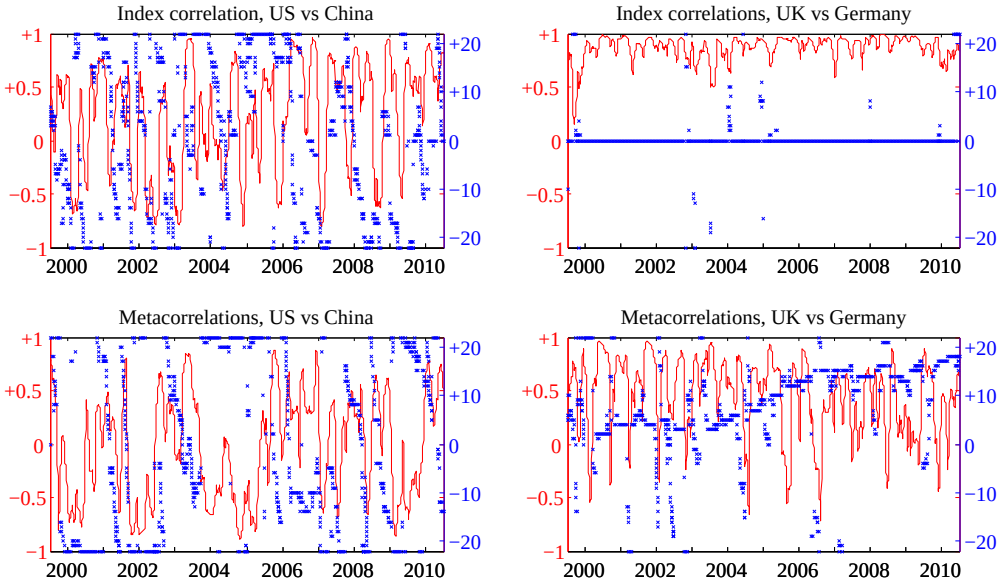

Fig. D.9: Market correlations: US-China, UK-Germany

Index correlations (top) and meta-correlations (bottom) for US-China and UK-Germany, Lag with maximum correlation (blue cross) and correlation at lag 0 for the cross-correlation of the indices. Both performed for a 66-day window.

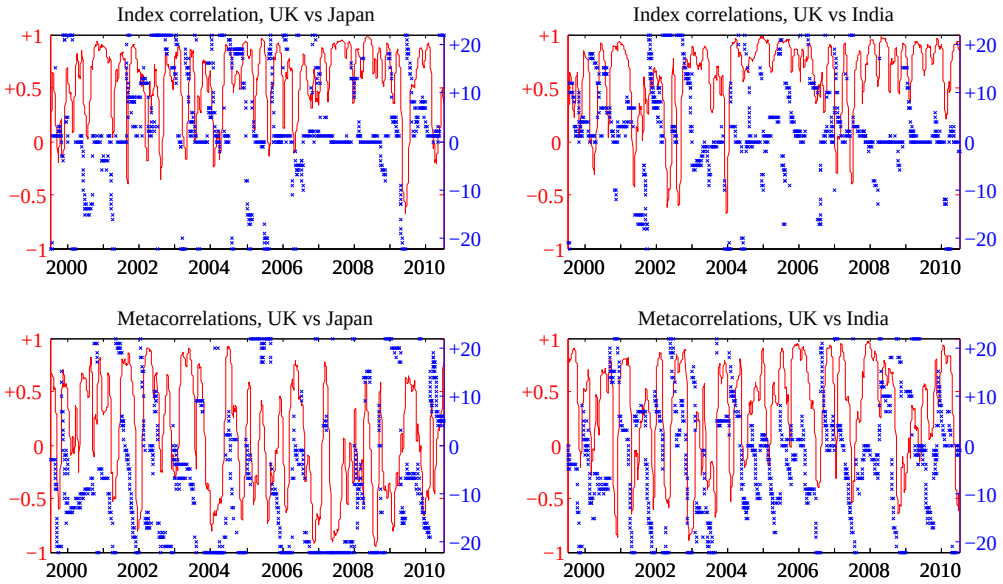

Fig. D.10: Market correlations: UK-Japan, UK-India

Index correlations (top) and meta-correlations (bottom) for UK-Japan and UK-India, Lag with maximum correlation (blue cross) and correlation at lag 0 for the cross-correlation of the indices. Both performed for a 66-day window.

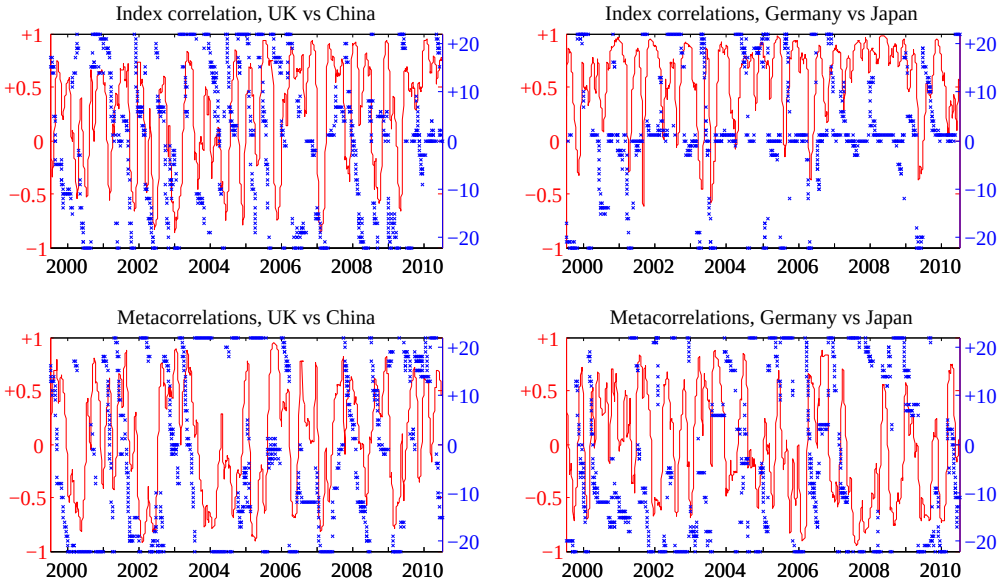

Fig. D.11: Market correlations: UK-China, Germany-Japan

Index correlations (top) and meta-correlations (bottom) for UK-China and Germany-Japan, Lag with maximum correlation (blue cross) and correlation at lag 0 for the cross-correlation of the indices. Both performed for a 66-day window.

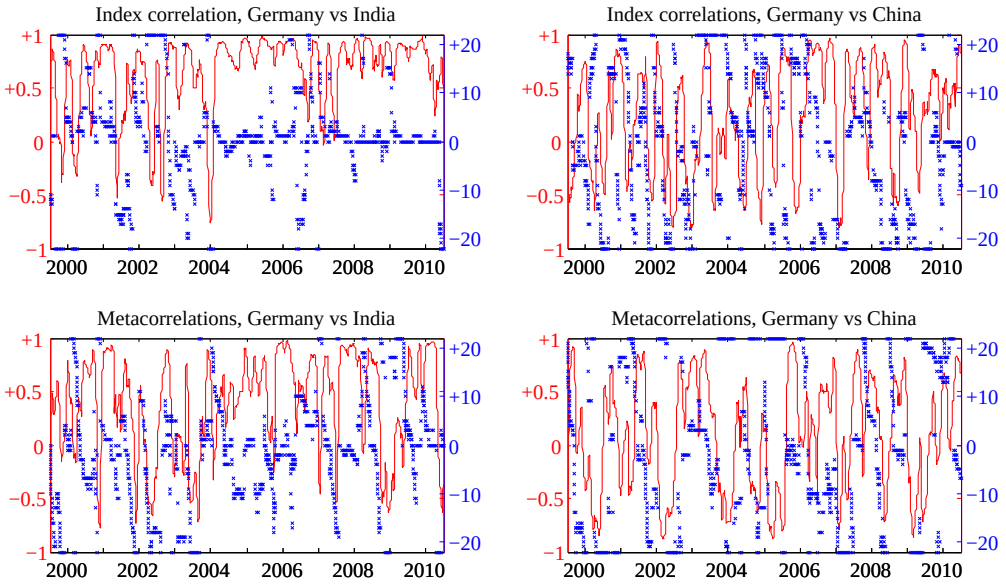

Fig. D.12: Market correlations: Germany-India, Germany-China
Index correlations (top) and meta-correlations (bottom) for Germany-India and Germany-China, Lag with maximum correlation (blue cross) and correlation at lag 0 for the cross-correlation of the indices. Both performed for a 66-day window.

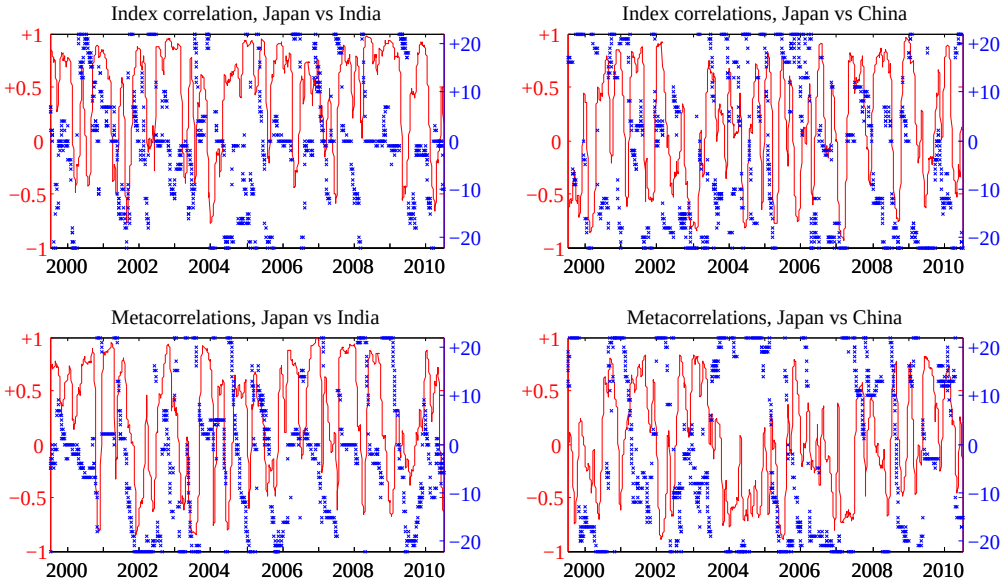

Fig. D.13: Market correlations: Japan-India, Japan-China
Index correlations (top) and meta-correlations (bottom) for Japan-India and Japan-China, Lag with maximum correlation (blue cross) and correlation at lag 0 for the cross-correlation of the indices. Both performed for a 66-day window.

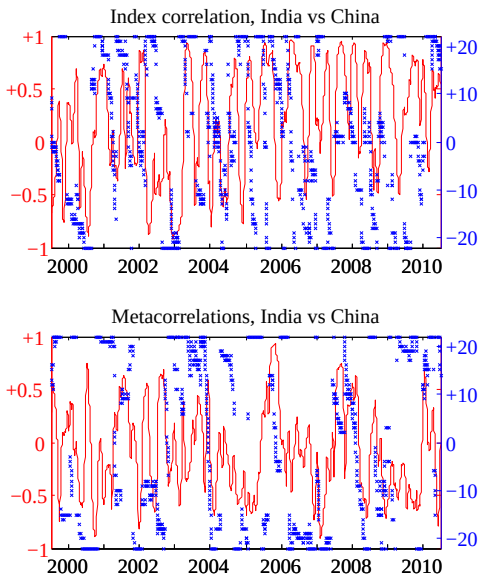

Fig. D.14: Market correlations: India-China

Index correlations (top) and meta-correlations (bottom) for India-China, Lag with maximum correlation (blue cross) and correlation at lag 0 for the cross-correlation of the indices. Both performed for a 66-day window.

D.5 Alternative Crosscorrelation Plots

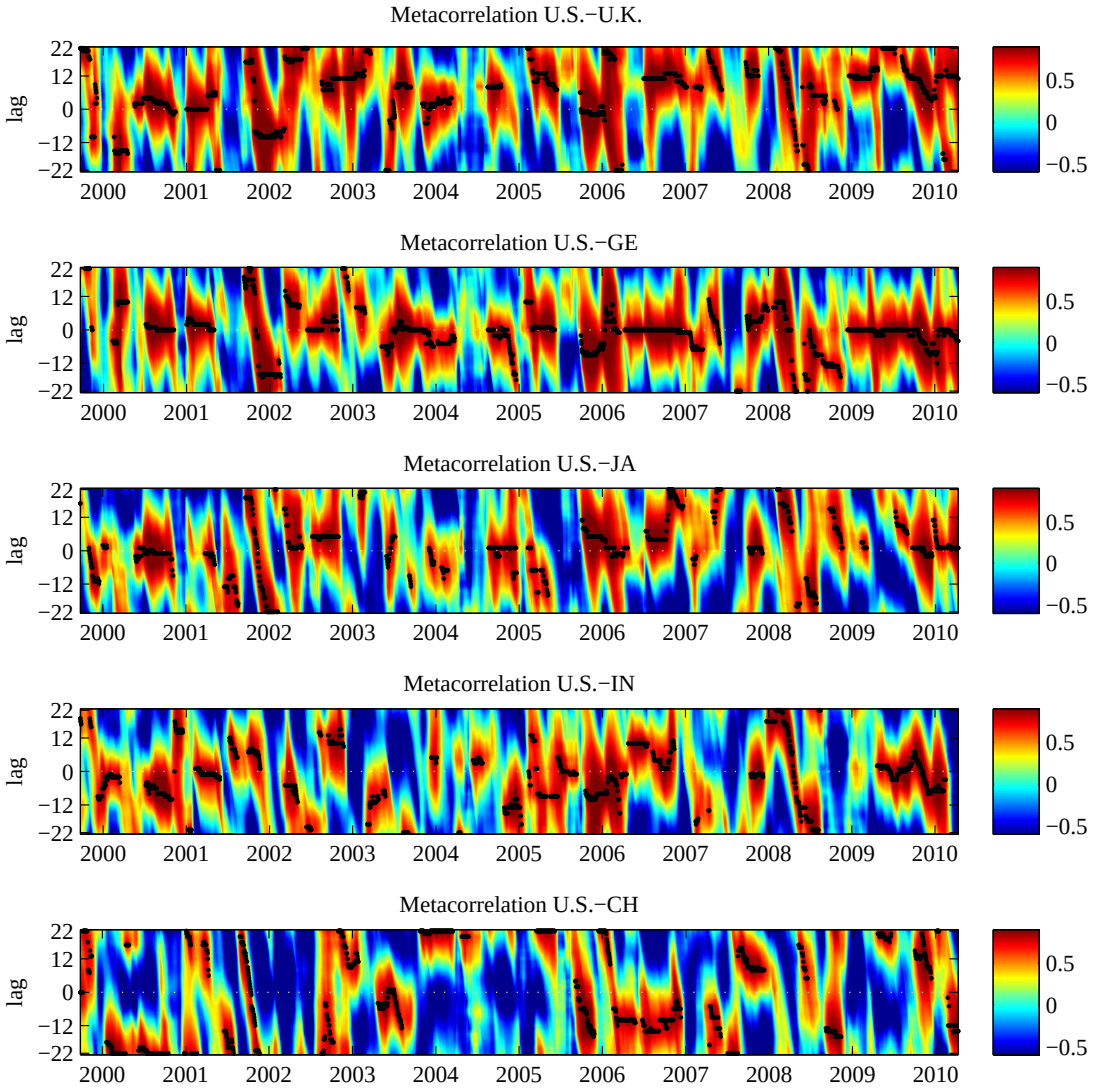

Fig. D.15: Cross-correlation plot of meta-correlations

Cross-correlation plot of meta-correlations. Black marker on maximum if the correlation is higher than .7, U.S. against all other markets. Performed for a 66-day window.

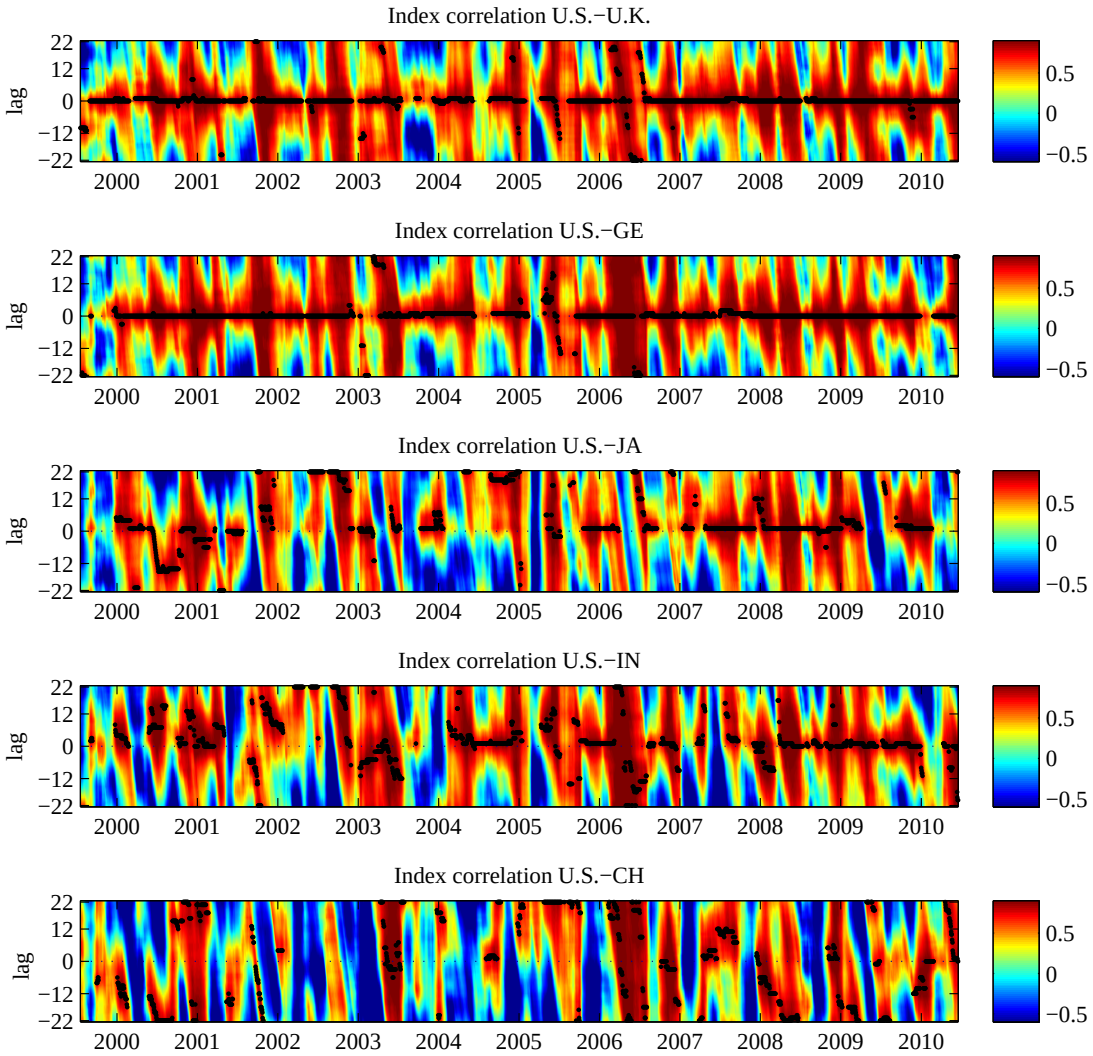

Fig. D.16: Cross-correlation plot of index correlations
Black marker on maximum if the correlation is higher than .7, U.S. against all other markets. Performed for a 66 day window.

E. ADDITIONAL PLOTS ON THE INTERBANK LOAN MARKET

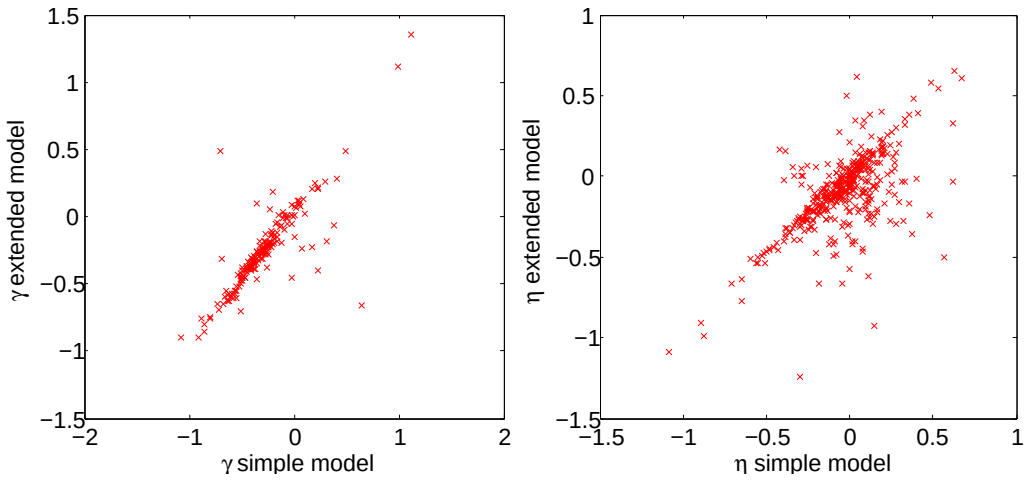

Fig. E.1: Comparing γ and η for the two models

The coefficients of the bank fixed effects in the left scatter plot ($n = 176$) are mostly close to a 45-degree line. The comparison of the preferential lending fixed effects $n = 412$ looks a little bit more noisy, still only about 5% of the observations are far from the 45-degree line.

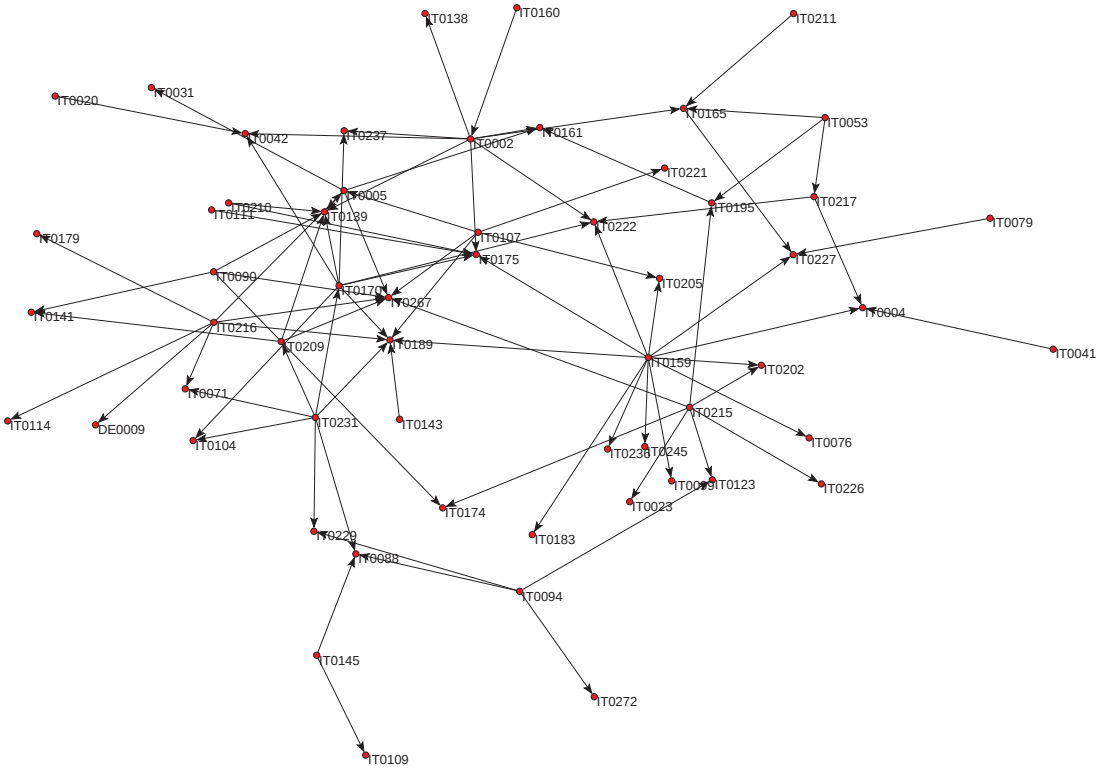

Fig. E.2: Network of non-preferential lending, 1999–2006

The "network of enemies" has a very special structure. Instead of a connected core we observe an almost circle like network with hubs that connect to the periphery but have relatively little links to other core hubs.

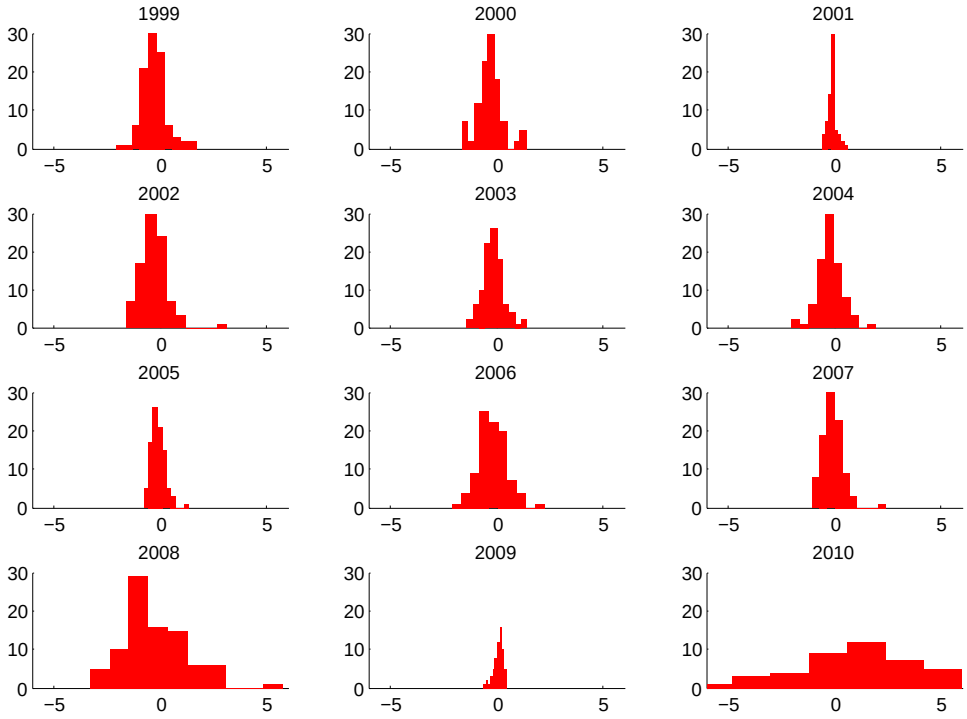

Fig. E.3: Spreads year by year

The histograms for the year by year estimated γ show similar distributions for 1999–2007 (exception: 2001). In 2008 amd 2010 the range of spreads is much wider. 2009 shows an increase of the mean value but also a much narrower distribution.

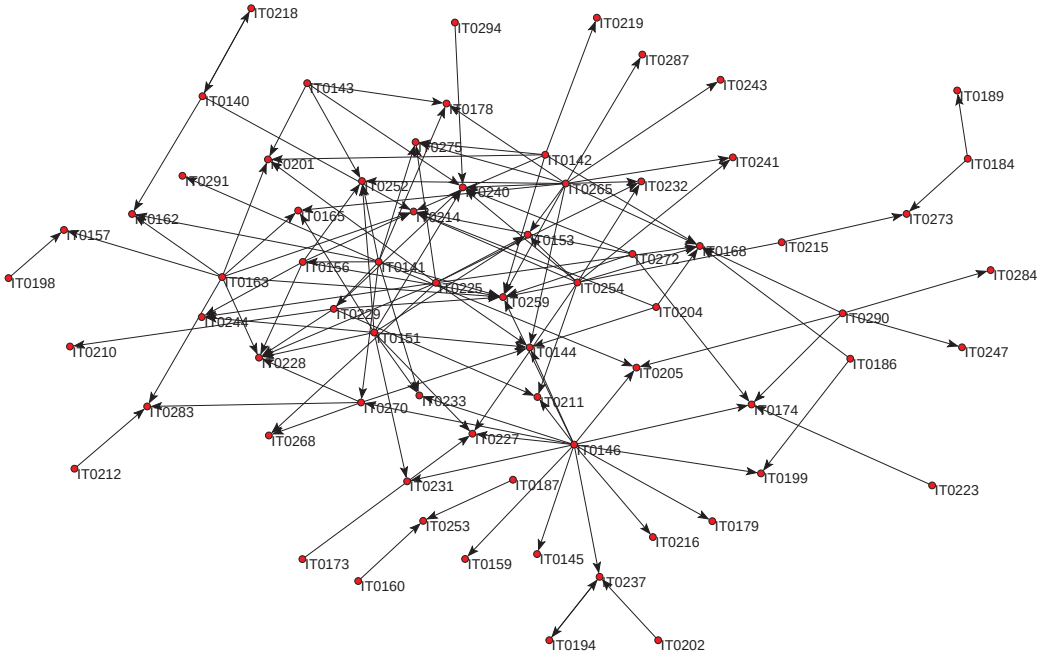

Fig. E.4: Network of non-preferential lending, post-Lehman

The network of non-preferential lending for the post Lehman period has similar characteristics like the network of preferential lending until 2006.

Eidesstattliche Erklärung

Ich erkläre hiermit an Eides Statt, dass ich meine Doktorarbeit "Networks in Financial Markets" selbständig und ohne fremde Hilfe angefertigt habe und dass ich alle von anderen Autoren wörtlich übernommenen Stellen, wie auch die sich an die Gedanken anderer Autoren eng anlehnenden Ausführungen meiner Arbeit, besonders gekennzeichnet und die Quellen nach den mir angegebenen Richtlinien zitiert habe. Über Teile der Arbeit die auf Zusammenarbeit mit anderen Forschern beruhen gibt Abschnitt 1.6 Auskunft. Die Arbeit hat bisher in gleicher oder ähnlicher Form oder auszugsweise noch keiner Prüfungsbehörde vorgelegen.

Kiel, den

LaTeX